Electrochemical Modeling of Bioenergy Generation from Wastewater by Microbial Fuel Cells

by

Yiming Li

A thesis

presented to the University of Waterloo

in fulfillment of the

thesis requirement for the degree of

Master of Applied Science

in

Civil Engineering

Waterloo, Ontario, Canada, 2025

© Yiming Li 2025

Author's Declaration

I hereby declare that I am the sole author of this thesis. This is a true copy of the thesis, including any required final revisions, as accepted by my examiners.

I understand that my thesis may be made electronically available to the public.

Abstract

As global water scarcity and environmental pollution continue to escalate, innovative wastewater treatment technologies are needed to ensure sustainable water resource management. Conventional wastewater treatment methods, such as activated sludge processes, are energy-intensive, costly, and contribute significantly to greenhouse gas emissions. Microbial fuel cells (MFCs) present a promising alternative, harnessing electroactive bacteria to simultaneously degrade organic pollutants and generate electricity. By leveraging microbial metabolism, MFCs can convert chemical energy in wastewater into usable electrical energy, offering a dual benefit of pollution reduction and renewable energy production.

This study focuses on developing a numerical simulation framework to optimize MFC performance, with an emphasis on real-world application at the Guelph Water Resource Recovery Centre (WRRC). A steady-state microbial fuel cell model was developed and validated using experimental data from previous studies. The model employs a finite difference method to solve mass balance equations for key reactants and products, including acetate, dissolved CO_2, protons, and oxygen. The simulation results highlight the influence of various operational parameters—such as substrate concentration, internal resistance, wastewater flow rate, and temperature—on the performance of a dual-chamber MFC. The study further compares MFC efficiency with conventional wastewater treatment processes, demonstrating a significantly higher chemical oxygen demand (COD) removal rate in MFCs (0.0633 kg COD/m^3/day), which is approximately 4.7 times greater than that observed at the WRRC.

The results emphasize the role of microbial activity and electrochemical interactions in optimizing power generation and pollutant degradation. Key limitations such as oxygen transport restrictions, internal resistance, and pH imbalances were identified, suggesting areas for improvement in MFC design. Numerical simulations were further extended to model full-scale integration within WRRC, providing insights into the feasibility of MFC technology as an alternative treatment strategy. Despite challenges in large-scale deployment, MFCs show strong potential for reducing wastewater treatment energy demands and mitigating environmental impacts.

This research contributes to the advancement of MFC applications in wastewater treatment by demonstrating the effectiveness of numerical modeling in predicting and optimizing system performance.

Acknowledgements

In the blink of an eye, my time on campus is drawing to a close. As I complete this thesis, I am grateful for the many people who have supported and encouraged me along this journey. Words alone cannot fully express the depth of my appreciation, but I offer my heartfelt thanks nonetheless.

First and foremost, I extend my deepest gratitude to my supervisor, Dr. Shunde Yin. Your wisdom, guidance, and unwavering support have shaped my academic journey in ways I could never have imagined. The opportunities you have provided me to learn and grow have been invaluable, and the lessons you have imparted—both in research and in life—will stay with me forever. Your meticulous approach to scholarship, your engaging teaching style, and the care you put into refining my work have left a profound impact on me. The principles you have instilled in me will continue to guide and inspire me throughout my life. I am also deeply grateful to my thesis committee members, Dr. Zhongming Lu and Dr. Giovanni Cascante, for their time, thoughtful feedback, and constructive suggestions. Their expertise and perspectives greatly enriched the quality of my work.

I would also like to express my sincere appreciation to my friends and my "academic siblings", Yutong Chai and An Ping. Your encouragement, camaraderie, and selfless support have made this journey more manageable and meaningful. The memories we have created together will always be cherished, and I am truly grateful to have shared this experience with you.

A heartfelt thank you goes to my family, whose unconditional love and support have been my greatest source of strength. To my parents, your patience, understanding, and unwavering belief in me have given me the courage to persevere through every challenge. This achievement is as much yours as it is mine.

Finally, I extend my gratitude to everyone who has contributed to my academic journey—professors, mentors, colleagues, and friends. Your encouragement and kindness have made a lasting impact on my life.

To all of you, thank you.

Dedication

I dedicate this thesis to my family, whose unwavering support, patience, and encouragement have been my foundation throughout this journey. To my parents, who have always believed in your love and sacrifices, have been my greatest motivation.

I also dedicate this thesis to my beloved cat, Tangbing. You have been my constant companion through the long nights of research, the countless hours of writing, and the moments of self-doubt. Your quiet presence, comforting purrs, and playful antics have brought me joy and relief during the most challenging times. You may not understand the significance of this work, but your unwavering companionship has made the journey more bearable and infinitely more enjoyable. This thesis is, in part, a testament to the warmth and comfort you have provided me every step of the way.

Thank you for being my furry source of love and support.

Table of Contents

Author's Declaration ii

Abstract iii

Acknowledgements iv

Dedication v

List of Figures ix

List of Tables xi

Chapter 1 Introduction 1

1.1 Need for Improvement in Wastewater Treatment 1

1.2 Current Wastewater Treatments and Their Challenges 1

1.2.1 Aerobic Treatment 2

1.2.2 Anaerobic Treatment 3

1.2.3 Biofilm Technology 5

1.3 Microbial Fuel Cells in Wastewater Treatment 5

1.4 Current Research Gaps in MFCs 7

1.4.1 High Operational Cost 7

1.4.2 Stacking 8

1.5 Research Scope 8

Chapter 2 Literature Review 10

2.1 Microbial Fuel Cell History and Development 10

2.2 Operating Principles of MFCs 12

2.3 Design Factors that Influence MFCs Performance 16

2.3.1 MFCs Electrode Material 17

2.3.2 Different Configuration of MFCs 20

2.4 Operational Factors that Influence MFCs Performance 28
2.4.1 Substrate 28
2.4.2 PH 31
2.4.3 Temperature 32
2.4.4 External Resistance 33
2.4.5 Flow Rate and Hydraulic Retention Time 34
2.5 Applications of MFCs in Different Industries 36
2.5.1 Agro Industry 36
2.5.2 Oil Industry 36
2.5.3 Dairy Industry 37
2.5.4 Textile Industry 37
2.5.5 Wastewater Treatment Plants 37
2.6 Challenges and Research Scope 38
Chapter 3 Modelling for Steady-State 40
3.1 Method of Approach 40
3.2 ADM1 Used in the Model 41
3.3 Model Development and Assumptions 43
3.4 Results and Discussion 47
3.5 Conclusion 54
Chapter 4 Modelling for Guelph WWTP 56
4.1 Introduce to Guelph WWTP 56
4.2 Analysis of Raw Influent and Effluent Wastewater Data 57
4.3 Model Development and Assumptions 58
4.3.1 Model Assumptions 58

4.3.2 Equations Generation 59
4.3.3 Boundary Conditions 62
4.4 Results and Discussion 63
4.4.1 Flow Rate 63
4.4.2 Initial Feed Concentration 66
4.4.3 Internal Resistance 69
4.4.4 Temperature 72
4.4.5 Voltage Output 73
4.4.6 Concentration over Time 75
4.4.7 COD 76
4.4.8 Monte Carlo-Based Uncertainty Analysis of MFC Performance 78
4.4.9 Conclusion 85
Chapter 5 Conclusion 86
References 89
Appendix A Raw Influent Data and Final Effluent Data from Guelph WWTP 110

List of Figures

Figure 1. Schematic Diagram of UASB Reactor (Farissi, Ramesh, Muthuchamy, & Muthukumar, 2022) 4
Figure 2. The Basic Setup of Microbial Fuel Cell (Watanabe, 2008) 6
Figure 3. Schematic Diagram of the MFC (Do, et al., 2018) 13
Figure 4. Schematic Diagram of the Single MFC (Hamedani, Abasalt, & Talebi, 2024) 21
Figure 5. Schematic Diagram of the Dual-Chamber MFC (Hoanga, et al., 2022) 23
Figure 6. Schematic Diagram of the Stacked MFC (Hamedani, Abasalt, & Talebi, 2024) 27
Figure 7. Conceptual model for ADM1 (Parker, 2005) 41
Figure 8. Power Density vs Current Density 48
Figure 9. Cell Voltage vs Current Density 49
Figure 10. Overpotentials for the Anode and Cathode 50
Figure 11. pH in Anode and Cathode Chamber 51
Figure 12. Reaction Rate for the Anode and the Cathode 52
Figure 13. Concentration for Each Component 53
Figure 14. Power Density vs. Current Density for Different Q_a 63
Figure 15. Voltage Changes Over Time Under Different Qa 64
Figure 16. COD Concentrations Over Time Under Different Q_a 65
Figure 17. Power Density vs. Current Density Under Different C 67
Figure 18. Voltage Over Time Under Different C 68
Figure 19. Power Density vs. Current under Different R_{int} 69
Figure 20. Polarization Curve under Different R_{int} 71
Figure 21. Polarization and Power Curve under Different T 72
Figure 22. Battery Output Voltage over Time 74
Figure 23. Concentration of Substances over Time 75
Figure 24. COD Removal over Time 77
Figure 25. Histogram of Simulated Current Outputs Across 1000 Monte Carlo Iterations 80
Figure 26. Histogram of Simulated Cell Voltage Values from Monte Carlo Simulations 80
Figure 27. Histogram of Power Density Output from Monte Carlo Simulations 81
Figure 28. Scatter Plot Showing the Relationship between k_{bio} and Power Density, Voltage and Current 82

Figure 29. Scatter Plot Showing the Relationship between R and Power Density, Voltage and Current 83
Figure 30. Scatter Plot Showing the Relationship between L_f and Power Density, Voltage and Current 84
Figure 31. Raw Influent Data from Guelph WWTP (Guelph, 2022) 110
Figure 32. Final Effluent Quality (Guelph, 2022) 111

List of Tables

Table 1. Energy Stored in Each Element within Wastewater (McCarty, Bae, & Kim, 2011) 2
Table 2. Sewage sludge treatment using dual-chamber MFCs (Mahmoudi, Alireza Mousavi, & Darvishi, 2024) 24
Table 3. Electricity Generation Using Different Substrates in MFCs (Mahmoudi, Alireza Mousavi, & Darvishi, 2024) 29
Table 4. Kinetic Processes of 24 Components in ADM1 (IWA, 2005) 42
Table 5. Parameters for Model Set-Up and Simulation 46
Table 6. Raw Wastewater Inflow Data 58
Table 7. Summary of Input Parameters Considered in Monte Carlo Uncertainty Analysis 79

Chapter 1 Introduction

1.1 Need for Improvement in Wastewater Treatment

Approximately 71% of Earth's surface is covered by water, with oceans containing about 97% in saline form. Consequently, only 3% of the planet's water is fresh, and merely 0.5% is available in liquid form within rivers, lakes, ponds, and groundwater. The remaining 2.5% of fresh water is locked in glaciers (Baker, Aldridge, & Omer, 2016). Since the earliest civilizations emerged along riverbanks, water has been used for domestic and agricultural purposes. Historically, raw sewage from human settlements was discharged into nearby water bodies, relying on their inherent capacity to dilute and disperse waste—a practice that was manageable when populations were smaller and wastewater volumes were relatively low. (Sangamnere, Misra, Bherwani, Kapley, & Kumar, 2023)

With accelerating economic growth and urbanization, the increasing water demand has driven substantial extraction from natural sources. This demand continues to intensify under the pressures of rapid industrial expansion, rising per capita consumption, shifting weather patterns due to climate change in densely populated areas, population growth, and migration from drought-stricken regions (Pearce, 2008). Consequently, the reuse and treatment of wastewater have emerged as crucial strategies for enhancing water availability, and water sanitation has become a critical global priority.

1.2 Current Wastewater Treatments and Their Challenges

Due to rapid industrialization, conventional wastewater treatment methods have become increasingly inadequate in meeting rising water sanitation demands, particularly in regions experiencing swift population growth and urban expansion. These methods, initially designed for lower waste volumes and fewer types of pollutants, have not kept pace with the heightened contamination now entering water bodies. As a result, they struggle to remove emerging pollutants and maintain water quality effectively.

Furthermore, these treatment systems rely on energy-intensive processes, leading to substantial operational costs and environmental impacts such as elevated greenhouse gas emissions. This reliance on high-cost, resource-heavy technologies not only significantly burdens municipal budgets but also complicates the pursuit of sustainable water solutions. (McCarty, Bae, & Kim, 2011). In this case, many low- to middle-income nations face inadequate sewage collection and treatment infrastructure, resulting in household and commercial wastewater discharge without or with only minimal treatment. In Latin America, for instance, only 15% of the total generated wastewater is

processed at formal treatment facilities. (Dhote, Ingoleb, & Chavhana, 2012). In 2014–15, India's class-I and class-II cities collectively generated 62,000 MLD of sewage. However, the total treatment capacity of existing, planned, and under-construction facilities amounts to just 23,277 MLD—leaving an unaddressed gap of nearly 62.46% in the country's sewage treatment capacity. (CPCB, 2021)

Currently, wastewater treatment typically consumes around 0.5 to 2 kWh/m³, depending on the treatment process and the wastewater's composition. Remarkably, wastewater contains three to ten times the energy necessary for its treatment, suggesting its potential as an energy resource. The principal energy forms in wastewater include organic matter, nutrients, and thermal energy. (McCarty, Bae, & Kim, 2011) Table 1 summarizes the specific amount of energy each element contains.

Table 1. Energy Stored in Each Element within Wastewater (McCarty, Bae, & Kim, 2011)

Types of Elements	The energy contained in Wastewater (kWh/m^3)
Organic Matter	~1.79
Nutritional Elements	~0.7
Thermal Energy	~7.0

Domestic wastewater contains two primary forms of energy: chemical and thermal, accounting for roughly 26% and 74% of the total energy potential, respectively. Chemical energy resides in carbon-based compounds such as chemical oxygen demand (COD) and nutrients like nitrogen and phosphorus. Meanwhile, thermal energy forms a larger share of overall energy content but often requires a heat pump for extraction and is highly sensitive to fluctuations in wastewater temperature. Consequently, harnessing the chemical energy from wastewater offers a promising pathway to transform treatment processes into energy-independent systems. (Gude, 2016)

1.2.1 Aerobic Treatment

In aerobic wastewater treatment (WWT), microorganisms operate in the presence of oxygen to degrade substrates or other organic material found in the wastewater. These microorganisms use organic matter as a source of carbon and energy. Aerobic biological treatment can be categorized into

two types: suspended growth systems and attached growth systems. In a suspended growth system—sometimes called mixed liquor—the microorganisms and the substrate remain suspended in the water. However, in an attached growth system, the microorganisms form a layer that adheres to a solid surface. (Sangamnere, Misra, Bherwani, Kapley, & Kumar, 2023)

The activated sludge process (ASP) is a well-established biological method that is currently used extensively in wastewater treatment (Fernandes, Jungles, Hoffmann, Antonio, & Costa, 2013). It involves aeration and the formation of biological flocs, made up of bacteria and protozoa. Among the various secondary treatment options, it is particularly effective for removing biodegradable organic matter and suspended solids. In this process, air (or oxygen) is supplied to the microorganisms, enabling them to oxidize organic pollutants and produce a waste sludge (or floc) containing the oxidized material (Peng, Wang, Yin, & Xu, 2019). Its high treatment efficiency and relatively low operating costs make it suitable for both domestic and industrial applications (Tran, et al., 2022). A significant drawback of the ASP is the substantial volume of waste activated sludge (WAS) it produces, requiring further treatment before safe disposal (Banu, Ushani, & Yukesh Kannah, 2017). Additionally, ASP demands extensive maintenance and incurs high operational costs, with aeration alone accounting for up to 75% of a wastewater treatment plant's energy consumption, making it a considerable energy burden.

Sludge management and disposal can account for as much as 60% of WWTP's total operating costs. According to the North Toronto Treatment Plant's 2020 annual report, a single WWTP can already cost around $2 million per year (Toronto water, 2020) . Beyond these financial challenges, greenhouse gas emissions, including carbon dioxide, nitrous oxide, and volatile substances—are also generated throughout the treatment process, further exacerbating environmental concerns (Li, Yu, & He, 2014).

1.2.2 Anaerobic Treatment

Anaerobic treatment is a type of biological wastewater that operates without needing oxygen or air. By employing anaerobic reactors, it is possible to reduce pollution levels and achieve effective solids stabilization significantly. (Daud, et al., 2018)

One breakthrough in the development of anaerobic treatment was the introduction of high-rate reactors, which separate biomass retention from liquid retention (Lettinga, Rebac, & Zeeman, 2001). Upflow anaerobic sludge blanket (UASB) reactors have shown considerable success among

the various anaerobic wastewater treatment methods. These reactors have been used to treat a wide range of effluents—including those from sugar, pulp and paper, dairy, chemical, potato starch, bean balancing, soft drinks, fish processing, noodle processing, yeast production, slaughterhouse, and coffee processing industries (Yetilmezsoy & Sakar, 2008). In this system, wastewater is introduced at the bottom of the reactor and flows upward through a blanket of biologically active sludge, typically in the form of granular aggregates. These aggregates remain stable and are not washed out under normal operating conditions, which leads to efficient treatment when the wastewater contacts the granules. Methane and carbon dioxide produced under anaerobic conditions promote internal mixing, aiding the formation and maintenance of these biological granules. (Daud, et al., 2018), which also leads to reduced carbon dioxide emissions, resulting from lower energy requirements and additional energy production in biogas, which can be utilized to operate the system. Figure 1 is a schematic diagram of a UASB reactor.

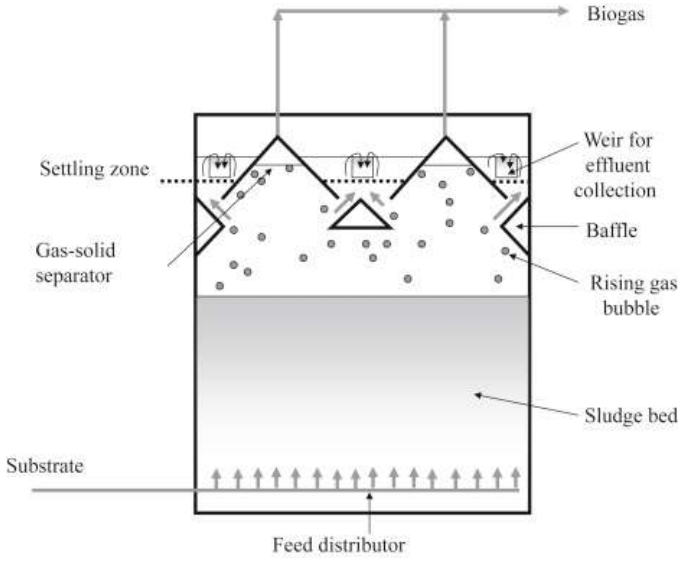


Figure 1. Schematic Diagram of UASB Reactor (Farissi, Ramesh, Muthuchamy, & Muthukumar, 2022)

However, there are still several disadvantages of UASB reactor technology. Anaerobic bacteria, particularly methanogens, are susceptible to a wide range of inhibitory substances. The initial start-up of this process can be slow, though it may be accelerated by using adapted seed sludge. Furthermore, a practical post-treatment step is necessary to remove any remaining biochemical oxygen demand (BOD), nitrogen, and odorous compounds. (Bobade & Lomte, 2015)

1.2.3 Biofilm Technology

Biofilm-based technologies highlight the critical role of microbial communities attached to surfaces. By forming these biofilms, microorganisms enhance the efficiency of wastewater treatment through improved pollutant degradation. (O'Toole, Kaplan, & Kolter, 2000). The biofilm development is a cyclic process, free-floating cells respond to environmental cues and begin attaching to a surface. As developmental signals drive their organization and growth, the biofilm matures into a structured community of microorganisms. Eventually, detachment signals cause some cells to leave the mature biofilm, returning to a planktonic state and completing the cycle. (Sangamnere, Misra, Bherwani, Kapley, & Kumar, 2023). As a result, novel technologies—particularly high-rate biofilm-based bioreactors—have been developed over time to overcome the limitations of traditional anaerobic–aerobic wastewater treatment systems.

An aerobic membrane bioreactor (MBR) serves as a dual-mechanism system in which membrane filtration and biodegradation processes occur simultaneously. While water and smaller dissolved molecules pass through the membrane, solids, biomass, and larger macromolecules are retained in the reactor (Seow, et al., 2016). Through this process, MBR have the ability to treat high-strength synthetic wastewater. However, biofilm-based wastewater treatment can face several challenges. First, the formation of biofilm on carriers can prolong the start-up phase. Excessive biofilm growth may also lead to the elutriation of particles. Additionally, controlling the thickness of the biofilm is often tricky. Finally, liquid distributors can be expensive for large-scale reactors in fluidized systems, and they frequently encounter issues such as clogging and the difficulty of ensuring uniform fluidization. (Seow, et al., 2016)

1.3 Microbial Fuel Cells in Wastewater Treatment

To address sustainability and economic challenges, microbial fuel cells (MFCs) have gained notable attention among researchers as a more promising option for wastewater treatment. A fuel cell is an electrochemical device that directly converts the chemical energy of its reactants (fuel and oxidant) into electrical power. Unlike batteries, which store energy, a fuel cell essentially acts as an energy converter, producing electricity as long as it is supplied with the necessary fuel and oxidant (Li X. , 2006). Like other fuel cells, MFCs convert chemical energy from wastewater into electricity by oxidizing carbonates into carbon dioxide (CO_2) and facilitating biochemical electron transport (Rahimnejad, Ghoreyshi, Najafpour, Younesi, & Shakeri, 2012). In MFCs, electrons and protons are

generated when substrates decompose at the anode. These charged particles then travel through a resistor and membrane to the cathode, where they react with oxygen to produce electricity (Sharma & Li, 2010), (Munoz-Cupa, Hu, Xu, & Bassi, 2021)

Compared to traditional activated sludge systems, MFCs offer higher substrate-to-energy conversion efficiency and greater volume reduction (Zhang, et al., 2019). Additionally, they can recover valuable by-products—such as silver (Ag) and chromium (Cr)—and produce lower greenhouse gas emissions, making them a more sustainable option for wastewater treatment (Li, Yu, & He, 2014), (Jadhav, Ghosh Ray, & Ghangrekar, 2017), (Rabaey & Verstraete, 2005). Figure 2 shows a process flow of an MFC reaction.

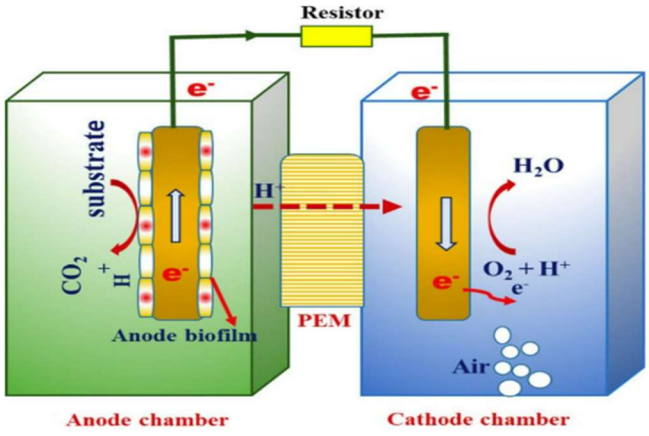


Figure 2. The Basic Setup of Microbial Fuel Cell (Watanabe, 2008)

A typical microbial fuel cell consists of three main components: an anode, a proton exchange membrane (PEM), and a cathode. The anode and cathode are connected by an electrical wire that completes the circuit. In MFCs, microorganisms in the anode chamber generate electrons, passing through the PEM to reach the cathode chamber, where oxygen is reduced. Like all fuel cells, the anode in an MFC must be made from non-toxic materials, resist fouling, and efficiently conduct electrons (Kumar, Singh, Zularisam, & Hai, 2017) .These properties ensure a suitable environment for microbial activity and high conductivity (N M, Meda, Patil, Moses, & P L, 2022), (Min, Kim, Oh, Regan, & Logan, 2005).

The cathode, which typically does not host microorganisms (except when methane production is desired through methanogens), relies on electrons and ions arriving from the anode to

maintain the cell reaction (N M, Meda, Patil, Moses, & P L, 2022). This electrode plays a central role in determining energy output (Chao, et al., 2020). For these reactions to occur, an oxidant—usually oxygen or air—is introduced into the cathode compartment (N M, Meda, Patil, Moses, & P L, 2022).

The proton exchange membrane separates the anode and cathode in a fuel cell, facilitating ion transport from the anode to the cathode and enabling the necessary electrochemical reactions (Moharir & Tembhurkar, 2018). In MFCs, the membrane also prevents waste by-products formed at the anode from contaminating the cathode, thus avoiding fouling and ensuring stable reactions (Ghasemi, Sedighi, & Usefi, 2022) (Mitov & Hubenova, 2015). Constructed from specialized materials (e.g., biopolymers, activated carbon sheets), this semi-permeable membrane is often modified with sulfonated graphene oxide and polyvinylidene fluoride to resist biofouling in wastewater environments (Ahmadian-Alam & Mahdavi, 2018).

1.4 Current Research Gaps in MFCs

Although microbial fuel cells have been recognized as promising for future wastewater treatment, they have not yet achieved widespread commercial adoption. One of the primary obstacles lies in scaling up MFC systems from laboratory or pilot-scale setups to full-scale operations. This chapter explores several key factors contributing to these challenges, including high costs, material limitations, and operational complexities, which must be addressed to enable broader commercial use of MFCs.

1.4.1 High Operational Cost

High operating expenses and limited power generation pose significant obstacles to the commercial use of MFC technology. Compared to conventional activated sludge systems for wastewater treatment, the capital costs for MFCs are substantially higher—approximately 30 times more. This significant cost difference is due to the specialized design and treatment processes employed in MFCs. Addressing these financial and performance challenges is essential for the broader adoption and commercial success of MFC technology in both wastewater treatment and energy generation. (Hassan, et al., 2024) A contributing factor to the high operational cost is the membrane material used in MFCs, which is produced from Nafion—an established commercial polymer electrolyte membrane commonly used in fuel cells. (Park, Tinh, & Kim, 2022).

Another elevated capital cost of MFCs largely comes from using expensive electrode materials, including current collectors, catalysts, and separators. These components significantly increase the system's overall cost. Moreover, the power output of MFCs is sometimes insufficient to continuously run sensors or transmitters, which limits their practical use. Although materials such as carbon cloth and carbon paper can provide relatively high-power output, their costs are still prohibitively high. (Hassan, et al., 2024) The high cost of these materials limits the large-scale adoption of MFCs across different applications. Overcoming these financial barriers and finding alternative materials with similar performance but lower expenses are essential to ensure broader usage and commercialization of MFC technology.

1.4.2 Stacking

Fuel cell stacks, which consist of multiple MFC units connected in parallel or series, are essential for scaling up bio-electrochemical technologies in wastewater treatment and energy generation. Testing and validating technological improvements in real-world conditions is possible by scaling up, leading to enhanced efficiency and effectiveness. Stacking and multiplying MFC units is a commonly used strategy for this purpose. Miniaturizing and stacking the reactors helps reduce ohmic losses—electrical and ionic resistance within the system—thereby improving energy conversion. As a result, overall performance increases, and higher power output can be achieved. (Hassan, et al., 2024)

1.5 Research Scope

In summary, microbial fuel cells have significant potential for wastewater treatment but have not yet achieved widespread commercial use due to key challenges in scaling up. One major obstacle is the high operating costs associated with specialized membranes and expensive electrode materials, making MFC systems considerably more costly than conventional activated sludge treatments. Furthermore, the limited power output of MFCs can make it difficult to continuously operate sensors and other devices, further limiting their broader adoption. Although linking multiple MFC units (stacking) can enhance efficiency by reducing ohmic losses and improving energy conversion, the high costs of current collectors, catalysts, and separators still pose challenges for large-scale applications.

Numerical simulation is a vital tool for addressing these challenges related to cost, performance, and scaling. Through precise computational modeling, researchers can predict the

performance of MFC systems under various conditions, refine reactor designs, and test new materials without repeated trial-and-error experimentation. This approach conserves both time and resources, facilitating faster innovation in MFC design. As MFCs progress toward commercial deployment, numerical simulations will be essential for optimizing reactor configurations, reducing costs, and enhancing power output—ultimately accelerating the path to practical, large-scale implementation of this promising technology.

This research utilizes numerical simulation to improve MFC. Computational models provide a more efficient and cost-effective method than traditional experimental techniques, enabling accurate predictions of reactor behavior, identifying potential problem areas, evaluating cost-effective alternatives, and optimizing stacking methods. These simulations help clarify the main design aspects that influence both efficiency and expenses, aiding in the quest for commercial viability.

This work aims to bridge the gap between laboratory achievements and practical, real-world applications by systematically exploring advanced methods for modelling the overall performance of an MFC system. Numerical simulation serves as a powerful tool for streamlining this transition. Simulation significantly reduces the time and financial commitments typically required for large-scale experimentation by providing insights into reactor performance and facilitating rapid design assessments. Consequently, the findings of this study can expedite innovation in MFC technology, guiding the field toward more sustainable, efficient, and commercially feasible solutions for wastewater treatment and energy production.

Chapter 2 Literature Review

2.1 Microbial Fuel Cell History and Development

Luigi Galvani, a physician and professor at the University of Bologna, is recognized as one of the pioneers of electrochemistry and bioelectricity. In his 1780 experiments, he observed frog leg muscles twitching when exposed to an electrical spark. Galvani (1792) hypothesized that this movement resulted from an "*electrical fluid*" travelling along the nerves to the muscles—a phenomenon he termed "*animal electricity*." (Galvani & Aldini, 1792)

At the same time, Alessandro Volta, a professor of experimental physics at the University of Pavia, repeated Galvani's experiments. However, Volta argued that the muscle contractions were not due to any inherent animal electricity but were caused by the metal cable used to connect the nerves and muscles. This disagreement, later known as the Galvani-Volta controversy, ultimately led Volta to develop one of the earliest battery forms. (Santoro, Arbizzani, Erable, & Ieropoulos, 2017) In the early 19th century, significant advances were made in electrochemical systems for power generation and energy storage. Notably, the lead-acid battery—developed in 1859 by French physicist Gaston Planté—remains a critical technology in today's battery market. William Grove, a Welsh lawyer, turned scientist, built the first acid fuel cell using hydrogen and oxygen. Often called the father of fuel cells, Grove published a letter in 1838 describing his "*gas battery*," which inspired many researchers. Although Wilhelm Ostwald later remarked that Grove's gas battery was primarily of theoretical interest, in 1889, Charles Langer and Ludwig Mond introduced the term "*fuel cell*" as they pursued the development of a practical device using air and coal gas. (Carrette, Friedrich, & Stimming, 2001)

In 1932, Francis Bacon developed the first successful hydrogen-oxygen fuel cell using an alkaline electrolyte, and by 1959 he had demonstrated a practical 5 kW system. Since then, advancements in fuel cell technology have been driven by contributions from NASA, national agencies, and vehicle manufacturers. (Carrette, Friedrich, & Stimming, 2001) Fuel cells are typically classified by the type of electrolyte they use—such as polymeric membranes, ceramics, or liquid electrolytes—as well as by the fuel type (for example, alcohol fuel cells) and the operating pH (alkaline or acidic). The chosen electrolyte and electrode materials dictate the operating temperature range, generally 60–200 °C for low-temperature systems and 600–1000 °C for high-temperature systems. (Carrette, Friedrich, & Stimming, 2001)

Each type of fuel cell comes with its advantages and disadvantages. High-temperature systems like solid oxide fuel cells (SOFCs) and molten carbonate fuel cells (MCFCs) tend to have slow start-up times. Yet, they do not require expensive precious metal catalysts, thereby reducing costs, and their waste heat can be recycled to boost overall efficiency, theoretically up to 85%. In contrast, low-temperature proton exchange membrane fuel cells (PEMFCs), operating between 60 and 110 °C, benefit from improved reaction kinetics without significant degradation; however, they rely on precious metals to catalyze key reactions at both the anode and cathode. Replacing these costly catalysts remains an ongoing challenge in the field. (Morozan, Jousselme, & Palacin, 2011)

The benefits of these fuel cells are often overshadowed by challenges such as high operating temperatures, high costs, and sometimes corrosive environments. (Kuntke, et al., 2012) In contrast, BFCs are particularly appealing because they function under mild conditions—ambient temperature and pressure—use neutral or near-neutral electrolytes and rely on affordable catalysts. Moreover, the anodic fuel in BFCs can range from simple organic molecules like glucose or acetate to more complex organic waste, including wastewater and urine. (Shukla, Suresh, Berchmans, & Rajendran, 2004)

Biological fuel cells (BFCs) are devices that directly convert the chemical energy of organic compounds into electrical energy via electrochemical reactions involving biochemical pathways. They are generally divided into two main types: enzymatic fuel cells (EFCs) and microbial fuel cells (MFCs) (Minteer, Liaw, & Cooney, 2007). In EFCs, specific enzymes catalyze redox reactions to generate current, whereas in MFCs, electroactive microorganisms oxidize organic substrates to produce electricity. Although enzymes typically offer high catalytic performance, biocompatibility, efficiency, and selectivity under mild conditions, they often suffer from reduced durability compared to microbial catalysts. (Atanassov, Banta, Barton, Cooney, & Liaw, 2007)

The concept of microbial fuel cells dates to the early 20th century when English botanist Michael Cresse Potter demonstrated that microorganisms could generate voltage and deliver current. BFCs received further attention in the 1960s when NASA explored converting organic waste into electricity for space missions and again in the 1980s when Bennetto and colleagues emphasized mediator-based electron transfer in MFCs (Stirling, et al., 1983). Since the early 2000s, research on MFCs has grown rapidly, as evidenced by a significant increase in related publications and citations (Rasmussen, Abdellaoui, & Minteer, 2016)

In practical applications, BFCs operate by directly converting the chemical energy of organics into electrical energy using either enzymes or microbes as catalysts (Logan B. E., 2009). The advantages of enzymes—such as high biocompatibility, excellent transformation efficiency, and remarkable selectivity—allow EFCs to function without a separation membrane, facilitating device miniaturization and opening up applications in wearable and implantable electronics. However, enzymes have a limited lifespan, a challenge exacerbated by the presence of pollutants. Researchers have developed mediatorless enzyme-based biocathodes and bioanodes to address these issues and employed micellar polymers to encapsulate enzymes. This encapsulation helps prevent enzyme denaturation by providing a biocompatible, hydrophobic, and pH-buffered microenvironment, thereby extending their active lifetime. (Rabaey, Boon, Siciliano, Verhaege, & Verstraete, 2004)

On the other hand, MFCs use whole microbial cells, eliminating the need for enzyme isolation and allowing multiple enzymatic reactions to occur under near-natural conditions. The microbes naturally regenerate the necessary enzymes. Despite these benefits, MFCs generally exhibit slower response times due to their more complex metabolic pathways. In this case, MFCs are typically considered for large-scale applications such as wastewater treatment or portable energy systems. EFCs are ideal for compact, miniaturized, and flexible bioelectrochemical devices. (Falk, Narvμez Villarrubia, Babanova, Atanassov, & Shleev, 2013)

2.2 Operating Principles of MFCs

Microbial fuel cells use bacteria to break down organic and inorganic substances and produce electricity. Figure 3 below shows a schematic diagram of a dual-chamber MFC. In microbial fuel cells, microorganisms serve as biocatalysts, facilitating the conversion of chemical energy into electrical energy (Singh Mathuriya & Yakhmi, 2016). A typical MFC comprises two compartments: an anaerobic anode chamber (negative electrode) and an aerobic cathode chamber (positive electrode). A proton exchange membrane usually separates these chambers and Figure 3 below shows a general configuration of a two-chamber MFC. (Mahmoudi, Alireza Mousavi, & Darvishi, 2024). The proton exchange membrane plays a vital role in MFCs by transporting protons from the anode to the cathode while preventing oxygen from entering the anode chamber.

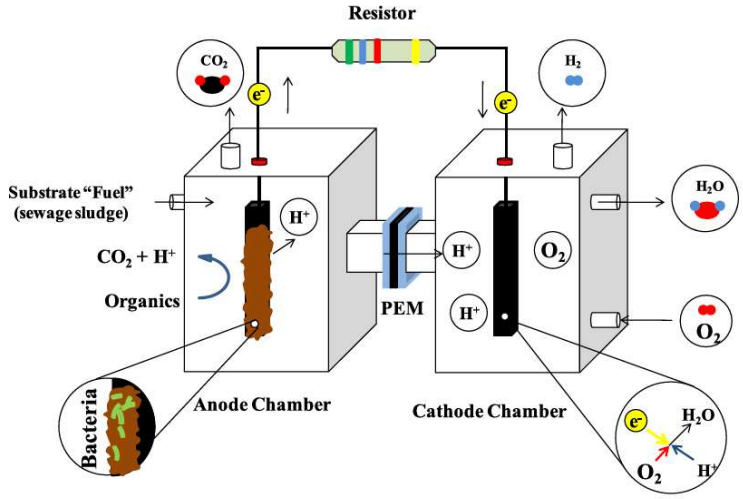


Figure 3. Schematic Diagram of the MFC (Do, et al., 2018)

In microbial fuel cells, bacteria in the anode chamber break down organic matter under anaerobic conditions, generating hydrogen ions (H^+) and electrons. These electrochemically active bacteria form a biofilm on the anode surface, facilitating the oxidation of organic compounds. Carbon dioxide is released as a by-product of this process. However, there is no net carbon emission into the environment since the CO_2 originates from renewable biomass, which initially absorbs carbon from the atmosphere through photosynthesis (Do, et al., 2018).

The electrons produced by the bacteria are transferred to the anode (negative terminal) and then travel through a conductive material to the cathode (positive terminal). This movement can either pass through a resistor or supply power to an external load, generating electricity to operate a device (Hernandez-Flores, et al., 2015) (Bimastyaji, 2017). Meanwhile, the H^+ ions migrate through a semi-permeable membrane to the cathode, driven by the electrochemical gradient created by their higher concentration near the anode. At the cathode, these electrons combine with dissolved oxygen and H^+ ions, forming pure water (Brown, 2012).

A variety of bacterial species play a role in electricity generation within MFCs, including *Geobacter metallireducens, Clostridium butyricum, Geobacter sulfurreducens, Aeromonas hydrophila, Rhodoferax ferrireducens,* and *Shewanella putrefaciens.* Most of these species belong to the group of metal-reducing bacteria. Recent studies indicate that microbial communities capable of producing mediators or electron shuttles can enhance electricity production in MFCs. Among these,

Pseudomonas aeruginosa, Alcaligenes faecalis, and *Enterococcus faecium* have been identified as key contributors (Liu, Cheng, & Logan, 2004) (Saratale, et al., 2017)

Despite significant progress, the microbial communities involved in electron transfer at the cathode and the biochemical mechanisms driving this process remain poorly understood. Further research is needed to clarify these pathways, as various extracellular electron transfer mechanisms have been proposed, but their precise functions and interactions require deeper investigation. In summary, extracellular electron transfer occurs through several mechanisms:

1. Direct electron transfer using the active sites of membrane-bound enzymes, such as cytochromes.
2. Direct electron transfer via biological nanowires, which are fibrous protein structures.
3. Mediated electron transfer through self-secreted electron shuttles.
4. Long-distance electron transfer through a conductive biofilm matrix, which consists of a network of nanowires and cytochromes associated with the matrix (He, et al., 2015).

In MFCs, organic substrates serve as electron donors for redox reactions at the anode, contributing to energy generation. Exoelectrogenic microbes attached to the anode oxidize these organic substrates, leading to the reduction of nicotinamide adenine dinucleotide (NAD^+) to NADH in the cytoplasm as part of their metabolic processes (Choi & Cui, 2012). NAD^+ and its reduced form, NADH, play essential roles as cofactors and electron carriers in cellular metabolism and energy production. Similarly, flavin adenosine dinucleotide (FAD) is reduced to $FADH_2$, while (CO_2) is released as a by-product. Both NADH and $FADH_2$ function as electron carriers, transferring electrons to the electron transport chain (ETC), which facilitates the production of adenosine triphosphate (ATP), the primary energy-carrying molecule in cells (Kumar, Singh, Wahid, & Din, 2015).

To ensure efficient electron transfer, the anode compartment must remain completely anaerobic. This is because the anode electrode should be the sole electron acceptor, preventing competition from alternative electron acceptors such as oxygen (O_2), nitrate (NO_3^-), nitrite (NO_2^-), or sulfate (SO_4^{2-}), which could otherwise reduce the efficiency of electron transfer (Khandaker, et al., 2021).

Microbial fuel cells inoculated with mixed bacterial cultures, such as sewage sludge, exhibit greater resistance to process disturbances, higher power output, and greater versatility in substrate utilization compared to other MFCs (Jiang , Zhao, Wei, & Wang, 2010). Efficient degradation of

biomass, particularly sewage sludge, is crucial for enhancing electricity generation in MFCs. Therefore, to improve productivity, increase the added value of sludge, and ultimately enhance MFC performance, pretreatment of sludge as a substrate is essential.

In MFCs, electrons generated by microbial metabolism are transferred to the cathode via an external circuit. Mediators such as methyl viologen, thionine, humic acid, methylene blue, and neutral red facilitate this electron transfer from microorganisms to the electrode. At the cathode, protons and electrons combine with an oxygen oxidant to form water. Electrode reactions are shown below using acetate as an example substrate. (Zeng, Choo, Kim, & Wu, 2010)

$$(CH_2O)_2+2H_2O \rightarrow 2CO_2+8H^++8e^-$$

$$O_2+4e^-+2H_2O \rightarrow 4OH^-$$

Electricity generation in microbial fuel cells is significantly influenced by the reduction of kinetics at the cathode. Research has demonstrated that the choice of electron acceptor plays a crucial role in minimizing potential losses within the cathode chamber (He, et al., 2015). An ideal electron acceptor should exhibit key properties such as a high redox potential, fast reduction kinetics, cost-effectiveness, stability, and easy accessibility. (He, et al., 2015)

In recent years, considerable efforts have been devoted to optimizing and understanding the reduction mechanisms of electron acceptors at the cathode surface. While oxygen is commonly used due to its abundance, affordability, and high redox potential, its effectiveness as a terminal electron acceptor is limited. This limitation arises from poor contact between oxygen and electrodes, as well as the slow reduction process on graphite or carbon electrodes. To improve MFC performance, researchers have investigated alternative electron acceptors with faster reduction rates and higher theoretical redox potentials as substitutes for oxygen (Pandit, Sengupta, Kale, & Das, 2011).

The fundamental reaction in an MFC involves the breakdown of organic substrates into carbon dioxide and water, with electricity generated as a by-product. Through the movement of electrons from the anode to the cathode via an external circuit, MFCs convert chemical energy into electrical energy. This technology has promising applications, including electricity generation, bio-hydrogen production, wastewater treatment, and biosensors (Santoro, Arbizzani, Erable, & Ieropoulos, 2017). However, this thesis primarily focuses on the application of MFCs in wastewater treatment.

2.3 Design Factors that Influence MFCs Performance

The performance of MFCs can be affected by a combination of system design, operating conditions, and biological factors. These elements play a crucial role in optimizing electron transfer processes and improving energy generation.

Several design factors significantly impact the formation and function of electro-active biofilms in MFCs. One of the most critical considerations is the electrode material, as it directly affects microbial attachment and electron transfer efficiency. The properties of the electrode, including conductivity, hydrophilicity, porosity, and chemical stability, strongly influence biofilm formation and overall performance (Kumar, et al., 2013) (Venkata Mohan, Velvizhi, Modestra, & Srikanth, 2014)

The electrode surface area-to-volume ratio is also essential for optimizing electron transfer efficiency. The presence or absence of a membrane and the type of membrane used can influence ion transfer and microbial community stability. The relative anode-cathode surface area and the type of cathode also play a role in biofilm development. Furthermore, factors such as MFC configuration and electrode spacing determine how effectively electrons are transferred within the system. (Saratale, et al., 2017)

The performance of MFCs is also significantly affected by various environmental and operating parameters. The operational mode, whether batch or continuous flow, impacts microbial adaptation and efficiency. External resistance influences the electron transfer rate, while redox potential plays a key role in maintaining electrochemical balance. Other important factors, such as shear rate, temperature, pH, and ionic concentration, affect microbial growth and metabolic activity (Karthikeyan, et al., 2015) (Venkata Mohan, Velvizhi, Modestra, & Srikanth, 2014).

The microbial community composition is influenced by whether the system operates under aerobic or anaerobic conditions, as well as the type of substrate used as a microbial energy source. Controlling these variables is essential for maintaining optimal conditions for biofilm development and efficient energy generation. (Saratale, et al., 2017) The biological factors in MFCs are equally crucial in determining electron transfer efficiency and biofilm formation. The availability, diversity, and abundance of microbial resources play a fundamental role in system performance. The type of microbial culture, whether Gram-positive or Gram-negative, and whether a pure or mixed culture is used, affects electron transfer capabilities. Microbial interactions, including competition and niche

formation, also influence the stability of electro-active biofilms (Saratale, et al., 2017), (Venkata Mohan, Velvizhi, Modestra, & Srikanth, 2014)

Furthermore, factors such as biofilm growth rate and the specific rate of electron transfer significantly impact energy production. Evaluating the electroactive microbial community's density, diversity, composition, and abundance is essential for maintaining a stable and functional system. Microbes capable of synthesizing redox mediators and producing nanowires for direct electron transfer further enhance MFC performance. (Saratale, et al., 2017) In addition, the relative exoelectrogen population and the substrate utilization rate determine overall system efficiency. A better understanding of microbial interactions and the careful selection of microbial strains can significantly improve electron transfer processes and energy production in MFCs. (Saratale, et al., 2017)

In conclusion, the development of electro-active biofilms and the efficiency of MFCs depend on a combination of system design, operational conditions, and biological parameters. By optimizing electrode materials, environmental factors, and microbial interactions, MFCs can achieve greater efficiency, enhanced stability, and improved performance in applications such as energy production and wastewater treatment. This chapter discusses how those parameters influence performance based on existing research and publications. (Saratale, et al., 2017)

2.3.1 MFCs Electrode Material

2.3.1.1 Anode Material

Microorganisms play a crucial role in the anode chamber by generating electrons. These electrons are transferred through an external circuit to the cathode, where they reduce electron acceptors. Similarly, to complete the circuit, the protons produced in the anode must pass through the proton exchange membrane to the cathode. As a result, this process simultaneously generates electrical power and facilitates the removal of organic waste. (Park, Christy, Kim, & Nahm, 2014)

The anaerobic anode compartment is a critical component of microbial fuel cells. It provides the necessary conditions for biomass degradation. This compartment typically contains a substrate, microorganisms, an optional mediator, and the anode electrode, which serves as the electron acceptor. The activation energy for anodic reactions must be reduced using appropriate catalysts. In the anode

chamber, the bacteria present typically act as natural catalysts. (Virdis, Rabaey, Yuan, & Keller, 2008), (Rahimnejad, Adhami, Darvari, Zirepour, & Oh, 2015)

Consequently, various studies have explored a wide range of materials to optimize electrode design. Ideal electrode materials should exhibit the following key characteristics:

1. Excellent electrical conductivity and low resistance
2. High biocompatibility to support microbial activity
3. Chemical stability and resistance to corrosion
4. Large surface area to maximize interaction with microbes
5. Sufficient mechanical strength and durability (Logan, et al., 2006).

Different types of anode materials have been used in microbial fuel cells, each with distinct advantages and disadvantages. One commonly used material is carbon cloth, which offers large relative porosity, a high specific area, and strong mechanical properties. It is also easy to connect for wiring purposes. However, it is relatively expensive, which may limit its application in large-scale systems (Ishii, Watanabe, Yabuki, Logan, & Sekiguchi, 2008). Another anode material is carbon paper, which is relatively porous and easy to work with. However, its main drawbacks include fragility and high cost, making it less durable in long-term applications (Kim, Jung, Regan, & Logan, 2007). Similarly, carbon felt is known for its high porosity and excellent electrical conductivity, making it an efficient choice for electron transfer. It is also relatively low-cost and has a wide surface area, which is beneficial for microbial attachment. However, its large resistance can hinder electron flow efficiency. (Kim, et al., 2002) (Do, et al., 2018)

Reticulated vitreous carbon (RVC) is another material used in MFCs, offering high electrical conductivity. However, it has notable disadvantages, including considerable resistance and fragility, which may affect its overall stability in microbial environments (He, et al., 2015). Stainless steel, available in various forms such as plates, mesh, foam, or scrubbers, is valued for its high conductivity, low cost, and easy accessibility. Despite these advantages, it has some challenges, including a low surface area and potential biocompatibility issues. (Do, et al., 2018)

Graphite rods and plates are also widely used due to their good electrical conductivity and chemical stability. These materials are relatively inexpensive and easy to access. However, corrosion can be a concern, and increasing the surface area for microbial attachment can be challenging. (Liu, Cheng, & Logan, 2005), (Do, et al., 2018)

Lastly, the graphite fiber brush has gained popularity as an anode material because of its high specific area, ease of construction, and accessibility. These characteristics make it an attractive option for MFC applications. However, clogging can be a significant issue, potentially affecting performance over time. (Ahn & Logan, 2010)

In summary, the selection of anode materials in MFCs depends on factors such as conductivity, porosity, durability, cost, and ease of use. Each material has advantages and drawbacks, which must be carefully considered when designing MFC systems. (Do, et al., 2018)

2.3.1.2 Cathode Material

The cathode electrode is a crucial component of microbial fuel cells, as it plays a significant role in determining the power output of the system (Saravanana, Senthil, Srinivasand, Jeevananthame, & Kamaleshe, 2022). Cathodes have a high redox potential, allowing them to efficiently capture protons. During operation, electrons travel from the anode to the cathode through an external circuit, while protons migrate through the proton exchange membrane. At the cathode electrode, these electrons and protons combine with oxygen, forming water molecules. This oxygen reduction reaction is facilitated by both microbial activity and abiotic catalysts. (Saravanana, Senthil, Srinivasand, Jeevananthame, & Kamaleshe, 2022), (Hamedani, Abasalt, & Talebi, 2024)

Many materials commonly used as anodes can also function as cathodes. Carbon-based materials, such as carbon cloth, carbon fiber, granular graphite, and carbon paper, are widely used for this purpose (Logan, et al., 2006). While platinum (Pt) electrodes are considered the most efficient cathodes due to their excellent catalytic properties, their high cost and susceptibility to degradation from toxic compounds in microbial environments limit their widespread application in air-exposed biocathodes. (Clauwaert, et al., 2007).

To address these challenges and reduce the overall cost of MFCs, researchers are exploring alternative, cost-effective cathode materials to replace Pt electrodes. Promising alternatives include activated carbon, carbon nanotubes (CNTs), and copper (Cu). Among these, CNTs are particularly effective in enhancing the power density of MFCs by increasing the available surface area, thereby improving oxygen reduction efficiency in the cathode chamber (Gorbunov, Jost, Pompe, & Graff, 2002), (Mahmoudi, Alireza Mousavi, & Darvishi, 2024). Ongoing advancements in cathode material development aim to optimize MFC performance while making the technology more economically viable for large-scale applications. (Mahmoudi, Alireza Mousavi, & Darvishi, 2024)

2.3.2 Different Configuration of MFCs

Proper configuration is one of the most crucial factors influencing the performance of microbial fuel cells. Over the years, researchers have explored various design modifications to enhance the efficiency and functionality of MFC technology. MFC reactors' size, shape, and structure vary significantly, and there is currently no standardized design. Instead, the choice of configuration largely depends on the designer's specific application and objectives.

MFCs have been utilized for sludge stabilization in different configurations, including single-chamber systems (Liu, Cheng, & Logan, 2004) and double- or multi-chamber designs (Samsudeen, Radhakrishnan, & Matheswaran, 2015). In the following sections, several studies focused on bioenergy recovery and sludge purification using MFCs with various configurations are reviewed, highlighting advancements in reactor design and their impact on performance.

2.3.2.1 Single Chamber

Single-chamber microbial fuel cells are among the most promising, simple, and cost-effective designs, particularly for scaling up real-world applications. Figure 4 shows a general single chamber MFC setup. Compared to dual-chamber MFCs, single-chamber MFCs eliminate the need for a separate cathode chamber and different electrolytes for the anode and cathode, making them more efficient and easier to operate (Wang, et al., 2018). The standard design consists of an anode compartment, with the anode and cathode electrodes positioned on opposite sides, and in some cases, a proton exchange membrane. However, many modern single-chamber MFCs opt for air-cathode configurations without PEM, offering lower cost, more straightforward construction, and higher power density. (Fan, Hu, & Liu, 2007).

One of the major advantages of single-chamber MFCs is that they rely on oxygen as the terminal electron acceptor, benefiting from its natural abundance, high redox potential, and stability (Silveira , de Aquino Neto, & Schneedorf, 2020). Additional advantages include lower energy consumption, reduced internal resistance, compact size (leading to higher volumetric power density), no aeration requirements, and greater design flexibility (Zhang, Wang, Fu, & Zhang, 2020). However, removing PEM can lead to oxygen diffusion into the anode chamber, lowering coulombic efficiency (CE). Nevertheless, this issue is partially mitigated by aerobic biofilm formation on the inner surface of the cathode, which helps consume any diffused oxygen and maintain anaerobic conditions in the anode chamber (Liu, Cheng, & Logan, 2004).

Despite these benefits, single-chamber MFCs present some challenges, including liquid leakage, evaporation, and excessive oxygen diffusion. To address this, Cheng et al. developed polytetrafluoroethylene (PTFE) diffusion layers, which improved oxygen diffusion control and prevented liquid leakage, ultimately enhancing both coulombic efficiency and power output (Cheng, Liu, & Logan, 2006). Additionally, the distance between the anode and cathode must be carefully controlled (typically 1–2 cm) to prevent excessive oxygen exposure, which can negatively impact anaerobic bacterial activity and increase the risk of short circuits (Fan, Hu, & Liu, 2007) (Mahmoudi, Alireza Mousavi, & Darvishi, 2024).

A variety of electrode materials have been explored to further optimize single-chamber MFCs. Typically, porous carbon paper is used as the anode, while carbon cloth with a platinum catalyst serves as the cathode. However, given the high cost of platinum, researchers are investigating alternative materials to make MFCs more economically viable. Winfield et al. (Winfield, Gajda, Greenman, & Ieropoulos, 2016) highlighted ceramics as a cost-effective alternative due to their ion exchange capabilities. Ceramics not only provide a stable environment for microbial growth but also improve energy production efficiency by acting as a size-selective separator, preventing pH fluctuations in the anolyte. (Hamedani, Abasalt, & Talebi, 2024)

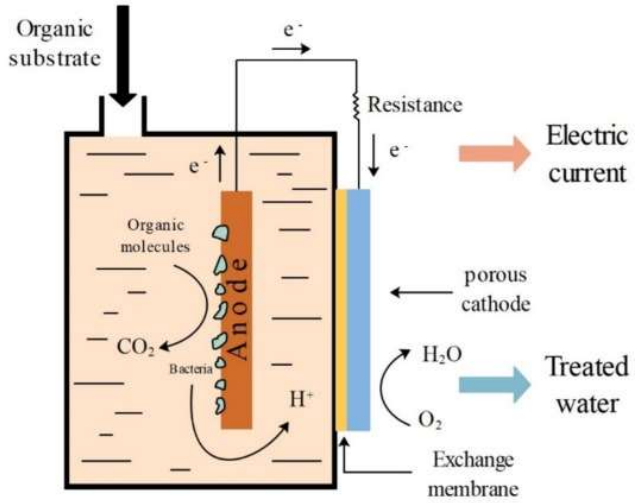


Figure 4. Schematic Diagram of the Single MFC (Hamedani, Abasalt, & Talebi, 2024)

Single-chamber microbial fuel cells have been extensively utilized for treating various types of sewage sludge, demonstrating effective organic matter removal and notable energy recovery potential. The performance of MFCs is largely influenced by the type of substrate used, leading to

variations in total chemical oxygen demand (TCOD), soluble chemical oxygen demand (SCOD), total suspended solids (TSS), volatile suspended solids (VSS), pH levels, removal efficiencies, voltage output, and power density. (Zhang, Chen, Zhou, Yuan, & Yuan, 2012)

In the case of primary sludge, TCOD concentrations ranged between 11,200 and 14,200 mg/L, achieving TCOD removal efficiencies of 69.8 ± 24.1%. Additionally, the removal efficiencies for TSS and VSS were 63.7 ± 19.6% and 68.4 ± 17.9%, respectively. The voltage output in these systems was 0.2 V, with a high-power density of 8,500 mW/m^3 (Ge, Zhang, Grimaud, Hurst, & He, 2013). In contrast, digested sludge showed lower TCOD removal efficiency (36.2 ± 24.4%), though it exhibited a higher voltage output of 0.62 V and a power density of 115 mW/m^2 (Zhang, Chen, Zhou, Yuan, & Yuan, 2012).

For raw sludge, removal efficiencies varied considerably across studies. One study on raw sludge with a TCOD of 49,700 mg/L reported a TCOD removal rate of 78.1 ± 0.2%, alongside a voltage output of 0.36 V and a power density of 190 ± 5 mW/m^2 (Zhang, Olias, Kongjan, & Angelidaki, 2011). Another study investigating raw sludge with a TCOD of 36,500 mg/L reported lower removal efficiencies, ranging from 42% to 20%, with power densities between 73 ± 5 mW/m^2 and 4 ± 0.5 mW/m^2, depending on the operational conditions. (Ge, Zhang, Grimaud, Hurst, & He, 2013).

The treatment of waste-activated sludge (WAS) also displayed notable variations in performance. One study reported a TCOD of 8,906 ± 1,225 mg/L, achieving a TCOD removal efficiency of 14.6 ± 0.9%. The removal efficiencies for TSS and VSS were 17.7 ± 1.4% and 18.8 ± 2.7%, respectively, with a voltage output of 0.60 V and a power density of 0.91 W/m^3 (Suor, et al., 2014). Another study using highly concentrated WAS (TCOD: 174.8 g/kg) reported an exceptionally high-power density of 1,036 ± 59 W/m^3, indicating significant energy recovery potential (Gulamhussein & Randall, 2020).

Overall, single-chamber MFCs provide several advantages over dual-chamber designs, making them a preferred choice for bioenergy recovery and wastewater treatment applications. Their performance varies depending on sludge type and operating conditions, with higher TCOD removal rates generally observed in primary and raw sludge, while WAS exhibits lower organic removal but higher power densities. These results underscore the feasibility of using single-chamber MFCs for simultaneous waste treatment and bioelectricity generation, contributing to sustainable wastewater

management. However, challenges related to oxygen diffusion and system stability need to be addressed through further research to optimize efficiency and scalability (Hamedani, Abasalt, & Talebi, 2024).

2.3.2.2 Dual Chamber

Dual-chamber microbial fuel cells are a widely used configuration that consists of two separate chambers—anodic and cathodic—which are connected by either a PEM or a salt bridge to facilitate ion transfer shown in Figure 5. (Yaqoob, et al., 2020) (Munoz-Cupa, Hu, Xu, & Bassi, 2021). Electrons generated in the anaerobic anode chamber are transferred through an external circuit, while protons migrate to the cathode, where they combine with oxygen to produce water (Hoanga, et al., 2022). This design allows for higher power densities compared to single-chamber MFCs, as the separation of microbial metabolic reactions and proton oxidation enhances efficiency (Behera, Kumari, Shankar, & Mondal, 2018).

Various electrode materials are commonly used in dual-chamber MFCs, including copper, carbon paper, carbon cloth, graphite, stainless steel mesh, and carbon or graphite brushes. These systems can function in either continuous or batch mode, making them suitable for both wastewater treatment and bioelectricity generation. However, their complex structure makes them challenging to scale up, and H-shaped MFCs, in particular, suffer from high internal resistance, which limits power generation efficiency (Jung & Pandir, 2019).

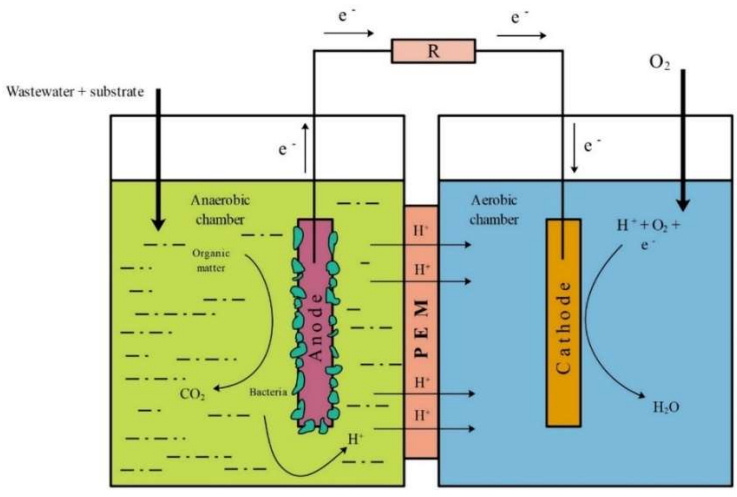


Figure 5. Schematic Diagram of the Dual-Chamber MFC (Hoanga, et al., 2022)

Dual-chamber microbial fuel cells (MFCs) have demonstrated significant potential for sewage sludge treatment, effectively achieving organic matter removal and bioelectricity generation. The performance of these systems depends on the substrate type, influencing TCOD, SCOD, TSS, VSS, pH levels, voltage output, and power density. (Xiao, Yang, & Liu, 2011)

The effectiveness of organic matter removal varies across different sludge types. Raw sludge exhibited TCOD removal rates between 19.2% and 40%, while secondary sludge and waste-activated sludge (WAS) showed higher TSS and VSS removal efficiencies, reaching 62% and 46%, respectively. Additionally, combining anaerobic sludge with raw sludge enhanced TSS removal (49.68%) and VSS removal (37.17%). Various pre-treatment methods, including ozonation and microwave treatment, further improved sludge degradation, achieving up to 55% removal efficiencies. (Jiang , Zhao, Wei, & Wang, 2010) (Xiao, Han, Liu, & Liu, 2014)

The power generation potential of dual-chamber MFCs also varies depending on the sludge type and operating conditions. The highest power density (0.599–0.853 kW/m^3) was recorded for anaerobic sludge mixed with raw sludge. Sterilized and pretreated sludge yielded power densities ranging from 25.5 to 40.8 mW/m^2, while secondary sludge achieved 46.8 to 55.88 mW/m^2. Depending on treatment conditions, waste-activated sludge exhibited power outputs between 1.24 W/m^3 and 24 W/m^3. The voltage output varied between 0.3 V and 0.74 V, with raw sludge producing the highest voltage. (Geng, et al., 2020)

Table 2. Sewage sludge treatment using dual-chamber MFCs (Mahmoudi, Alireza Mousavi, & Darvishi, 2024)

Substrate Type	TCOD (mg/L)	SCOD (mg/L)	TSS (g/L)	VSS (g/L)	pH	% Removal TCOD	% Removal TSS	% Removal VSS	Voltage (V)	Power Density
Aerobic sludge digestion	6900 ± 50	365 ± 10	3.40	1.83	7.1 ± 0.1	-	34.5	38.7	0.41–0.43	36.8–40.1 mW/m^2
Sterilized sludge	11,380 ± 100	27.7 ± 2	2.60	1.92	6.9 ± 0.1	-	32.8	34.6	0.34–0.36	25.5–28.6 mW/m^2

Base pretreated sludge	11,380 ± 100	27.7 ± 2	2.60	1.92	6.9 ± 0.1	-	25.5	26.7	0.41–0.43	37.1–40.8 mW/m²
Raw sludge	11,380 ± 100	27.7 ± 2	2.60	1.92	6.9 ± 0.1	-	25.1	22.8	0.30–0.32	19.9–22.6 mW/m²
Raw sludge	12,300 ± 115	220 ± 4	9430 ± 88 (TS)	7760 ± 82 (VS)	6.9	19.2 ± 0.2	-	-	0.74 ± 0.01	9.1 ± 0.1 W/m³
Raw sludge + Anaerobic sludge	9720 ± 110	225 ± 21	13.88 ± 0.24	13.88 ± 0.24	7.71 ± 0.1	-	49.68 ± 0.10	37.17 ± 0.14	0.505–0.600	0.599–0.853 kW/m³
Secondary sludge	10,560 ± 110	3190 ± 20	11.45 ± 0.18	11.45 ± 0.18	12.3 ± 0.1	-	-	-	0.47–0.52	46.80–55.88 mW/m²
Raw sludge	10,850	281	-	-	6.8–7.0	46.4	-	-	0.687	8.5 W/m³
Secondary excess sludge	2560 ± 186	128 ± 22	7.35 ± 0.527	6.2 ± 0.371	6.95 ± 0.2	-	-	-	-	27.65 W/m³
WAS	8790 ± 80	70 ± 4	-	4.9 ± 0.3	-	49 ± 3.4	-	-	0.605	1.24 W/m³
Raw sludge	~1700	~70	-	-	-	-	40	-	0.105	10 ± 2 mW/m²
2h ozonation	~1500	~230	-	-	-	-	55	-	0.154	21 mW/m²
4h ozonation	~1420	~250	-	-	-	-	55	-	0.125	10 mW/m²
Microwave	~1400	~570	-	-	-	-	55	-	0.170	42 mW/m²
ASS	10,622 ± 940	519 ± 28	11.4 ± 0.9	6.4 ± 0.8	-	62	46	34	0.67	38.1 W/m³

WAS 1	8180 ± 1122	431 ± 44	9.3 ± 0.5	5.6 ± 0.6	-	28	26	18	-	11.7 W/m³
WAS 2	9034 ± 1655	464 ± 131	8.5 ± 0.8	6.0 ± 0.7	-	29	35	27	0.63	24 W/m³

Despite their promising potential, dual-chamber microbial fuel cells face several challenges that hinder their large-scale application. Issues such as high internal resistance, pH imbalances in the cathode, structural complexity, and high operational costs reduce overall efficiency and increase maintenance requirements. Additionally, the intricate design of dual-chamber systems complicates their scalability and practical implementation in wastewater treatment. Another drawback of dual-chamber MFCs is the accumulation of cationic species (Na^+, K^+, NH_4^+, Ca^{2+}, Mg^{2+}) in the cathode chamber, leading to increased pH levels and reduced MFC performance (Rozendal, Hamelers, & Buisman, 2006). Maintaining anaerobic conditions in the anode and adequate oxygen supply in the cathode is essential for sustained power output. Additionally, continuous oxidation at the cathode is required for optimal operation, posing a technical challenge. (Mahmoudi, Alireza Mousavi, & Darvishi, 2024)

To enhance their feasibility for real-world applications, further research is needed to optimize reactor configurations, improve power output, enhance power density, and develop cost-effective waste disposal strategies. Addressing these challenges will make MFC technology more efficient, practical, and economically viable for sustainable wastewater treatment and bioelectricity generation. (Zhang, Olias, Kongjan, & Angelidaki, 2011)

2.3.2.3 Stacked MFC

To improve power production and COD removal efficiency, researchers have explored stacked and multi-chamber microbial fuel cells. Stacked MFCs are designed by connecting multiple units in series or parallel, shown in Figure 6, enhancing voltage or current output. Studies indicate that parallel-connected MFCs exhibit superior efficiency and COD removal due to a higher bio-electrochemical reaction rate compared to series configurations (Lee, Ban, Oh, Park, & Choi, 2016). Aelterman et al. (Aelterman, Rabaey, Pham, Boon, & Verstraete, 2006) demonstrated that six integrated MFCs using graphite granules as electrodes and Ultrex CMI7000 PEM as a separator achieved high energy density in both parallel and series arrangements. (Mahmoudi, Alireza Mousavi, & Darvishi, 2024)

Similarly, multi-chamber MFCs have been investigated for their potential to improve pollutant removal and power generation. Researchers have achieved significant COD removal and enhanced power output by linking individual unit chambers in series or parallel. Liang et al. (Liang, et al., 2018) reported 90% COD removal with a power density of 125 W/m³ in a stacked MFC system. Another study introduced a multi-anode, single-cathode microbial fuel cell, which achieved a power output of 24 W/m³ under optimal conditions (Kim , et al., 2011). Further advancements were made by incorporating cassette electrodes, resulting in a maximum power density of 150 W/m³ and 20% Coulombic efficiency (Miyahara, Hashimoto, & Watanabe, 2013). Additionally, research demonstrated an even higher COD removal efficiency of 97%, along with a power output of 50.9 W/m³ in a stacked MFC system (Wu, et al., 2016).

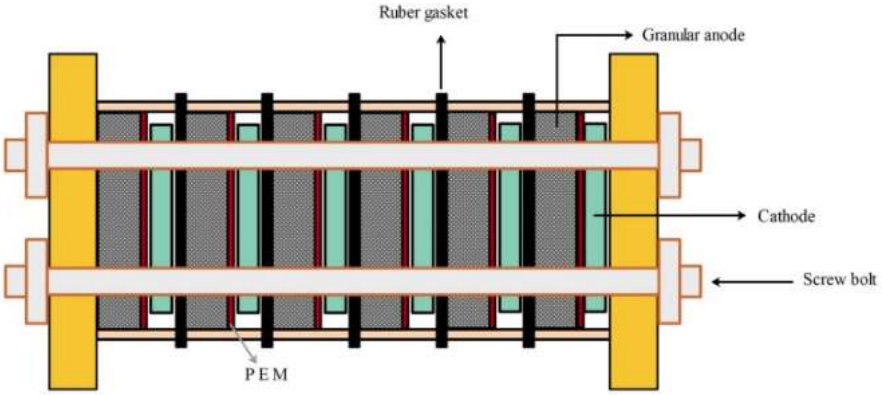


Figure 6. Schematic Diagram of the Stacked MFC (Hamedani, Abasalt, & Talebi, 2024)

However, stacked MFCs present several challenges, including charge inversion, voltage reversal, and biofilm degradation when organic substrates fail to sustain the increasing current load (Slate, Whitehead, Brownson, & Banks, 2019). The use of bipolar electrodes has been proposed as a potential solution to minimize energy losses due to resistance while also simplifying assembly. Studies have shown that Coulombic efficiency in individual MFC units remains unaffected mainly by stacking configurations, while stacking significantly enhances overall power output, making the system functionally comparable to conventional power sources (Yang, et al., 2016).

Regarding fluidic connectivity, series and parallel configurations offer distinct advantages. While non-fluidic stacked MFCs can be connected in either series or parallel, fluidically connected MFCs can only be arranged in parallel to prevent short-circuiting (Fraiwan & Choi, 2016). Comparative studies have indicated that parallel-configured MFCs achieve higher Coulombic

efficiency—up to six times greater than series-connected MFCs—while also providing better protection against short circuits, making them more suitable for high bio-electrochemical rate reactions (Aelterman, Rabaey, Pham, Boon, & Verstraete, 2006).

Despite these advantages, high manufacturing costs remain a significant limitation of stacked MFCs due to the requirement for multiple fluid streams and additional electrical connections (Dun, Hu, Bi, & Cao, 2009). Nevertheless, stacked and multi-chamber MFCs hold significant potential as high-efficiency power sources for sustainable bioelectricity generation and wastewater treatment, provided that scalability and cost-effectiveness are further improved.

2.4 Operational Factors that Influence MFCs Performance

2.4.1 Substrate

In microbial fuel cells, the substrate is one of the most fundamental biological factors influencing electricity generation (Pant, Van Bogaert, Diels, & Vanbroekhoven, 2010). Within biological processes, substrates serve as both a carbon source (nutrient) and an energy provider for microbial metabolism (Liu, Liu, Zhang, & Su, 2009). Additionally, the type of substrate affects the composition of the bacterial community in the anodic biofilm, which in turn impacts MFC performance, including coulombic efficiency (CE) and power density (PD) (Zhang, Min, Huang, & Angelidaki, 2011)

A wide range of substrates for power generation in MFCs have been investigated. These include fermentable substrates such as xylose, glucose, and sucrose, as well as non-fermentable substrates like butyrate and acetate (Zhang, Min, Huang, & Angelidaki, 2011). More complex substrates, containing both fermentable and non-fermentable components, have also been utilized, including domestic wastewater, paper recycling wastewater, food processing wastewater, aquatic sediment organic matter, and corn stover hydrolysate (Pant, Van Bogaert, Diels, & Vanbroekhoven, 2010). A comprehensive list of substrates used in MFC studies is provided in Table 3. (Divya Priya & Pydi Setty, 2019), (Mahmoudi, Alireza Mousavi, & Darvishi, 2024)

Table 3. Electricity Generation Using Different Substrates in MFCs (Mahmoudi, Alireza Mousavi, & Darvishi, 2024)

Type of Substrate	Type of MFC	Power Density (mW/m^3)	Current Density (mA/m^2)	Coulombic Efficiency (%)
Domestic waste water	Single Chamber	26	125	12
Palm oil effluent	Dual Chamber	45	190	0.8
Sodium acetate	Dual Chamber	38	130	47
Brewery wastewater	Single Chamber	–	669	2.5
Wastewater	Single Chamber	2400	–	60
Excess sludge	Single Chamber	40	–	–
Sewage sludge	Single Chamber	115	–	7.8
Sewage Sludge	Dual Chamber	843.5	828.5	3.07
Raw sludge	Dual Chamber	10	0.17	3.2
2h ozonation treated sludge	Dual Chamber	21	0.25	3.7
4h ozonation treated sludge	Dual Chamber	10	0.17	2.8
Microwave treated sludge	Dual Chamber	42	0.35	6.3

Mixture of WAS to Potato = 1:4	Dual Chamber	6.8	193.1	31.1

Several studies have demonstrated the effectiveness of different substrates in improving MFC efficiency. Vegetable waste composites have been used in mediator-less single-chamber MFCs, achieving a power density of 57 mW/m^2 and 62% COD removal efficiency (Venkata Mohan, Mohanakrishna, & Sarma, 2010). Other research has reported higher power densities when using glucose (286 mW/m^2) and acetate (212 mW/m^2) as substrates with ferricyanide as the catholyte (Min & Logan, 2004). Additionally, using acetate and glucose has led to power densities of 90 and 66 W/m^3, respectively (Rabaey, Clauwaert, Aelterman, & Verstraete, 2005).

Experiments investigating substrate efficiency in various MFC configurations have considered parameters such as COD removal, coulombic efficiency, and electricity production (Molognoni, et al., 2014). Agro-food waste has shown promising results, but using mixed substrates may increase microbial diversity and system complexity (Capodaglio, Cecconet, & Molognoni, 2017). However, highly fermentable substrates can reduce coulombic efficiency and promote methanogenesis, leading to energy loss (Pinto, Srinivasan, Manuel, & Tartakovsky, 2010). Additionally, substrate concentration is a key factor in MFC optimization, as it influences microbial growth and electron transfer rates. While researchers continue to explore the use of pure and mixed cultures for performance enhancement, wastewater remains a micronutrient-rich and carbon-abundant source for microbial metabolism. Synthetic wastewater with controlled nutrient concentrations is being investigated to achieve more stable and efficient MFC operation (Ullah & Zeshan, 2020).

Among the various substrates, sewage sludge has gained increasing attention due to its potential for energy recovery. When sewage sludge is used as a substrate, the degradation of organic matter leads to the release of intracellular compounds, thereby increasing the solubility of COD in the liquid phase (Kiani Raad, Farrokhi, Alireza Mousavi, Darvishi, & Mahmoudi, 2020). The higher COD concentration enhances microbial activity, which subsequently increases current generation in the MFC (Raad, Farrokhi, Mousavi, Darvishi, & Mahmoudi, 2020) (del Campo, Lobato, Cañizares, Rodrigo, & Fernandez Morales, 2013). In this process, COD particles are first hydrolyzed by microbial activity into soluble COD, which is then consumed by microorganisms, converting it into electricity and metabolic by-products.

The choice of substrate plays a critical role in optimizing MFC performance, as it directly affects microbial activity, biofilm formation, and electron transfer efficiency. Understanding how different substrates influence MFC output is essential for enhancing power generation and improving wastewater treatment efficiency in future applications. (Mahmoudi, Alireza Mousavi, & Darvishi, 2024)

2.4.2 PH

pH is a crucial operational parameter influencing both wastewater treatment efficiency and power generation in MFCs (He, Huang, Manohar, & Mansfeld, 2008). The electrolyte pH in the anode chamber affects microbial metabolism, altering the concentration of protons (H^+) and electrons (e^-), which impacts ion balance, membrane potential, and biofilm formation (Tremouli, Martinos, & Lyberatos, 2017). A higher pH difference between the anode and cathode enhances current and voltage output. Studies indicate that bacteria require a near-neutral pH for optimal growth, with maximum current generation observed between pH 7 and 8, while both acidic and alkaline conditions reduce power production (Sajana, Ghangrekar, & Mitra, 2013).

He et al. (He, Huang, Manohar, & Mansfeld, 2008) demonstrated that varying the anode pH between 5 and 10 significantly influences both anodic and cathodic reactions, with optimal MFC performance occurring within the pH range of 8–10. However, at near-neutral pH, the lower proton concentration increases internal resistance compared to chemical fuel cells using acidic electrolytes (Behera & Ghangrekar, 2009). Ren et al. (Ren, Ward, & Regan, 2007) reported that in dual-chamber MFCs, power generation declines at a final pH of 5.2 due to acidic fermentation byproducts but improves when pH is adjusted to 7. Similarly, pH regulation in sewage sludge-based MFCs can enhance voltage and current production (Vologni, Kakarla, Angelidaki, & Min, 2013).

The influence of substrate type was also significant, as different microbial consortia demonstrated varied power densities. Acidiphilium cryptum at pH 4 yielded a power density of 12.7 mW/m^2, while Geobacter sulfurreducens (pH 7) and Rhodoferrac ferrireducens (pH 7) generated 14.7 mW/m^2 and 33 mW/m^2, respectively. P. vulgaris, another microbial strain at pH 7, exhibited a power density of 32 mW/m^2, suggesting that bacterial metabolism plays a crucial role in energy conversion efficiency. The findings indicate that higher pH levels (8–10) generally enhance power generation, particularly in single-chamber MFCs, whereas power output is significantly lower in acidic conditions. Additionally, wastewater-based substrates demonstrated varying performance levels,

reinforcing the importance of substrate selection in MFC optimization (Malekmohammadi & Ahmad Mirbagheri, 2021).

Furthermore, pH influences the electron and proton production mechanisms, impacting electron transfer and coulombic efficiency. Higher pH enhances current density and COD removal. (Behera, Jana, More, & Ghangrekar, 2010), whereas lower pH can improve organic matter degradation due to methane-producing microorganisms. In dual-chamber MFCs, both excessively high and low pH levels negatively affect performance. (He, Huang, Manohar, & Mansfeld, 2008), while higher pH improves single-chamber MFCs.

Microbial activity also alters pH over time. If the initial pH is below 8, the output pH increases due to slower proton exchange across the membrane than proton production, causing proton accumulation in the anode and a subsequent pH drop (Cheng, Liu, & Logan, 2006). Conversely, if the initial pH exceeds 8, microbial metabolism produces weak acids, leading to a gradual decline of the pH as microbial activity remains high (He, Huang, Manohar, & Mansfeld, 2008). Therefore, maintaining an optimal pH balance is essential for improving MFC performance and ensuring efficient microbial activity.

2.4.3 Temperature

Temperature plays a significant role in MFC performance by influencing bacterial kinetics, proton mass transfer, and oxygen reaction rates catalyzed by platinum on the cathode (Liu, Cheng, & Logan, 2005). Most MFC studies are conducted at room temperature or higher (20–35°C), as lower temperatures (4–30°C) require longer startup times for stable power generation. Below 15°C, MFCs struggle to generate appreciable power even after one month of operation. However, if an MFC is initially started at 30°C, reproducible power cycles can be maintained even at 4°C and 10°C (Cheng, Liu, & Logan, 2006). Additionally, studies have shown that power density doubles at 40°C compared to 30°C, but it decreases sharply—by fourfold—when the temperature increases to 50°C (Adelaja, Keshavarz, & Kyazze, 2015).

Microbial decomposition processes are also temperature-dependent, with mesophilic microorganisms operating optimally between 35 and 40°C (Bohn, Björnsson, & Mattiasson, 2007). Outside this range, microbial activity declines, affecting overall system efficiency. Higher temperatures generally enhance MFC power production, particularly in wastewater treatment applications (Ahn & Logan, 2010). While MFCs perform better at elevated temperatures, they exhibit

greater resilience than conventional anaerobic systems in colder environments (4–15°C), maintaining reasonable efficiency (Bohn, Björnsson, & Mattiasson, 2007). This makes MFCs a viable option for wastewater treatment in cold regions with low urban wastewater flow rates (Krieg, Mayer, Sell, & Holtmann, 2019).

Electroactive anodic consortia in MFCs enable COD removal and electricity generation even at 4°C (Larrosa-Guerrero, et al., 2010). Li et al. (Li L. H., Sun,, Yuan, Kong, & Li, 2013) examined power generation across 10–55°C, finding that current density increased up to 33°C before declining at higher temperatures, with no stable power output between 43 and 55°C. Similarly, Liu et al. (Liu, Climent, Berna, & Feliu, 2011) observed an optimal temperature of 45°C. These findings highlight the importance of temperature optimization for maximizing MFC efficiency while maintaining system stability across different environmental conditions.

2.4.4 External Resistance

External resistance is a critical factor in microbial fuel cells performance, impacting power generation, coulombic efficiency, and system stability. While electroactive bacteria can adapt to varying resistances, selecting an optimal external resistance minimizes energy losses and improves overall efficiency (Clauwaert, et al., 2008). Properly chosen external resistance not only boosts output power and coulombic efficiency but also suppresses methane production, ensuring more electrons are directed toward electricity generation rather than methanogenesis (Pinto, Srinivasan, Guiot, & Tartakovsky, 2011). Additionally, external resistance regulates current output and cell voltage, enabling better control over system operations. (Malekmohammadi & Ahmad Mirbagheri, 2021).

Like other power sources, MFCs aim to maximize power output, which depends on the voltage and current density balance. Lowering external resistance reduces voltage but increases current density, necessitating an optimized trade-off to achieve peak power density. Maximum power density occurs when internal and external resistances are equal, a condition that can be identified using polarization curves (Woodward, Perrier, Srinivasan, Pinto, & Tartakovsky, 2010). However, internal resistance varies with factors such as pH, temperature, and wastewater composition, requiring adjustments to external resistance for optimal performance. (Pinto, Srinivasan, Manuel, & Tartakovsky, 2010), (Corbella & Puigagut, 2018)

Research shows that reducing external resistance enhances both pollutant removal efficiency and power generation. For instance, Liu et al. (Liu, Cheng, & Logan, 2005) found that lower external

resistance correlates with higher maximum power output. Aelterman et al. (Aelterman, Versichele, Marzorati, Boon, & Verstraete, 2008) observed that decreasing resistance from 50 Ω to 25 Ω and further to 10.5 Ω increased current density and power output. Although COD removal efficiency remains high in MFCs, it improves only marginally with decreasing resistance (Ahn & Logan, 2012).

External resistance also significantly affects MFC startup time. Higher resistance accelerates microbial growth and shortens startup time, while lower resistance delays biofilm formation. For example, increasing external resistance from 10 Ω to 1,000 Ω reduced startup time from 3 days to 0.6 days, indicating faster microbial colonization at higher resistances (Zhang, et al., 2017). However, once the system is operational, reducing resistance enhances current generation (Katuri, Scott, Head, Picioreanu, & Curtis, 2011).

Very low external resistances ($\leqslant$10 Ω) can hinder startup by slowing microbial growth, resulting in thin and compact biofilms, whereas higher resistance promotes greater biomass yield (Zhang, et al., 2017) (Katuri, Scott, Head, Picioreanu, & Curtis, 2011). Therefore, a gradual reduction from high to low resistance is recommended to achieve optimal power generation (Ahn & Logan, 2012). Sudden changes in resistance from the adaptation level can reduce efficiency and power output, leading to performance variability.

External resistance also influences microbial community structure and metabolic diversity (Suzuki, et al., 2018). Since anodic biofilm formation depends on external resistance, changes in resistance alter microbial populations and energy transfer mechanisms. Studies suggest that low external resistance accelerates energy output, active biomass formation, and maximum power density but reduces the voltage evolution rate of microbial populations (Zhang, et al., 2017).

In summary, external resistance is a vital parameter for optimizing MFCs in both power generation and wastewater treatment. Balancing resistance with system conditions enhances efficiency, accelerates startup, and influences microbial biofilm development. A stepwise reduction from high to low resistance is recommended for stable operation, ensuring effective pollutant removal and maximum power output.

2.4.5 Flow Rate and Hydraulic Retention Time

Hydraulic Retention Time (HRT) is a crucial parameter in wastewater treatment systems, including MFCs, as it directly influences system design, operation, and overall cost (Sobieszuk, Zamojska-

Jaroszewicz, & Makowski, 2017). HRT represents the average time wastewater remains in the reactor and is determined by the ratio of reactor volume to influent flow rate (Xu, Li, Tang, & Hu, 2015). A longer HRT typically leads to higher treatment efficiency but increases operational costs, making it essential to balance retention time with economic feasibility. For MFCs to be competitive with conventional treatment processes, their HRT should be optimized to align with traditional systems (Kim, Yang, & Logan, 2015).

Increasing HRT enhances chemical oxygen demand removal efficiency and coulombic efficiency (CE) due to the prolonged interaction between microbes and organic matter (Sobieszuk, Zamojska-Jaroszewicz, & Makowski, 2017). Longer retention times also improve the removal of pollutants such as total nitrogen (TN), ammonium, nitrate, and pharmaceutical contaminants (Hang, Chang, Chao, Jane, & Chang, 2018). However, in continuous-flow MFCs, HRT is even more critical in stabilizing system performance (Sobieszuk, Zamojska-Jaroszewicz, & Makowski, 2017).

While longer HRT enhances pollutant removal, it can negatively impact electricity generation. Studies show that increasing HRT from 8 to 16 hours reduces the output voltage from 0.21 V to 0.13 V due to a decline in the average COD concentration in the reactor (Ahn & Logan, 2012) (Ma, Jiang, Lay, & Zhou, 2016). Microbial diversity also increases with longer HRT, which can influence system performance. Since HRT and flow rate are inversely related, a higher flow rate leads to lower retention time, increasing dilution and reducing electricity generation (You, Greenman, & Leropoulos, 2018).

As HRT is directly proportional to removal efficiency but inversely related to current density, an optimal balance must be established to achieve both effective treatment and power generation. Initial microbial conditions significantly affect the ideal HRT, and variations in retention time often stem from microbial community differences rather than reactor configurations. Given that MFCs are dynamic systems, the optimal HRT may change over time (Sobieszuk, Zamojska-Jaroszewicz, & Makowski, 2017). Reported optimal HRT values in different studies vary, with 15.5 hours (Li, Yao, Kong, & Liu, 2008), 20 hours (Huang, Zeng, & Angelidaki, 2008), 11.3 hours (Liu H. , Cheng, Huang, & Logan, 2007), and 24 hours (Haavisto, Kokko, Lay, & Puhakka, 2017) being identified as ideal conditions. Ultimately, optimizing HRT is crucial for maximizing both wastewater treatment efficiency and energy production, ensuring that MFCs remain practical and competitive alternatives in sustainable wastewater treatment applications.

2.5 Applications of MFCs in Different Industries

Microbial Fuel Cells have emerged as a promising technology for simultaneously treating various industrial wastewater and resource recovery. This chapter overviews MFC applications across different industries, summarizing key parameters such as waste pollutants, microorganisms used, electrode materials, power generation, and resources recovered.

2.5.1 Agro Industry

MFCs have been widely applied in the agro-industry to treat different types of agricultural waste. Various organic-rich waste streams have been explored for bioelectricity generation, COD removal, and valuable resource recovery. Food crop waste containing wheat straw, corn straw, and rice straw has been treated using Cellulomonas species with carbon cloth electrodes, generating 123 mW/m^2 and recovering bioelectricity, cellulose, hemicellulose, and energy (Roy, et al., 2023) (Pandit, et al., 2021). Winery and brewery wastewater has been processed using MFCs with titanium anodes and platinum-coated carbon cloth cathodes, leading to electricity generation and COD and BOD removal (Pandit, et al., 2021). Lignocellulosic wastes such as sugarcane bagasse, wood chips, and crop residues have been treated using lignolytic fungi, particularly white rot fungi, producing 8.78 W/m^3 and recovering lignin, cellulose, and hemicellulose (Kumar, et al., 2019). Mustard tuber and molasses wastewater treated with Brevibacillus borstelensis STR II using carbon cloth electrodes generated 246 mW/m^2 and facilitated COD removal and bioelectricity production (Pandit, et al., 2021). Palm oil mill effluent has been processed using carbon cloth electrodes, resulting in power outputs ranging from 45 to 304 mW/m^2, thereby aiding in COD removal and electricity generation energy (Roy, et al., 2023), (Pandit, et al., 2021).

2.5.2 Oil Industry

The oil industry generates various wastewater pollutants, including fats, grease, and polyphenols. MFCs have demonstrated potential in treating these effluents while producing electricity and valuable byproducts. Palm oil wastewater treated using Pseudomonas aeruginosa with polyacrylonitrile carbon electrodes produced 451.26 mW/m^2, facilitating electricity recovery (Nor, et al., 2015). Olive oil wastewater treated with Geobacter spp. in an MFC setup with platinum electrodes achieved a power output of 124.6 mW/m^2, enabling electricity generation (Sciarria, et al., 2013). Tannery wastewater containing heavy metals, tannins, oils, and grease has been processed using a mixture of bacterial species, including K. pneumoniae, Bacillus firmus, Pseudomonas, and K. quasipneumoniae, utilizing

carbon electrodes to generate 7371 mW/cm³ while producing electricity and biogas (Chauhan, Sharma, Varjani, Sindhu, & Bhargava, 2022). Additionally, wastewater containing spent engine oil treated using isolated cellulolytic bacteria and microalgae in an MFC with graphite electrodes generated between 16 and 34.88 mW/m², contributing to bioelectricity recovery (Verma, Singh, & Mishra, 2023).

2.5.3 Dairy Industry

MFCs in the dairy industry are primarily used for bioenergy generation, COD removal, and biofuel production. Dairy wastewater treated using Acutodesmus dimorphus produced 192–161 mW/m² while generating biodiesel and bioethanol (Chokshi, Pancha, Ghosh, & Mishra, 2016). Farm wastewater treated using Cyanophyta and Chlorophyta facilitated biodiesel production (Hena, Fatimah, & Tabassum, 2015). Dairy wastewater processed using Botryococcus braunii enabled the production of bioethanol and a reduction in COD, BOD, and TSS (Nurmayani, Sugiarti, & Putra, 2016). Fresh cheese wastewater treated with Chlorella pyrenoidosa facilitated electricity generation along with biomass and lipid productivity of 230–270 mg L^{-1} day^{-1} and 58.84–77.41 mg L^{-1} day^{-1}, respectively (Pandey, Srivastava, & Kumar, 2020).

2.5.4 Textile Industry

Textile wastewater is known for its high organic load and dye content. MFCs have been explored for both electricity generation and pollutant removal. Textile dye wastewater treated using bacterial community DC5 with anaerobic anodes and aerobic cathodes produced 197.94 mW/m², contributing to electricity generation and dye degradation (Patel, Bapodra, Madamwar, & Desai, 2021). Aromatic dye wastewater containing Congo red treated using anaerobic anodes and cathodic aeration resulted in electricity generation of 35.94 mW/m³ (Saket, Mittal, Bala, Joshi, & Yadav, 2022). Real dye textile wastewater treated using microalgae, specifically Chlorella vulgaris, produced 123.2 ± 27.5 mW/m³, enabling biodiesel and biomass production along with heavy metal recovery (Logroño, et al., 2017).

2.5.5 Wastewater Treatment Plants

MFCs have also been applied in municipal and industrial wastewater treatment plants to enhance energy recovery and nutrient removal. The Cronulla Wastewater Treatment Plant utilized anaerobic microorganisms with graphite felt anodes and carbon-fiber brush cathodes to enable phosphate and ammonium removal while generating electricity (Ye, et al., 2019). Sewage treatment using Geobacter

spp. in MFCs with graphite electrodes removed 80% of the organic load and produced 26 mW/m² of electricity (Liu, Cheng, & Logan, 2004).

Microbial Fuel Cells have demonstrated immense potential in wastewater treatment and resource recovery across various industries. These bioelectrochemical systems not only help in pollutant removal but also facilitate the production of bioelectricity, biofuels, and other valuable byproducts. However, further research is needed to optimize power generation, scalability, and cost-effectiveness for industrial-scale applications. (Jothinathan, Pandey, Choure, & Rathinavel, 2024)

2.6 Challenges and Research Scope

Microbial Fuel Cells represent a promising technology with the potential to significantly impact both sustainable energy production and wastewater treatment. As environmental concerns and the demand for renewable energy sources continue to rise, MFCs are gaining increasing attention for their ability to convert organic matter in wastewater into electricity while simultaneously reducing pollution. Their integration into broader environmental sustainability initiatives could enhance public perception and accelerate their adoption. However, despite these advantages, challenges such as scalability, operational efficiency, and cost-effectiveness must be addressed before MFCs can achieve widespread commercial success. The future of MFCs is expected to evolve with continuous advancements in biotechnology, materials science, and system optimization. Research efforts are currently focused on improving

MFC efficiency in electricity generation and wastewater treatment performance, enabling their application in industrial-scale wastewater management. Additionally, integrating MFCs into existing wastewater treatment infrastructure could enhance energy recovery from waste streams while reducing operational costs. The development of hybrid systems combining MFCs with other renewable energy sources, such as solar or wind, may further improve the stability and reliability of power output. (Kumar, Boda, Shah, Kumar, & Sarkar, 2024)

Given these potential benefits, this thesis aims to provide a numerical simulation framework to help wastewater treatment plants predict how various operating factors influence MFC performance. By developing a robust computational model, this research will enable plant operators to evaluate the optimal conditions for MFC operation before actual deployment. This predictive approach can help refine system configurations, enhance efficiency, and reduce the risks associated with scaling up MFC technology. Through numerical simulations, wastewater treatment facilities will

be better equipped to integrate MFCs into their operations, ensuring effective energy recovery and pollutant removal while minimizing costs and uncertainties associated with real-world implementation.

Chapter 3 Modelling for Steady-State

3.1 Method of Approach

To validate the microbial fuel cell (MFC) model developed in this study, experimental data from a previously conducted study were used as a reference. The referred experimental setup comprised an MFC device constructed from transparent polyacrylic plastic with anode and cathode compartments of equal volume (5.5 mL) and identical dimensions (5.5 × 1.0 × 1.0 cm). Graphite felt electrodes (4.5 × 1.0 × 0.5 cm) were employed in both compartments, with the cathode electrode coated with 0.3 mg cm^{-2} of platinum powder to enhance catalytic activity. A cation-exchange membrane separated the compartments, and liquid flow was maintained using peristaltic pumps. (Zeng, Choo, Kim, & Wu, Modelling and simulation of two-chamber microbial fuel cell, 2010)

The MATLAB simulation developed for this study follows a structured approach to model the steady-state performance of an MFC. The code begins by defining key assumptions and governing electrochemical reactions at the anode and cathode. The primary responses include acetate oxidation at the anode, generating protons and electrons, and oxygen reduction at the cathode. The model assumes fixed overpotentials for both electrodes.

The model employs static memory allocation to optimize computational efficiency by preallocating matrices for species concentrations, reaction rates, overpotentials, and cell voltage. The mass balance equations for acetate, dissolved CO_2, H^+, bacteria, oxygen, OH^-, and cations are iteratively solved within a loop that systematically varies the current density. The simulation accounts for charge transfer coefficients, reaction rate constants, and half-saturation constants to accurately represent reaction kinetics.

The core numerical approach involves solving a set of coupled differential equations using an explicit finite difference method. The anode and cathode reaction rates are iteratively updated based on electrochemical kinetics, and the cell voltage is computed considering overpotentials and resistive losses due to membrane and electrolyte conductivity. The steady-state values of key parameters, such as acetate concentration, overpotentials, and cell voltage, are extracted and stored for analysis. The simulation results are compared against experimental data to validate the accuracy of the model and refine parameter estimates.

3.2 ADM1 Used in the Model

The ADM1 (Anaerobic Digestion Model No. 1) model is discussed in detail in a report by the IWA Task Group for Mathematical Modelling of Anaerobic Digestion Processes. (IWA, 2005) The ADM1 model serves as a structured framework that explains the primary processes involved in converting complex organic matter into methane, carbon dioxide, and inert byproducts. Figure 7 presents an overview of the substrates and conversion processes included in the model.

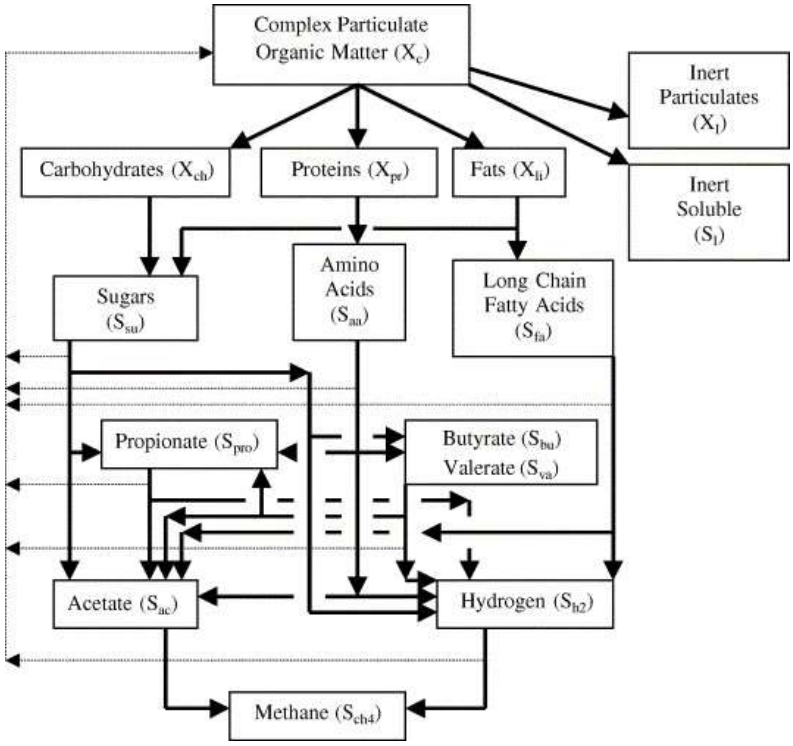


Figure 7. Conceptual model for ADM1 (Parker, 2005)

The ADM1 provides a structured framework for describing anaerobic digestion, detailing converting complex organic matter into methane, carbon dioxide, and inert byproducts. The model incorporates five key stages: disintegration, hydrolysis, acidogenesis, acetogenesis, and methanogenesis. (Parker, 2005) (IWA, 2005)

1. Disintegration & Hydrolysis: Complex particulate matter, including carbohydrates, proteins, and lipids, is broken down into simpler compounds through extracellular enzymatic activity. These processes are governed by first-order reaction kinetics.

2. Acidogenesis: Fermentative bacteria convert monosaccharides and amino acids into volatile fatty acids (VFAs) such as acetate, propionate, butyrate, valerate, and hydrogen and carbon dioxide. (IWA, 2005)
3. Acetogenesis: VFAs and long-chain fatty acids (LCFAs) are further metabolized by acetogenic bacteria into acetate, hydrogen, and carbon dioxide. (IWA, 2005)
4. Methanogenesis: Methanogenic archaea produce methane through two pathways—acetoclastic methanogenesis (acetate breakdown) and hydrogenotrophic methanogenesis (CO_2 reduction via hydrogen).

ADM1 represents these processes using state variables: soluble species (denoted as "S"), including monomers, volatile acids, hydrogen, and methane, and particulate species (denoted as "X"), encompassing active biomass and non-biodegradable materials. The model employs Monod kinetics for microbial reactions and first-order kinetics for hydrolysis and microbial decay. (Parker, 2005) Additionally, using non-competitive rate multipliers, ADM1 incorporates various inhibition mechanisms, such as pH imbalances, hydrogen accumulation, and free ammonia. Gas-liquid mass transfer processes for methane, carbon dioxide, and hydrogen are also included, requiring separate mass balances for the liquid and gas phases. (Parker, 2005) Unlike other models such as ASM, which focus on microbial growth, ADM1 prioritizes substrate conversion, making it a comprehensive tool for simulating anaerobic digestion dynamics.

ADM1 describes kinetic processes of 24 components. Tables 4 summarize these 24 components. (IWA, 2005)

Table 4. Kinetic Processes of 24 Components in ADM1 (IWA, 2005)

Parameter	Name	Unit
S_{Su}	Monosaccharide	$kgCOD \cdot m^{-3}$
S_{Aa}	Amino Acid	$kgCOD \cdot m^{-3}$
S_{Fa}	Long-chain Fatty Acid	$kgCOD \cdot m^{-3}$
S_{Va}	Valerate	$kgCOD \cdot m^{-3}$
S_{Bu}	Butyrate	$kgCOD \cdot m^{-3}$

S_{Pro}	Propionate	$kgCOD \cdot m^{-3}$
S_{Ac}	Acetate	$kgCOD \cdot m^{-3}$
S_{H2}	Hydrogen	$kgCOD \cdot m^{-3}$
S_{CH4}	Methane	$kgCOD \cdot m^{-3}$
C_{Su}	Monosaccharide-Degrading Microorganisms	$kgCOD \cdot m^{-3}$
C_{Aa}	Amino Acid-Degrading Microorganisms	$kgCOD \cdot m^{-3}$
C_{Fa}	Fatty Acid-Degrading Microorganisms	$kgCOD \cdot m^{-3}$
C_{Va}	Valerate-Degrading Microorganisms	$kgCOD \cdot m^{-3}$
C_{Bu}	Butyrate-Degrading Microorganisms	$kgCOD \cdot m^{-3}$
C_{Pro}	Propionate-Degrading Microorganisms	$kgCOD \cdot m^{-3}$
C_{Ac}	Acetate-Degrading Microorganisms	$kgCOD \cdot m^{-3}$
C_{H2}	Hydrogen-Degrading Microorganisms	$kgCOD \cdot m^{-3}$

3.3 Model Development and Assumptions

To simplify the simulation, this article assumes that acetate is oxidized at the anode and the reduction of dissolved oxygen occurs at the cathode. In the anode chamber, the chamber is operated under anoxic or anaerobic conditions, where a Monod-type equation is adopted. Furthermore, since both anode and cathode reactions are electrochemical reactions and controlled by electrical potential, the Butler-Volmer expression is applied for simulation. Equations 1 and 2 describe the electron transfer reaction on the anode and the cathode, respectively. Equations 3 and 4 represent the reaction rate in the anode and cathode, respectively.

$$(CH_2O)_2+2H_2O \rightarrow 2CO_2+8H^++8e^- \quad (1)$$

$$O_2+4e^-+2H_2O \rightarrow 4OH^- \quad (2)$$

$$r_a = k_a e^{\left(\frac{\alpha F}{RT}\eta_a\right)} \frac{C_a}{K_a + C_a} \quad (3)$$

$$r_c = -k_c e^{\left((\beta-1)\frac{F}{RT}\eta_c\right)} \frac{C_O}{C_O + K_O} X \quad (4)$$

where k_a and k_c are rate constants of the anode and cathode reaction under standard conditions, η_a and η_c are overpotential at the anode and cathode. X represents the concentration of biomass in the anode chamber, while Ca and Co represent the concentration of acetate in the anode and the concentration of dissolved oxygen in the cathode. K_a and K_O represent the half velocity rate constant for acetate and dissolved oxygen respectively. There are also several constants in the equation, which is *F*, the Faraday constant, *R*, the gas constant and *T* for operating temperature. Moreover, α represents the charge-transfer coefficient of the anode reaction and β is the charge-transfer coefficient of the cathodic reaction.

It is also assumed that carbon dioxide and acetate do not diffuse into the membrane, and the gas phase formed by releasing carbon dioxide bubbles is not considered. Therefore, four components in the anode compartment need to be balanced, acetate, dissolved CO_2, hydrogen ions, and biomass, while the cathode compartment has two components, dissolved oxygen and hydroxide ion. The mass balance of acetate, dissolved CO_2, hydrogen ion and biomass could be calculated by the following equations

$$V_a \frac{dC_{Ac}}{dt} = Q_a\left(C_{Ac}^{in} - C_{Ac}\right) - A_m r_a \quad (5)$$

$$V_a \frac{dC_{CO2}}{dt} = Q_a\left(C_{CO2}^{in} - C_{CO2}\right) - 2A_m r_a \quad (6)$$

$$V_a \frac{dC_H}{dt} = Q_a\left(C_H^{in} - C_H\right) - 8A_m r_a \quad (7)$$

$$V_a \frac{dX}{dt} = Q_a \frac{\left(X^{in} - X\right)}{f_X} + A_m Y_{ac} r_a - V_a K_{dec} X \quad (8)$$

In the equations above, the subscripts 'a' and 'in' refer to the anode and the feed flow, respectively. The terms V, Q, and A_m represent the compartment volume, feed flow rate, and membrane cross-sectional area, respectively. In Equation 8, f_x denotes the reciprocal of the wash-out fraction, Y_{ac} represents the bacterial yield, and K_{dec} is the decay constant for acetate utilizers.

In the cathode compartment the mass balances of dissolved O_2 and hydroxyl in the cathode expressed by Equations 9 and 10, respectively

$$V_c \frac{dC_{O2}}{dt} = Q_c\left(C_{O2}^{in} - C_{O2}\right) - A_m r_c \tag{9}$$

$$V_c \frac{dC_{OH}}{dt} = Q_c\left(C_{OH}^{in} - C_{OH}\right) - 4A_m r_c \tag{10}$$

After balancing mass and charge transfer, the current density and the flux of ions transferring the membrane can be simulated by using Equation 11.

$$i = F\sum_n z_n N_n \tag{11}$$

where z_n represents the charge number of the nth species, N_n is the superficial flux of the nth species, and i denotes the cell current density. The anode overpotential was calculated by using the Butler-Volmer equation, The Butler-Volmer equation describes the relationship between the overpotential η and the reaction rate j at an electrode, as mentioned in Equation 12. For large overpotentials, the Tafel approximation simplifies this equation into:

$$\eta_a = \frac{RT}{\alpha F} ln \frac{j}{j_0} \tag{12}$$

Where j is the actual reaction rate (current density), j_0 is the exchange current density, α is the charge transfer coefficient. At steady state, the concentration balance in the anode chamber gives

$$C_{AC} = C_{Ac}^{in} - \frac{r_a A_m}{Q_a} \tag{13}$$

By substituting this into the reaction rate equation and rearranging, we obtain:

$$\frac{j}{j_0} = \frac{(Q_a + V_a K_{dec} f_x)}{A_m Y_{ac} f_x k_1}\left(\frac{K_a}{C_{Ac}^{in} - r_a \frac{A_m}{Q_a}} + 1\right) \tag{14}$$

Taking the logarithm and applying the Tafel equation gives the final form:

$$\eta_a = \frac{RT}{\alpha F} ln \frac{(Q_a + V_a K_{dec} f_x)}{A_m Y_{ac} f_x k_1} \tag{15}$$

This equation accounts for electrochemical activation losses (via Butler-Volmer and Tafel equations), substrate concentration dependence (via Monod kinetics), and flow conditions in the anode (via mass balance on acetate). This formulation is commonly used in the MFC system model to predict how changes in flow rate, bacterial yield, and acetate concentration affect the anode overpotential in microbial fuel cells. After getting η_a and η_c, the cell voltage then can be calculated:

$$U_{cell} = U^o - \eta_a + \eta_c - \left(\frac{d^m}{k^m} + \frac{d}{k^s}\right) i \tag{16}$$

where d^m and d are the thickness of the membrane and the distance between the electrodes. k^m and k^s are the conductivities of the membrane and the solution, respectively and U^0 is the open-circuit voltage.

All fixed operating conditions and parameters used during the simulations are listed in Table 5 for the modelling system. Since the electrical conductivity of the aqueous solution (k_s) is not sensitive to the simulation result, k_s is assumed based on theoretical data during the simulation and parameters of the capacitances of the anode and cathode.

Table 5. Parameters for Model Set-Up and Simulation

Symbol	Value	Unit	Description
F	96485.4	Coulombs mol^{-1}	Faraday's constant
R	8.3144	J mol^{-1} K^{-1}	Gas constant
T	30	℃	Temperature
d^m	2×10^{-4}	Thickness of membrane	Thickness of membrane
k^s	5	Ohm^{-1} m^{-1}	Electrical conductivity of the aqueous solution
A_m	5×10^{-4}	m^2	Area of membrane
k_{bio}	0.05	Sm^{-1}	Electrical conductivity of the membrane

Q_s	2025 $\times 10^{-5}$	$m^3\ h^{-1}$	Flow rate
R	91000	Ohm	Total resistance
R_{in}	1000	Ohm	Internal resistance
U_0	0.77	volt	Cell open circuit potential
Y_{ac} (Zeng, Choo, Kim, & Wu, 2010)	0.05		Bacterial yield
K_{dec} (Zeng, Choo, Kim, & Wu, 2010)	8.33×10^{-4}	h^{-1}	Decay constant for acetate utilisers
f_x	122	-	Reciprocal of wash-out fraction
α	0.051	-	Charge transfer coefficient of anode
β	0.663	-	Charge transfer coefficient of cathode
K_A	0.592	mol m^{-3}	Half velocity rate constant for acetate
K_{O2}	0.004	mol m^{-3}	Half velocity rate constant for dissolved oxygen

3.4 Results and Discussion

The power density plot, Figure 8 below, shows the relationship between power density and cell current density in a microbial fuel cell. The curve follows a characteristic trend observed in fuel cells, where power density initially increases with current density, reaches a peak, and then declines as

current density continues to rise. The interplay of activation losses, ohmic losses, and mass transport limitations primarily governs this trend.

At lower current densities, power density increases steadily as the MFC operates efficiently, with minimal internal losses and a sufficient supply of substrate for microbial metabolism. The linear increase in power density during this phase is primarily due to activation losses, which dominate at low currents as electrons are transferred from bacteria to the anode. The power density reaches a maximum at approximately 8 A/m^2, indicating the optimal operating point for the MFC under the given experimental conditions. At this peak, the microbial community is effectively oxidizing the electron donor, and the system is operating with balanced electrochemical reactions and minimal energy losses.

Beyond the peak, the power density declines as current density increases further. This drop is attributed to significant ohmic losses and mass transport limitations. Ohmic losses arise from the electrolyte, electrode materials, and external circuit resistance, impeding efficient electron flow. Additionally, substrate and oxygen diffusion limitations can hinder microbial activity and cathodic reactions at higher currents, reducing overall performance.

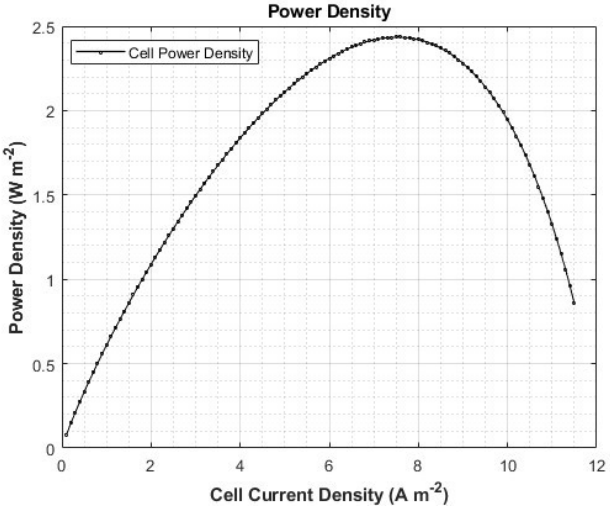


Figure 8. Power Density vs Current Density

The voltage-current density curve, Figure 9, follows a typical fuel cell polarization behavior, showing a steady decline in voltage as current density increases. This trend is primarily due to the combined effects of activation losses, ohmic losses, and mass transport limitations. At low current

densities, the cell voltage remains relatively high, close to the open-circuit voltage (OCV), which is around 0.8 V. In this region, the MFC experiences activation losses, which are primarily caused by the energy barriers associated with the electrochemical reactions at the anode and cathode. These losses are more pronounced at the beginning, leading to a sharp initial voltage drop.

As the current density increases beyond this initial region, the voltage decreases more gradually. This middle portion of the curve is dominated by ohmic losses, which result from the internal resistance of the system. Ohmic resistance arises from the electrodes' electrical resistance, the electrolyte's ionic resistance, and the cation-exchange membrane's resistance. This linear region indicates that electron and ion transport limitations begin to affect performance, but the cell is still operating efficiently within this range.

Mass transport limitations make the voltage decline steeper at higher current densities. This occurs because the supply of reactants (acetate oxidation at the anode and oxygen reduction at the cathode) cannot keep up with the increasing demand for electrochemical reactions. The rate of acetate oxidation at the anode increases with current density, but oxygen reduction at the cathode faces diffusion limitations, leading to a sharp voltage drop. Oxygen transport to the cathode is often a limiting factor in MFCs, and insufficient oxygen availability can cause increased cathodic overpotential, further reducing cell voltage.

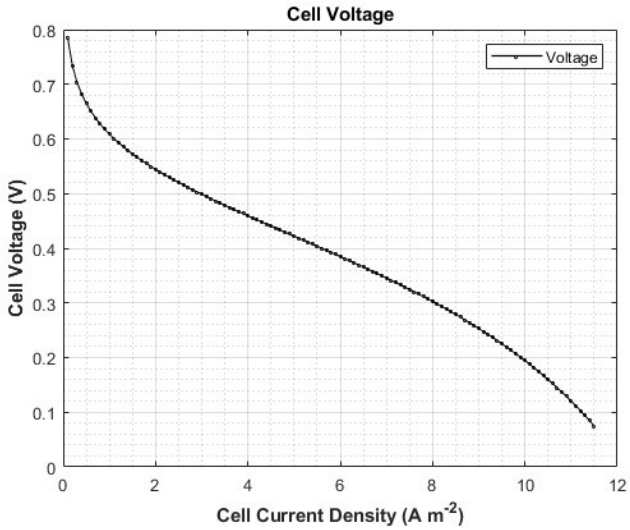


Figure 9. Cell Voltage vs Current Density

Overpotential represents the deviation of electrode potential from its equilibrium value due to kinetic, ohmic, and mass transport losses. The anode and cathode exhibit distinct behaviors crucial in determining the overall cell performance.

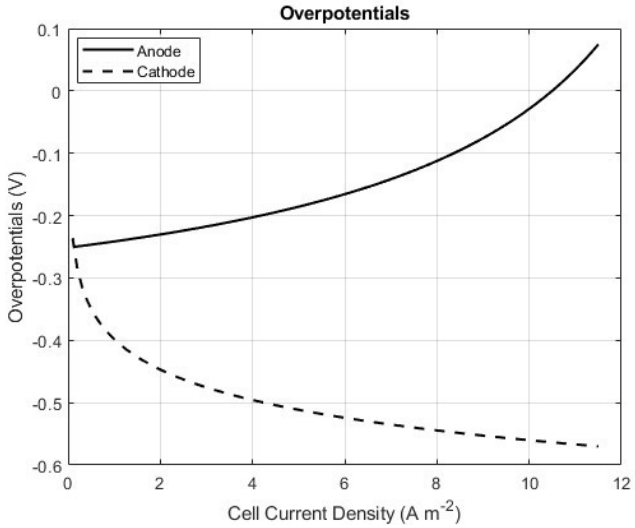


Figure 10. Overpotentials for the Anode and Cathode

As Figure 10 shown. At low current densities, both the anode and cathode overpotentials are relatively small, indicating minimal losses and efficient electron transfer at the electrodes. As the current density increases, the overpotentials at both electrodes deviate further from their initial values. The anode overpotential exhibits an increasing trend, which is expected as the microbial oxidation of the electron donor becomes kinetically limited at higher reaction rates. This behavior is typical due to activation losses arising from the energy barrier required for microbial extracellular electron transfer. Additionally, ohmic losses from the electrolyte and electrode materials contribute to increased anode overpotential.

On the other hand, the cathode overpotential follows a decreasing trend, becoming more negative as current density rises. This indicates increasing polarization losses at the cathode, which may be attributed to mass transport limitations and the inherent sluggish oxygen reduction kinetics in MFCs. Since the cathode reaction relies on oxygen diffusion and catalytic reduction, a higher current density exacerbates mass transport limitations, leading to a more significant drop in potential. The cathode overpotential decreases sharply at first and then levels off, suggesting that oxygen availability at the cathode surface becomes a significant limiting factor at higher currents. The combined effects

of these overpotentials contribute to the overall voltage losses in the system, limiting the maximum achievable power output. Reducing anode overpotentials can be achieved by optimizing microbial activity and electrode material properties, while cathode overpotential reductions may require improvements in catalyst loading, electrode surface area, or mass transport enhancement strategies such as forced aeration.

Figure 11 depicts the variation of pH at the anode and cathode compartments of a microbial fuel cell (MFC) as a function of cell current density. It shows a clear divergence in pH behavior between the two electrodes, which is a direct result of the electrochemical and biochemical reactions occurring at each electrode.

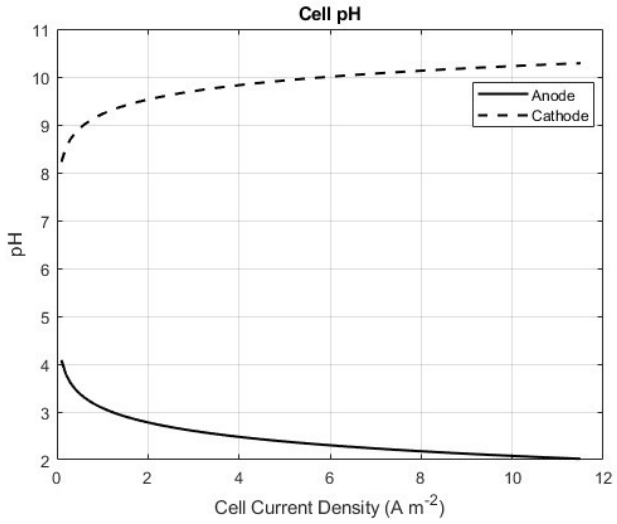


Figure 11. pH in Anode and Cathode Chamber

At the anode, the pH decreases as current density increases, stabilizing at a value around 2.5 at higher current densities. This acidic environment is primarily due to the oxidation of organic substrates by electroactive bacteria, which produces protons H^+ as a byproduct. The microbial oxidation rate increases as the current density rises, leading to a higher proton accumulation in the anode chamber. The continuous generation of protons, combined with limited buffering capacity and restricted proton transport through the cation-exchange membrane, contributes to the acidification of the anode chamber. A significantly low pH in the anode chamber can negatively impact microbial activity, potentially inhibiting bacterial metabolism and reducing MFC performance.

In contrast, the cathode pH follows an increasing trend with rising current density, reaching values above 10. This alkalization effect occurs due to the oxygen reduction reaction (ORR) at the cathode, which consumes protons and generates hydroxide ions OH^-. The ORR intensifies as the current density increases, leading to further hydroxide ion accumulation and a subsequent rise in cathode pH. High cathode pH can impact the efficiency of oxygen reduction and may lead to precipitation of salts, such as calcium or magnesium hydroxides, on the cathode surface, which could cause electrode fouling.

The reaction rates of acetate oxidation r_a and oxygen reduction rate r_c as a function of cell current density in a microbial fuel cell were shown in Figure 12. The trends observed in the plot align with the fundamental electrochemical reactions occurring at the anode and cathode of the MFC. The reaction rate of acetate oxidation, represented by the solid line, increases proportionally with current density. This behavior is expected since acetate oxidation at the anode is the primary source of electrons for the MFC. As the current density increases, more acetate is oxidized by the electroactive bacteria to supply the necessary electrons for the external circuit. This trend suggests that the microbial metabolism is not significantly limited by substrate availability at the tested current densities. However, at very high current densities, mass transport limitations or microbial activity constraints could eventually lead to deviations from this linear trend.

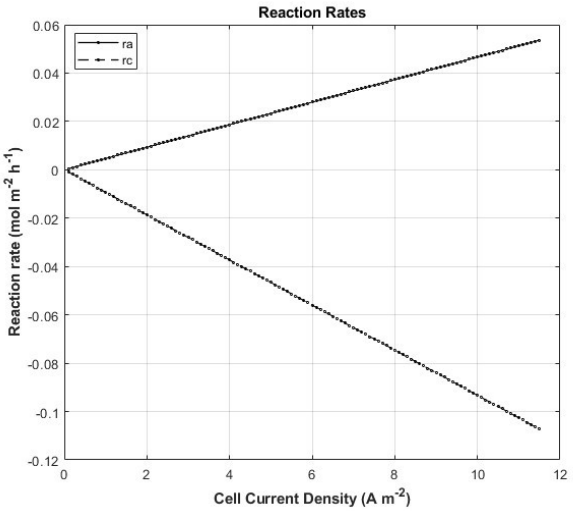


Figure 12. Reaction Rate for the Anode and the Cathode

Conversely, the oxygen reduction reaction rate, shown as the dashed line, decreases proportionally with increasing current density. This negative correlation directly results from the cathodic oxygen reduction reaction, where electrons arriving from the anode combine with protons and oxygen to form water. The observed trend indicates that the rate of oxygen reduction is directly linked to the electron supply from acetate oxidation, maintaining charge balance in the system. However, the decline in r_c at high current densities suggests that mass transport limitations at the cathode, such as oxygen diffusion resistance, could affect the reduction process's efficiency.

The last step in the simulation is to simulate the variation in concentrations of different species, including acetate, CO_2, cations, oxygen, and bacteria, as a function of cell current density in a microbial fuel cell. The trends observed in Figure 13 reflect the electrochemical and biological processes governing MFC performance.

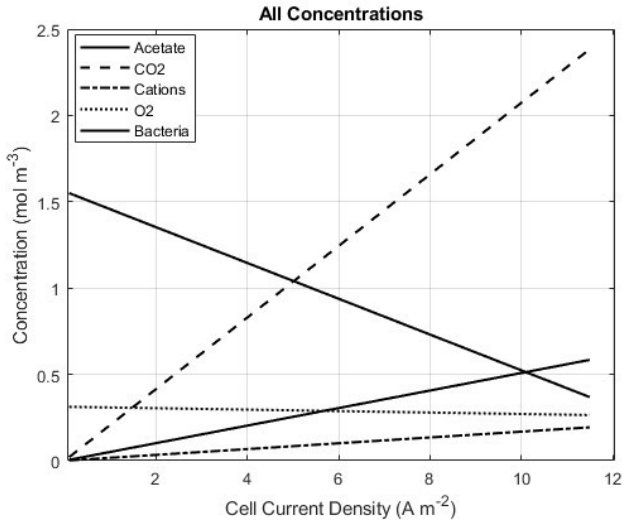


Figure 13. Concentration for Each Component

As the cell current density increases, the concentration of acetate decreases steadily. This trend is expected because acetate serves as the primary electron donor in the anode compartment. Microbial communities oxidize acetate to generate electrons, which are transferred to the anode, producing CO_2 as a byproduct. The decreasing acetate concentration suggests that microbial oxidation becomes more active with increasing current density, leading to enhanced substrate consumption. Conversely, the concentration of CO_2 increases with current density, following a nearly linear trend. This increase is directly linked to acetate oxidation, where CO_2 is produced as a metabolic byproduct.

The correlation between acetate depletion and CO_2 production confirms that microbial metabolism intensifies with rising current density, resulting in higher CO_2 release.

The concentration of cations and oxygen remains relatively low but shows a slight increasing trend. Cations, likely representing protons and other positively charged species, accumulate due to electrochemical reactions and ion transport through the membrane. The slight increase in oxygen concentration at the cathode may be attributed to oxygen diffusion limitations, which can impact the oxygen reduction reaction efficiency. The bacterial concentration exhibits an increasing trend initially but stabilizes at higher current densities. This behavior suggests that the availability of acetate initially stimulates microbial growth, but at higher current densities, growth becomes constrained, possibly due to factors such as pH imbalance, mass transport limitations, or substrate depletion.

3.5 Conclusion

The simulation results presented in this chapter offer a comprehensive evaluation of microbial fuel cell performance under varying current densities, shedding light on the complex interplay between electrochemical and biological processes. The power density curve revealed a characteristic peak, indicating an optimal operating point beyond which performance declines due to mass transport limitations. This finding emphasizes the critical need to identify and maintain an efficient operating range for MFCs to maximize energy output. Furthermore, overpotential analysis showed that activation and ohmic losses at both the anode and cathode increased with rising current density, leading to significant voltage drops. These losses underscore the importance of optimizing electrode materials and configurations to minimize internal resistance and enhance overall system efficiency.

The pH distribution results highlighted substantial disparities between the anode and cathode compartments. Proton accumulation at the anode caused acidification, while oxygen reduction reactions at the cathode led to alkalization. These pH imbalances underscore the necessity of implementing effective pH regulation strategies to sustain stable microbial activity and improve electrode performance. Without proper pH control, microbial metabolism and electrochemical reactions can be severely hindered, resulting in reduced energy conversion efficiency. Additionally, reaction rate analysis revealed that acetate oxidation at the anode and oxygen reduction at the cathode followed inverse trends, ensuring charge balance within the system. However, oxygen transport limitations became apparent at higher current densities, potentially impeding cathodic reactions and

degrading overall MFC performance. This suggests that enhancing oxygen diffusion and improving cathode catalytic activity could alleviate these limitations.

Cell voltage curve further corroborated these findings, showing a steady decline as current density increased due to the combined effects of activation, ohmic, and mass transport losses. This trend highlights the inherent trade-offs between power output and energy efficiency in MFC operation. Moreover, acetate, CO_2, cations, oxygen, and bacteria concentration profiles provided more profound insights into the biochemical-electrochemical interactions within the system. The depletion of acetate and the corresponding rise in CO_2 concentration confirmed efficient substrate utilization, while bacterial concentration trends indicated that microbial growth was initially promoted but later constrained by factors such as pH imbalance and substrate depletion.

These simulation results underscore the intricate dependencies between electrochemical and microbial processes in MFCs. These insights deepen our understanding of MFC operation and provide a solid foundation for further experimental validation and potential advancements in microbial fuel cell technology.

Chapter 4 Modelling for Guelph WWTP

4.1 Introduce to Guelph WWTP

The model has been further refined to enhance its ability to accurately represent real-world wastewater treatment and evaluate the potential of MFC technology as an alternative treatment method. Additional complexity has been incorporated to simulate mass transfer and substrate diffusion across multiple substrates more precisely. To ensure realistic conditions, wastewater quality data from an existing treatment facility have been utilized as input samples, allowing the model to reflect actual wastewater characteristics and operational challenges.

The Guelph Water Resource Recovery Centre (WRRC) is a vital infrastructure facility operated by the City of Guelph's Wastewater Services Division. It provides tertiary treatment for domestic, commercial, institutional, and industrial wastewater collected from the City of Guelph and parts of the neighbouring Township of Guelph/Eramosa. Located at 530 Wellington Street West, the WRRC is a Class IV treatment plant with a rated capacity of 64,000 m^3/day. Following disinfection and dechlorination, the treated effluent is discharged into the Speed River. (Guelph, 2022)

Wastewater enters the facility through two sanitary trunk sewers, where it is lifted to the Headworks by Archimedes screw pumps for preliminary treatment, including screening and grit removal. The flow is then distributed among four treatment plants: Plant 1: 16,000 m^3/day; Plant 2: 13,000 m^3/day; Plant 3: 13,000 m^3/day and Plant 4: 22,000 m^3/day. (Guelph, 2022)

The treatment process includes primary and secondary treatment using conventional activated sludge processes, with chemical phosphorus removal achieved through ferric chloride injection. Ammonia removal occurs via rotating biological contactors (RBCs) for Plants 1, 2, and 3, while Plant 4 incorporates ammonia removal within its secondary treatment process. Effluent from Plant 4 is directed either to the RBCs or tertiary sand filters, depending on the plant's flow rate. Final disinfection is performed using sodium hypochlorite and dechlorination with sodium bisulfite before discharge into the Speed River. (Guelph, 2022)

The WRRC also incorporates sludge treatment and resource recovery. Primary sludge is thickened in the primary clarifiers, while waste activated sludge from secondary clarifiers undergoes thickening in a rotating drum thickener (RDT). Thickened sludge is anaerobically digested and further processed through belt filter presses. The dewatered sludge is treated using the Lystek process,

producing a Canadian Food Inspection Agency-approved fertilizer for land application. (Guelph, 2022)

With its advanced treatment processes and focus on environmental sustainability, the Guelph WRRC plays a vital role in wastewater management, ensuring compliance with regulatory standards and protecting local waterways.

4.2 Analysis of Raw Influent and Effluent Wastewater Data

The raw influent and treated effluent wastewater data from the Guelph Water Resource Recovery Centre in 2022 provide a detailed overview of the plant's treatment efficiency (Appendix A). The comparison between influent and effluent quality reveals significant reductions in organic matter, suspended solids, and nutrient concentrations, highlighting the effectiveness of the facility's treatment processes. (Guelph, 2022)

The pH levels in the influent remained relatively stable throughout the year, with an annual average of 7.53, while the effluent pH was slightly lower, averaging 7.1. This slight decrease is expected due to biological treatment processes and chemical additions used in nutrient removal. The concentration of Carbonaceous Biochemical Oxygen Demand ($CBOD_5$) in the raw influent averaged 204 mg/L, while the effluent $CBOD_5$ was drastically reduced to approximately 2.1 mg/L, demonstrating a highly effective organic matter removal process. Similarly, the Biochemical Oxygen Demand (BOD_5) levels in the influent averaged 225 mg/L, whereas the treated effluent contained only about 2.5 mg/L, confirming the plant's ability to significantly reduce oxygen-demanding substances before discharge into the receiving water body.

Total Suspended Solids (TSS) also experienced substantial removal. The influent had an annual average of 278 mg/L, which was reduced to only 2.3 mg/L in the treated effluent. This indicates that the plant's sedimentation, filtration, and biological treatment systems effectively capture and remove particulate matter. Nutrient removal was equally efficient. Total Phosphorus (TP) levels in the influent were recorded at an annual average of 5.09 mg/L, while the effluent TP concentration was reduced to 0.12 mg/L. Similarly, Total Kjeldahl Nitrogen (TKN) decreased from 35.9 mg/L in the influent to 1.79 mg/L in the effluent. Ammonia, represented as Total Ammoniacal Nitrogen (TAN), saw a significant reduction from 23.9 mg/L in the influent to 0.70 mg/L in the treated effluent, indicating an effective nitrification process.

In addition to nutrient and organic matter reduction, microbial quality improvements were evident in the effluent data. The concentration of E. coli in the final effluent was significantly reduced, averaging 17.8 CFU/100 mL, indicating effective disinfection and compliance with regulatory standards for pathogen control.

Seasonal variations in influent quality were also observed. During winter, influent CBOD5 and BOD5 concentrations were higher, with winter averages of 226 mg/L and 242 mg/L, respectively, compared to summer averages of 188 mg/L for CBOD5 and 212 mg/L for BOD5. The effluent data showed that TAN levels were slightly higher in winter at 1.11 mg/L compared to 0.41 mg/L in the summer. This could be attributed to seasonal temperature effects on microbial activity and nitrification efficiency. TSS concentrations were slightly higher in the summer, but overall removal performance remained consistent throughout the year.

A summary of the raw wastewater inflow data is calculated and shown in Table 6.

Table 6. Raw Wastewater Inflow Data

	S_{Su}	S_{Bu}	S_{Pro}	S_{AC}
Unit ($kgCOD/m^3$)	0.0594	0.00891	0.00891	0.0159

4.3 Model Development and Assumptions

Based on the steady-state model developed before, further assumptions are made to simulate a more complex wastewater stream.

4.3.1 Model Assumptions

To establish a computational model for microbial fuel cells, several assumptions are made to simplify the system and focus on the key governing mechanisms. The primary assumptions are as follows:

1. Biofilm Properties: The density at all points within the biofilm is assumed to be uniform, and the active microorganisms are evenly distributed throughout the biofilm.
2. Anode-Biofilm Interface: The anode surface is in complete contact with the biofilm, and their mass transfer resistance is considered negligible.

3. Cathode Potential Stability: The cathode potential remains stable and is maintained at a fixed value throughout the entire operation cycle of the MFC.
4. Electron Transfer in MFCs: Electrons are transferred solely by conductive biofilms, with other electron transfer processes ignored.
5. Mass Transfer in Biofilm: Mass transfer within the biofilm is considered to occur only in the thickness direction, reducing the problem to a one-dimensional transport model.
6. Environmental Conditions: The system operates at a neutral pH and maintains a temperature of approximately 30°C.

These assumptions provide a foundation for the mathematical modeling and numerical simulation of MFC performance, allowing for a focused analysis of electron transport, mass transfer, and bioelectrochemical reactions within the system.

4.3.2 Equations Generation

In the anode chamber, organic substrates diffuse from the bulk liquid phase into the biofilm, where electroactive bacteria metabolize them under anaerobic conditions. The model assumes a uniform microbial community within the biofilm, consisting of fermentative bacteria, methanogens, and exoelectrogens. Organic matter degradation follows typical anaerobic digestion pathways, with fermentative bacteria hydrolyzing complex substrates into smaller volatile fatty acids (VFAs), such as acetate, butyrate, and propionate. The exoelectrogens oxidize these VFAs, producing electrons and protons. In the cathode chamber, oxygen is assumed to be the primary electron acceptor, with uniform diffusion from the bulk solution to the cathode surface. The overall reaction rate can be expressed as follows:

$$(\Sigma R)_{su,bulk} = -q_{su,bulk}V_a - A_m J_{s,Su} \tag{17}$$

Carbohydrates in the anode chamber undergo microbial degradation and acidification, producing acetic acid, butyric acid, propionic acid, and hydrogen gas. Where $\sum R_{Su,bulk}$ represents the reaction rate of glucose in the anode chamber ($kgCOD \cdot day^{-1}$), $q_{Su,bulk}$ denotes the reaction rate of glucose in the anode chamber per unit volume ($kgCOD \cdot m^{-3} \cdot day^{-1}$).$V_a$ is the volume of the anode chamber, and $J_{s,su}$ refers to the glucose transfer rate between the anode chamber solution and the biofilm.

$$(\Sigma R)_{Bu,bulk} = -q_{Bu,bulk}V_a + (1 - Y_{Su})f_{Bu,Su}q_{su,bulk}V_a - A_m J_{s,Bu} \tag{18}$$

Butyrate is degraded by microorganisms, producing acetic acid and hydrogen gas. Where Y_{Su} represents the biomass yield coefficient for glucose in the anode chamber ($kgCOD_X/kgCOD_S$), and $f_{Bu,Su}$ denotes the conversion rate of glucose to butyrate in the anode chamber ($kgCOD_s/kgCOD_S$).

$$(\Sigma R)_{Pro,bulk} = -q_{Pro,bulk}V_a + (1 - Y_{Su})f_{Pro,Su}q_{su,bulk}V_a - A_m J_{s,Pro} \quad (19)$$

Propionate is degraded by propionate-utilizing microorganisms, producing acetic acid and hydrogen gas. In the anode chamber, methanogens degrade acetate, producing methane gas. The overall reaction rate expression for acetate production and degradation is as follows and the coefficients 0.8 and 0.57 in the equation are stoichiometric coefficients derived from microbial metabolic pathways in the anode chamber

$$(\Sigma R)_{Ac,bulk} = -q_{Ac,bulk}V_a + (1 - Y_{Su})f_{Ac,Su}q_{su,bulk}V_a + (1 - Y_{bu})0.8q_{Bu,bulk}V_a + (1 - Y_{Pro})0.57q_{Pro,bulk}V_a - A_m J_{s,Ac} \quad (20)$$

The model assumes that electron transport within the anode biofilm occurs solely through direct extracellular electron transfer (EET). This process relies on nanowires and outer membrane cytochromes produced by exoelectrogenic bacteria, forming a conductive network that channels electrons towards the anode surface. The microbial biofilm is viewed as homogeneous, with a uniform distribution of bacteria and consistent electrical conductivity throughout its structure.

The degradation of organic substrates follows a dual-limiting Monod equation, which accounts for both substrate concentration and the local electrochemical potential gradient within the biofilm. As the anode biofilm serves as the electron acceptor, local redox potential gradients affect electron flow within the conductive biofilm structure. The Butler-Volmer equation is used to model the charge transfer process at the anode surface, incorporating the concentration of electroactive species and local overpotential losses.

Moreover, the degradation rate of carbohydrates within the biofilm is determined by the proportion of carbohydrate-degrading microorganisms present. The corresponding reaction rate equation illustrates this relationship, accurately reflecting microbial activity and substrate utilization in the biofilm environment.

$$(\Sigma R)_{su,f} = -q_{su,f}X_{Su} \quad (21)$$

Where $\sum R_{Su,f}$ represents the reaction rate of glucose within the biofilm ($kgCOD \cdot day^{-1}$), $q_{Su,bulk}$ denotes the reaction rate of glucose within the biofilm per unit biomass ($kgCOD_S \cdot$

$kgCOD_X^{-1}\cdot day^{-1}$).$X_{Su}$ represents the volumetric fraction of active glucose-degrading microorganisms within the biofilm ($kgCOD_X\cdot m^{-3}$)

$$(\Sigma R)_{Bu,f} = -q_{Bu,f}X_{Bu} + \left(1 - Y_{Su,b}\right)f_{Bu,Su,b}q_{su,f}X_{Su} \tag{22}$$

Where $Y_{Su,b}$ represents the biomass yield coefficient for glucose in the biofilm ($kgCOD_X$ /$kgCOD_S$), and $f_{Bu,Su,b}$ denotes the conversion rate of glucose to butyrate in the biofilm ($kgCOD_s$ /$kgCOD_S$).

$$(\Sigma R)_{Pro,f} = -q_{Pro,f}X_{Pro} + (1 - Y_{Su})f_{Pro,Su}q_{su,f}X_{Su} \tag{23}$$

$$(\Sigma R)_{Ac,f} = -q_{Ac,f}X_{ac} + (1 - Y_{Su})f_{Ac,Su}q_{su,f}X_{Su} + (1 - Y_{bu})0.8q_{Bu,f}X_{Bu} + (1 - Y_{Pro})0.57q_{Pro,f}X_{Pro} \tag{24}$$

In MFC, acetate in the system is degraded by electroactive bacteria within the biofilm, generating electrons. The potential balance equation within the biofilm is:

$$\frac{dj}{dx} + \frac{\gamma_1 F q_{E.Ac}X_a f_e^0}{\tau} + \frac{F r_{res}X_a\gamma_2}{\tau} = 0 \tag{25}$$

where: j is the current density within the anode biofilm (A/cm), γ_1 is the number of moles of electrons transferred per mole of substrate ($mol\cdot kgCOD_S^{-1}$), f_e^0 is the energy conversion coefficient, γ_2 is the number of electrons transferred during endogenous microbial respiration ($mole\cdot kgCOD_X^{-1}$), r_{res} is the endogenous respiration rate (day^{-1}) and τ is the time conversion constant. Due to the presence of a conductive nanowire network, the biofilm exhibits conductivity, and its internal potential and current density follow Ohm's law:

$$\frac{d\eta}{dz} + k_{bio}J = 0 \tag{26}$$

Where k_{bio} is the biofilm conductivity, and η is the potential at a given point in the biofilm. Substituting Equation 24 into Equation 25 and rearranging, the relationship between biofilm potential and acetate degradation rate is:

$$k_{bio}\frac{d\eta}{dz} - \frac{\gamma_1 q_{E.Ac}X_a f_e^0}{\tau} - \frac{r_{res}X_a\gamma_2}{\tau} = 0 \tag{27}$$

The bioelectrochemical reaction rate of acetate degradation in the biofilm depends on the local potential, expressed as

$$q_{Ac} = q_{Ac}^{max} \frac{S_{Ac}}{K_{Ac} + S_{Ac}} \left(1 + \exp\left(\frac{F\eta}{RT}\right)\right) \phi_a = 0 \tag{28}$$

Where q_{Ac}^{max} is the maximum reaction rate constant for acetate, ϕ_a is the volumetric fraction of electroactive bacteria within the biofilm, K_{Ac} is the half-saturation constant, and S_{Ac} is the acetate concentration.

4.3.3 Boundary Conditions

Assuming no current is generated in the anodic solution and at the biofilm surface, the first boundary condition at the biofilm-liquid interface is:

$$\frac{d\eta}{dz}\Big|_{z=Lf} = 0 \tag{29}$$

For the second boundary condition, the actual cell voltage can be expressed as:

$$U_{cell} = U_{anode} - U_{cathode} - IR_{int} \tag{30}$$

The external resistance relation and The relation between current and electrode area can be expressed as:

$$U_{cell} = IR_{ext} \tag{31}$$

$$I = jA \tag{32}$$

Substituting into the previous equations, the boundary condition at the anode electrode surface is:

$$\eta\Big|_{z=0} - \left(Ak_{bio}(R_{ext} + R_{int})\right) + \frac{d\eta}{dz}\Big|_{z=0} = U_{catho} - E \tag{33}$$

The model equations are solved using the control volume method. The differential mathematical equations are transformed into difference equations through linearization for computation. The model equations are programmed and solved using MATLAB software.

4.4 Results and Discussion

4.4.1 Flow Rate

The relationship between power density and current density for different flow rates (Q_a) in a microbial fuel cell is illustrated in Figure 14. The three curves represent various flow rate conditions: a reduced flow rate $0.5Q_a$, a baseline flow rate (Q_a), and an increased flow rate $1.5Q_a$. The observed trends emphasize the impact of flow rate on the electrochemical performance of the MFC, especially regarding power output.

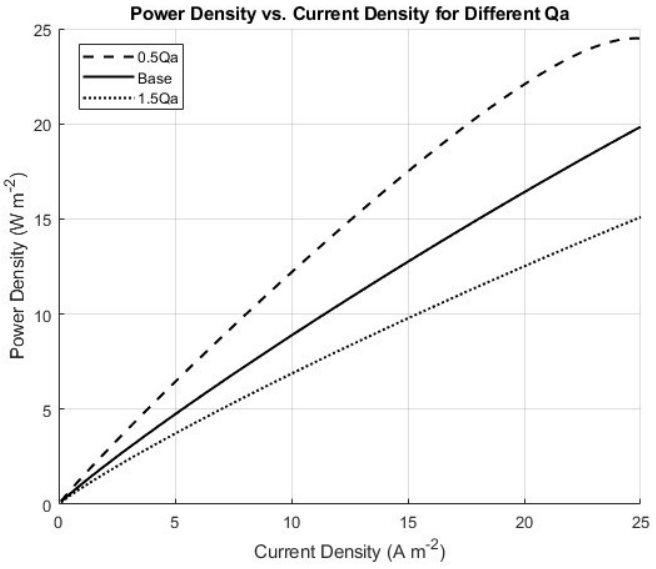


Figure 14. Power Density vs. Current Density for Different Q_a

At lower current densities, all three conditions display a similar linear trend, indicating that ohmic losses dominate in this region. However, as current density increases, the flow rate becomes more significant. The highest power density is observed at the lowest flow rate, with the power output reaching a peak before declining. This suggests that at lower flow rates, the substrate retention time in the anode chamber is extended, leading to more efficient microbial activity and electron transfer. The baseline flow rate follows a similar but slightly lower path, demonstrating a balance between substrate availability and mass transfer limitations. Conversely, the increased flow rate results in the lowest power density at any current density. This indicates that excessive flow may lead to insufficient retention time for microbial metabolism, thereby reducing electron generation efficiency. The decrease in power output at high flow rates suggests that while convective mass transfer

improves, it does not offset the diminished microbial conversion efficiency. This underscores a critical trade-off in MFC operation: while adequate flow is required to replenish reactants and eliminate metabolic byproducts, excessive flow can result in ineffective substrate utilization and lowered electrochemical performance.

The results highlight the need to optimize flow rate to balance substrate retention and mass transport. A lower flow rate increases power output by allowing more time for microbial reactions; however, excessively low flow rates can lead to diffusional limitations. On the other hand, excessively high flow rates decrease power density due to shorter substrate residence times, resulting in incomplete substrate conversion. Grasping this relationship is essential for designing MFC systems that maximize power generation while ensuring adequate mass transfer conditions. Figure 15 shows the voltage changes over time when varying Q_a.

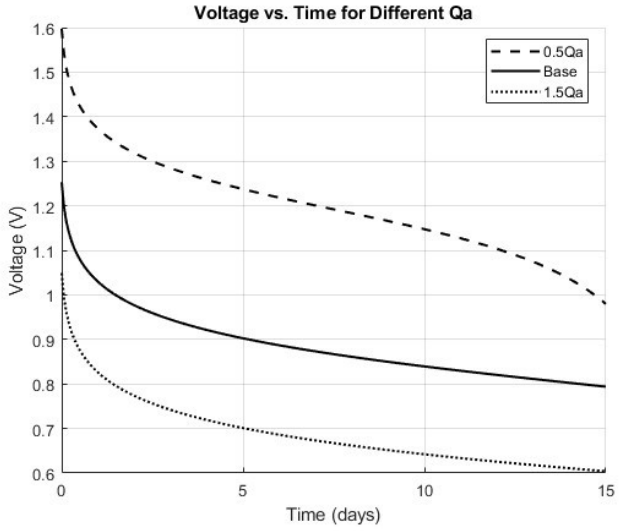


Figure 15. Voltage Changes Over Time Under Different Qa

At the outset, all three conditions showcase relatively high voltage levels, with the lowest flow rate Q_a producing the highest initial voltage, followed closely by the baseline and high flow rate conditions. Over time, voltage for all scenarios diminishes, reflecting a decline in system efficiency due to factors such as substrate depletion, biofilm adaptation, or electrode fouling. The most significant voltage drop occurs in the high flow rate condition Q_a, where voltage rapidly falls within the first few days and eventually stabilizes at the lowest level (~0.6 V) by the end of the 15-day

period. This indicates that a very high flow rate shortens retention time, limiting the microbial utilization of substrates and resulting in diminished bioelectrochemical efficiency.

Conversely, the lowest flow rate Q_a maintains the highest voltage throughout the period, displaying a gradual decline instead of a sharp drop. This prolonged voltage stability implies that extended substrate residence time promotes microbial activity, facilitating stable electron transfer and enhancing power generation. The baseline flow rate presents an intermediate pattern, showing moderate voltage stability that balances substrate availability with mass transfer limitations. The consistent performance observed in the low-flow condition suggests that a reduced flow rate enables microbes to degrade organic matter, thus enhancing sustained energy generation effectively.

These findings highlight the critical importance of optimizing flow rate in MFC operations. A lower flow rate extends substrate availability, culminating in a more stable and sustained voltage output, whereas excessively low flow rates can lead to diffusional limitations. On the other hand, an overly high flow rate diminishes system efficiency due to reduced substrate retention time, which constrains microbial metabolism and accelerates voltage decline. This underscores the vital need to maintain an optimal flow rate to balance microbial growth, substrate conversion, and electrochemical performance for the long-term operation of MFCs.

Flow rate is also a critical factor that influences the COD removal rate of the MFC system, Figure 16 indicates the time process of COD concentration under different flow rates.

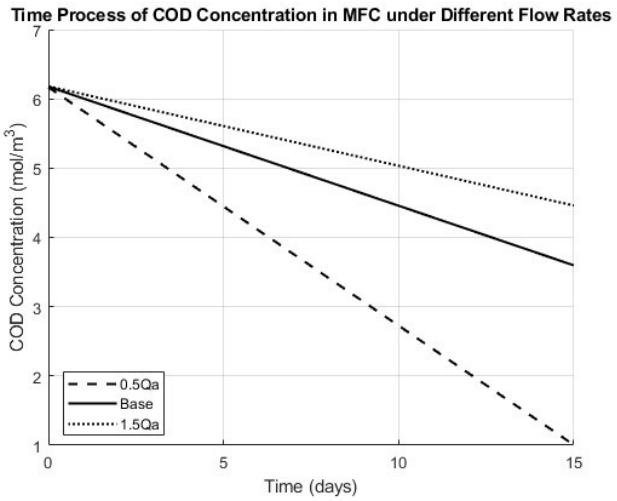


Figure 16. COD Concentrations Over Time Under Different Q_a

At the lowest flow rate, the COD concentration decreases rapidly, reaching its minimum value by the end of the 15-day period. This indicates that a longer HRT permits microorganisms more time to metabolize organic matter, resulting in a more efficient COD removal process. The extended residence time in the anode chamber enhances microbial degradation and electron transfer, ultimately improving the MFC's performance regarding substrate utilization.

The baseline flow rate displays an intermediate trend, with COD concentration decreasing moderately. This scenario balances substrate availability with flow rate, ensuring a satisfactory COD removal rate while providing a consistent supply of organic matter for microbial metabolism. The steady decline in COD concentration illustrates that the system operates under stable conditions, where substrate consumption is efficient but not maximized as it would be in low-flow conditions. Conversely, at the highest flow rate, the COD concentration decreases at the slowest rate, indicating less effective organic matter degradation. The shorter retention time limits the exposure of organic compounds to microbial activity, reducing the extent of COD removal. This suggests that while higher flow rates enhance mass transfer, they may lead to incomplete substrate utilization, resulting in lower treatment efficiency and potentially affecting the overall power generation capacity of the MFC.

These findings underscore the importance of optimizing flow rate to establish a balance between COD removal efficiency and substrate availability for power generation. While a lower flow rate promotes degradation by extending microbial interaction, excessively low flow rates can cause mass transfer limitations. Conversely, higher flow rates may decrease microbial retention time, leading to reduced COD removal efficiency. Therefore, selecting an optimal flow rate should consider both treatment performance and the MFC system's energy output. Future research should explore dynamic flow rate adjustments based on real-time COD monitoring to enhance MFC performance for both wastewater treatment and bioelectricity generation.

4.4.2 Initial Feed Concentration

Figure 17 illustrates the relationship between power density and current density for various acetate concentrations in a microbial fuel cell. The three curves represent conditions where acetate concentration is halved from baseline concentration, at baseline concentration, and increased to 1.5 times the baseline concentration. These trends highlight the influence of substrate availability on power generation and electrochemical performance.

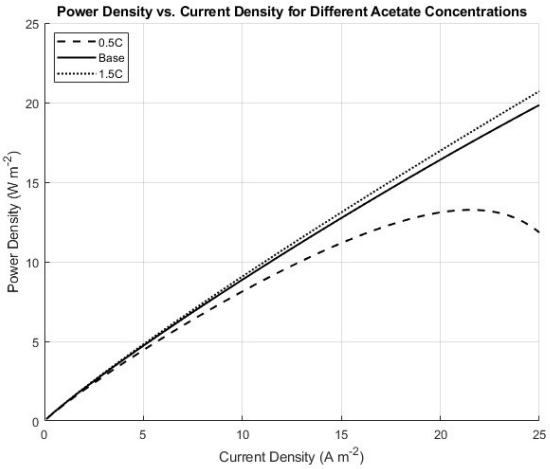


Figure 17. Power Density vs. Current Density Under Different C

At lower current densities, all three conditions exhibit comparable linear trends, indicating that the availability of acetate does not significantly affect power density in this range. This suggests that, in the initial phases, power generation is primarily influenced by ohmic resistance rather than by substrate limitations. As current density increases, however, distinct differences arise between the curves, highlighting the impact of acetate concentration on peak power output and overall system efficiency. The highest acetate concentration (1.5C) delivers the maximum power density across all current densities, with the baseline condition (C) closely trailing. This shows that a higher acetate concentration enhances microbial metabolism and electron transfer, leading to improved power generation. The linear relationship observed between power density and current density indicates that increased acetate availability promotes higher metabolic activity without immediate substrate limitations. Conversely, the lower acetate concentration (0.5C) causes a significant drop in power density, particularly at higher current densities. Here, power output peaks and then begins to decline, suggesting that substrate limitations critically impact performance as current demand grows. The decline at elevated current densities indicates that inadequate acetate availability hinders microbial activity once a certain threshold is surpassed, resulting in decreased power production.

Ultimately, these results underscore the importance of substrate concentration for optimizing MFC performance. While increased acetate concentrations elevate power density by fostering more excellent microbial activity and electron transfer, insufficient substrate limits power output at high current densities. It is crucial to maintain an optimal acetate level for consistent and effective power

generation, as excessive substrate limitations can hamper system performance, whereas overly high concentrations may yield diminishing returns. The voltage changes over time are also simulated under different feed concentrations shown in Figure 18.

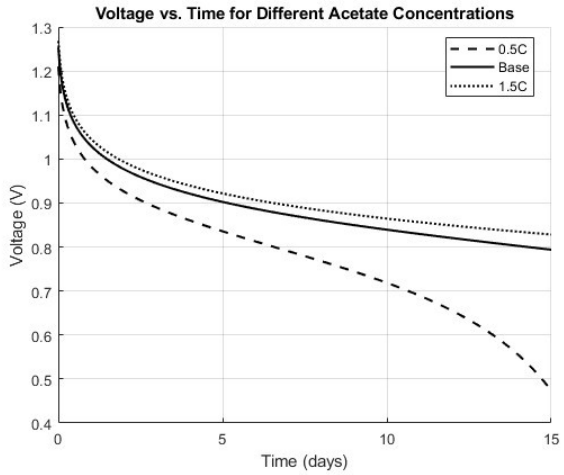


Figure 18. Voltage Over Time Under Different C

At first, all three conditions experience a sharp voltage drop, which is anticipated due to the swift acetate consumption by electrogenic bacteria as the system starts functioning. The condition with the highest concentration (1.5C) maintains the highest voltage during the entire experiment, closely followed by the baseline concentration (C). This suggests that greater substrate availability enhances microbial activity, improving and sustaining voltage output. In these two conditions, the voltage decline is relatively gradual, indicating that an ample supply of acetate allows for continuous electron transfer and stable biofilm function.

In contrast, the condition with reduced acetate (0.5C) shows a more pronounced voltage decrease over time. After the initial drop, the voltage persistently declines, reaching its lowest point (~0.5 V) by the end of the 15-day period. This pattern signifies that limited acetate hampers microbial metabolic processes, resulting in decreased electron generation and, consequently, a dip in voltage. The steep decline indicates that as acetate becomes limited, the biofilm lacks electron donors, leading to reduced electrochemical efficiency.

These observed trends underscore the vital importance of acetate concentration in ensuring stable and effective operation of MFCs. Higher acetate availability corresponds with better voltage retention by facilitating continuous microbial metabolism and electron transfer, whereas inadequate

substrate leads to voltage instability and degradation of the system. Nonetheless, while increasing acetate concentration boosts voltage output, excessively high concentrations may yield diminishing returns, as shown by the slight difference between the 1.5C and baseline conditions. Therefore, optimizing substrate concentration is crucial for striking a balance between sustained energy production and efficient substrate use in MFCs.

4.4.3 Internal Resistance

The power density-current curve of the microbial fuel cell at different internal resistances provides critical insight into the electrochemical performance of the system. The plot displays power density as a function of current for various internal resistances, including 100 Ω, 500 Ω, 1000 Ω, and 2000 Ω. Figure 19 illustrates how internal resistance influences power generation and the optimal operating conditions for maximizing energy output.

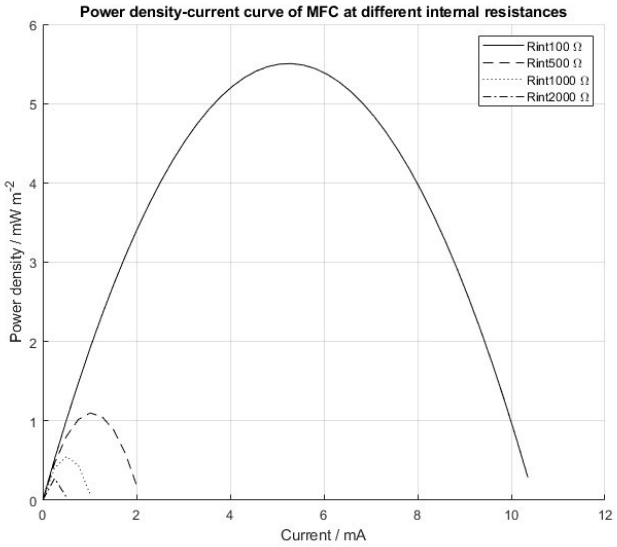


Figure 19. Power Density vs. Current under Different R_{int}

At the lowest internal resistance of 100 Ω, the power density curve shows a well-defined peak at a higher current. This indicates that the system can sustain a higher current flow while maintaining significant power output. This observation suggests that lower internal resistance facilitates efficient electron transfer, thereby reducing losses associated with charge transport. Under these conditions, the power density reaches its highest value, demonstrating that minimizing internal resistance is crucial for enhancing MFC performance. As internal resistance increases, the peak power density

decreases, and the current at which maximum power occurs shifts to lower values. The power output for 500 Ω is lower than for 100 Ω, yet it still maintains a recognizable peak. However, for 1000 Ω and 2000 Ω, power density values are significantly reduced, and the curves appear flatter, with peaks occurring at much lower current levels. This trend indicates that electron transport becomes less efficient as internal resistance rises, leading to higher voltage losses and reduced overall power generation.

The influence of internal resistance on power density highlights the importance of optimizing system design to minimize resistive losses. Reducing internal resistance enhances electron transfer efficiency, increasing power output and energy conversion efficiency. Nevertheless, in practical applications, internal resistance cannot be eliminated entirely, as it is influenced by factors such as electrode material properties, biofilm conductivity, and electrolyte composition. Therefore, decreasing internal resistance through improved electrode design, enhanced biofilm conductivity, and effective system architecture is vital for boosting MFC performance.

These results highlight that internal resistance is a limiting factor in MFC operation, impacting both peak power output and the associated optimal current. Future optimizations should concentrate on strategies to reduce internal resistance, such as employing highly conductive electrode materials, refining electrolyte composition, and improving microbial electron transfer mechanisms. By tackling these factors, MFC efficiency can be significantly enhanced, making it a more viable technology for sustainable energy generation.

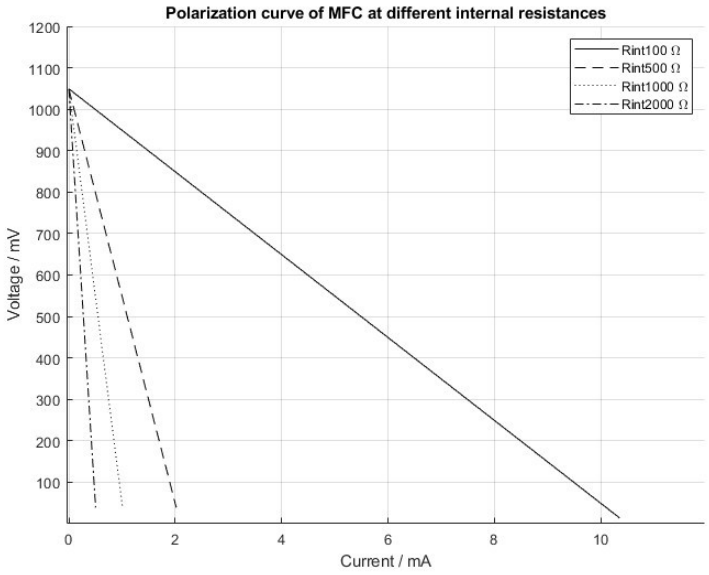


Figure 20. Polarization Curve under Different R_{int}

Figure 20 illustrates that with the lowest internal resistance of 100 Ω, voltage decreases linearly as current rises, resulting in the maximum current output under all tested conditions. This finding signifies that the system can sustain a higher electron flow with minimal resistive losses, thereby improving electrochemical performance. The notably high current in this case indicates that minimizing internal resistance enhances electron transfer efficiency, which is crucial for optimizing power generation in MFC systems. As internal resistance increases, the polarization curve becomes steeper, leading to a more rapid voltage drop with increasing current. The potential for current output is significantly reduced for internal resistances of 500 Ω, 1000 Ω, and 2000 Ω. This shows that higher internal resistance results in more significant energy losses, limiting the MFC's ability to maintain high current flow. The steep voltage decline at elevated resistances indicates that resistive losses inhibit system performance. This trend is especially striking at 2000 Ω, where the voltage nearly reaches zero at low current levels, underlining severe limitations in electron transport due to excessive resistive losses.

These results underscore how critical internal resistance is for MFC efficiency. Lower internal resistance facilitates higher current production by reducing energy losses and enhancing charge transfer efficiency within the system. In contrast, elevated internal resistance severely restricts current output, causing voltage drops and overall performance decline. The findings stress the

necessity of optimizing system elements, such as electrode materials, electrolyte conductivity, and biofilm characteristics, to lower internal resistance and improve MFC function.

4.4.4 Temperature

The microbial fuel cell's polarization and power density curves, shown below at various operating temperatures, provide insight into the system's electrochemical performance and energy output. The plot illustrates the variation in cell voltage and power density as functions of current density across a temperature range from 278 K to 303 K. The observed trends shown in Figure 21 highlight the effect of temperature on MFC efficiency, particularly concerning activation losses, ohmic resistance, and overall power generation.

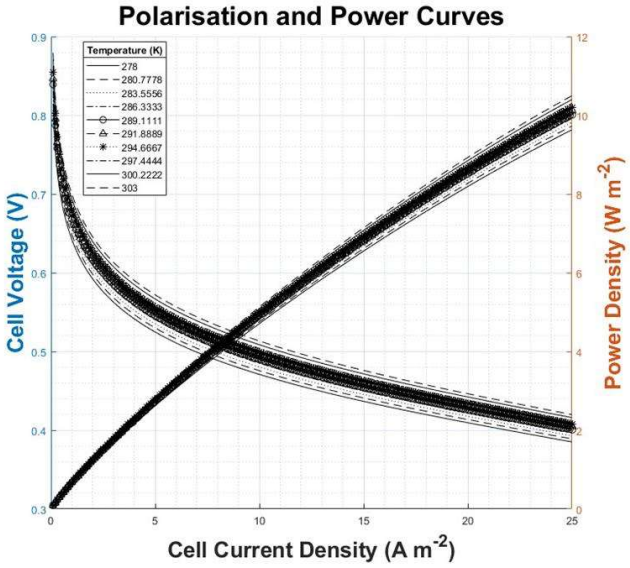


Figure 21. Polarization and Power Curve under Different T

The polarization curves, represented by cell voltage versus current density, exhibit a characteristic decline as current density increases. At lower current densities, the voltage drop is steep, indicating significant activation losses associated with the initial electron transfer reactions at the electrodes. As current density increases, the voltage decline becomes more gradual, reflecting the transition to ohmic losses, which are primarily influenced by the internal resistance of the system. The effect of temperature on polarization behavior is evident, as higher temperatures result in higher voltage at a given current density. This indicates that increased temperature enhances reaction kinetics, lowers activation energy barriers, and improves charge transport within the system. The

power density curves, plotted against current density, exhibit a typical parabolic shape, where power density increases with current density until it reaches a peak, after which it declines due to mass transport limitations. The maximum power density occurs at higher temperatures, with the peak shifting to higher current densities as temperature increases. This behavior indicates that elevated temperatures enhance microbial metabolism and electron transfer processes, leading to improved energy conversion efficiency. However, beyond a certain temperature threshold, excessive metabolic activity and increased diffusion rates may result in substrate depletion and reduced electrochemical efficiency.

The observed trends underscore the crucial role of temperature optimization in MFC operation. Higher temperatures enhance overall system performance by improving reaction kinetics and charge transfer, but excessively high temperatures could also introduce stability concerns related to microbial viability and mass transport limitations. These findings suggest that MFC efficiency can be maximized by maintaining an optimal operating temperature that balances microbial activity, substrate utilization, and electrochemical reaction rates.

4.4.5 Voltage Output

After simulating how operating factors influence MFC performance, the voltage output of the Guelph WWTP is determined. The plot illustrates the variation in battery output voltage over a 14-day period, offering insights into the stability and efficiency of energy storage in a microbial fuel cell system. The voltage initially increases, reaching a peak of approximately 505 mV within the first few days. After this stabilization phase, the voltage remains relatively constant for a significant duration before gradually declining toward the end of the experiment. This trend shown in Figure 22 suggests dynamic changes in microbial activity, substrate availability, and charge accumulation within the system.

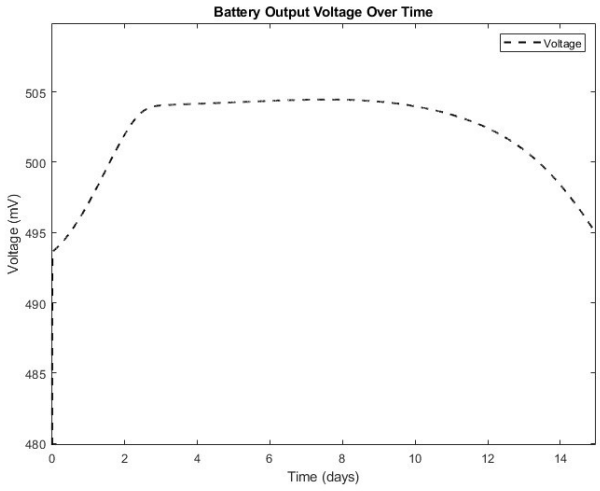


Figure 22. Battery Output Voltage over Time

During the initial phase, the increasing voltage indicates the establishment of bioelectrochemical reactions within the MFC. As microorganisms begin metabolizing organic matter, the electron transfer to the electrode becomes more efficient, leading to a rise in voltage. The rapid increase in voltage within the first few days suggests that the microbial community quickly adapts to the system conditions, attaining a stable electrogenic state. This phase is critical for MFC operation, as it determines how quickly the system reaches optimal performance. The plateau phase, where voltage remains nearly constant, signifies a stable energy output. This indicates that microbial activity has reached a steady-state condition, where substrate availability and electron transfer kinetics are well balanced. The relatively constant voltage output during this period demonstrates the MFC's efficiency in maintaining a continuous supply of electrons for power generation. This phase is crucial for the practical applications of MFC technology, as it ensures reliable and predictable power output for energy storage or direct utilization.

Towards the end of the period, the voltage begins to decline gradually, which may be attributed to substrate depletion, biofilm deterioration, or changes in system conditions such as pH fluctuations and mass transfer limitations. The decline in voltage suggests that the microbial fuel cell is experiencing reduced metabolic activity, leading to lower electron production. This phase highlights the importance of maintaining optimal conditions, such as replenishing organic substrates or optimizing flow rates, to sustain long-term energy generation.

The observed voltage trend underscores the potential of MFCs as a sustainable energy source, demonstrating stable power output over extended periods. However, the eventual decline in voltage emphasizes the need for system optimization to prolong energy production efficiency.

4.4.6 Concentration over Time

The concentration profile of various substances in the anode chamber over time, Figure 23, provides valuable insight into the metabolic dynamics of the microbial community within the microbial fuel cell. Initially, glucose is present at a high concentration, close to 0.95 kgCOD/m³, but it undergoes rapid depletion within the first two days. This suggests that fermentative bacteria actively metabolize glucose, forming intermediary metabolites such as butyrate, propionate, and acetate. The sharp decline in glucose concentration indicates that it is the primary substrate fueling microbial activity at the start of the experiment.

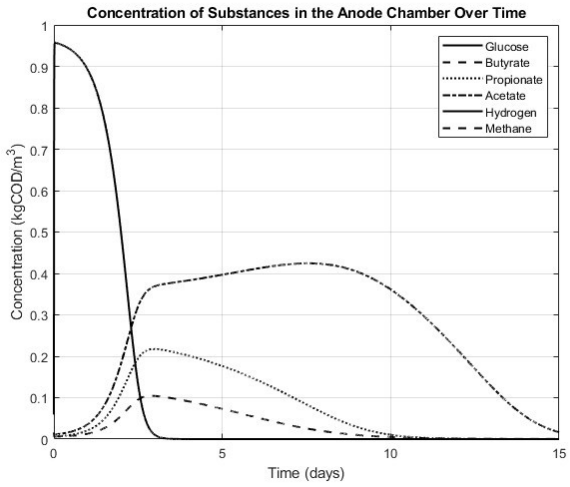


Figure 23. Concentration of Substances over Time

As glucose is consumed, the concentration of intermediate fermentation products increases. Acetate, in particular, shows the highest accumulation among the volatile fatty acids (VFAs), reaching a peak concentration of approximately 0.45 kgCOD/m³ around days 6 to 7. Butyrate and propionate also accumulate, but at lower concentrations, indicating differences in metabolic conversion rates among microbial groups. These trends suggest that fermentative pathways produce acetate as a dominant intermediate, which is a key substrate for both electrogenic bacteria and methanogens. The subsequent decline in acetate concentration after reaching its peak indicates that it

is actively consumed, either through direct electron transfer to the anode or by methanogenic conversion

The concentration of hydrogen shows an early peak before declining rapidly, indicating that hydrogenotrophic microbial processes are taking place. The low and transient levels of hydrogen suggest its utilization by electrogenic bacteria or its rapid conversion into methane. The methane concentration follows a distinct pattern, gradually increasing to a peak around days 10 to 12 before declining. This behavior corresponds to the decrease in acetate and hydrogen concentrations, indicating that both acetolactic and hydrogenotrophic methanogenesis are active in the system. The progressive rise and subsequent decrease in methane imply that methanogenic pathways become dominant after the depletion of glucose and the accumulation of VFAs.

The trends observed in the plot illustrate a sequential metabolic process in the anode chamber, beginning with glucose fermentation, then VFA accumulation, and concluding with methane production. The rapid depletion of glucose highlights its role as the primary energy source, while acetate emerges as a crucial intermediate, playing a significant role in electron transfer and methane formation. The gradual decrease in all substrate concentrations toward the end of the observed period suggests that the system reaches a quasi-stable state, where substrate availability limits further microbial activity.

4.4.7 COD

The COD removal rate of the MFC is also simulated. Figure 24 illustrates the reduction of COD in wastewater over a period of 15 days within a microbial fuel cell. COD is a crucial parameter that indicates the amount of organic matter present in the wastewater and serves as a measure of microbial degradation efficiency. The observed trend shows a gradual decline in COD concentration, underscoring the metabolic activity of microorganisms in breaking down organic substrates.

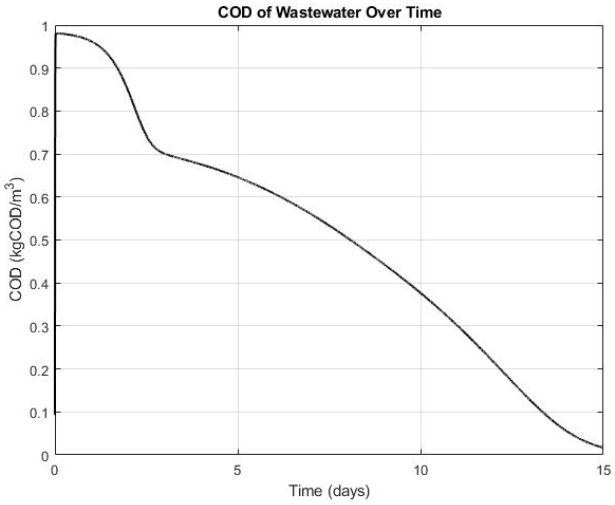


Figure 24. COD Removal over Time

During the first few days, a rapid decrease in COD is observed, suggesting active microbial metabolism as bacteria adapts to the environment and begin consuming available substrates. This phase is likely dominated by fermentative and electrogenic bacteria, which degrade complex organic matter into simpler compounds, generating electrons for bioelectricity production. Around days 3 to 5, the rate of COD removal appears to slow down, possibly due to the transformation of substrates into intermediate compounds such as volatile fatty acids (VFAs). This phase could correspond to a shift in microbial activity, during which certain intermediate products accumulate before being further degraded. The decline in COD resumes more significantly after this transition phase, suggesting that VFAs and other intermediates are subsequently consumed by electrogenic bacteria, leading to a further reduction in organic content.

After day 5, a steady and continuous decrease in COD is observed, with concentrations nearing zero by the end of the 15-day period. This indicates that microbial communities efficiently degrade the remaining organic matter, resulting in high COD removal efficiency. The gradual decrease suggests that substrate availability becomes limited, potentially reducing microbial activity towards the end of the period. This trend aligns with the expectation that as organic matter diminishes, microbial metabolism slows down, leading to lower electron transfer and power output.

The results emphasize the effectiveness of MFCs in wastewater treatment by demonstrating significant COD removal over time. The initial rapid degradation phase, followed by a stabilization

period and a subsequent continued decline, highlights the sequential metabolic pathways involved in organic matter breakdown.

The COD removal rate of the MFC was determined using simulation data, yielding a rate of 0.0633 kg COD/m³/day over a 15-day period. This figure was derived by assessing the changes in COD concentration, which decreased from 1.0 kg COD/m³ to 0.05 kg COD/m³ by the end of the 15 days. The removal efficiency from this analysis reached 95%. In comparison to the WWTP's original COD removal efficiency, derived from influent and effluent CBOD5 data in the wastewater quality tables, the removal rate calculated from the CBOD5 dataset was 0.01346 kg COD/m³/day over 15 days, based on an influent CBOD5 concentration of 204 mg/L and a 2.1 mg/L effluent CBOD5 concentration, with an assumed retention time of 15 days. The results indicate that the MFC system exhibits a significantly higher COD removal rate compared to the conventional WWTP process. The 0.0633 kg COD/m³/day removal rate of the MFC is nearly 4.7 times higher than the 0.01346 kg COD/m³/day removal rate observed in the WWTP. This suggests that MFC technology has the potential to offer superior organic pollutant degradation capabilities, making it an efficient alternative for wastewater treatment.

4.4.8 Monte Carlo-Based Uncertainty Analysis of MFC Performance

Microbial fuel cells are inherently complex bioelectrochemical systems influenced by biological variability, material properties, and operational conditions. While deterministic simulations provide insights into the relationships between parameters and outputs, they often overlook the uncertainty present in real-world implementations. This chapter introduces a Monte Carlo simulation approach to capture the sensitivity and robustness of MFC performance in the presence of uncertain inputs. The goal is to quantify how fluctuations in key parameters—reaction rate constant k_{bio}, external resistance R, and biofilm thickness L_f influence critical outputs: current, voltage, and power density.

These parameters were chosen based on sensitivity analyses conducted in earlier simulations, as well as their representation in the governing electrochemical and transport equations of the system. The selection also reflects practical considerations, including the variability in microbial kinetics, operational load settings, and dynamic biofilm growth observed in laboratory and field-scale MFC systems.

The uncertain parameters were modeled as independent normally distributed variables. The mean values were chosen based on baseline simulation inputs, while the standard deviations were

selected to represent approximately ±20% variation, capturing expected fluctuations due to experimental variability, environmental conditions, and operational constraints. The distributions are summarized in Table 7.

Table 7. Summary of Input Parameters Considered in Monte Carlo Uncertainty Analysis

Parameter	Symbol	Mean Value	Standard Deviation	Unit	Justification
Reaction rate constant	k_{bio}	0.05	0.01	$mol \cdot m^{-2} \cdot h^{-1}$	Reflects biofilm activity, substrate composition, and microbial kinetics.
External resistance	R	10,000	2,000	Ω	Represents variability in external circuitry and load resistance.
Biofilm thickness	L_f	5.0×10^{-5}	1.0×10^{-5}	m	Captures effects of biofilm growth, shear, and substrate diffusion.

A total of 1000 Monte Carlo iterations were performed. In each simulation run, the values of k_{bio}, R, and L_f were randomly sampled from their respective distributions. These sampled parameters were then input into the simplified electrochemical model, which was consistent with the framework described in Chapter 4. The distributions of output variables—current, voltage, and power density—were visualized using histograms, and the influence of each uncertain input on each output was assessed using scatter plots.

The current distribution, Figure 25, demonstrated a moderately right-skewed shape, with most simulated values clustering near the mean and a tail extending toward lower current values. This skewness reflects the influence of high resistance samples within the Monte Carlo iterations, which reduce the current according to Ohm's law. In contrast, lower-resistance simulations yielded notably higher current outputs, consistent with the expected inverse relationship between external resistance and electron flow.

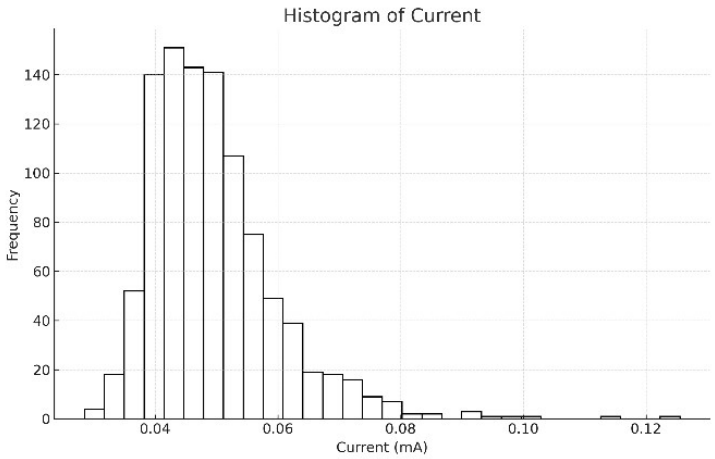


Figure 25. Histogram of Simulated Current Outputs Across 1000 Monte Carlo Iterations

Voltage output exhibited a narrower and more symmetrical distribution, shown in Figure 26, indicating that it is less susceptible to variability in the selected parameters. This stability is primarily due to the relatively fixed values of the cathodic potential and internal resistance within the system. Although the anode potential is affected by both k_{bio} and L_f, the voltage drop across the internal circuit is partially constrained, resulting in a narrower range of voltage values. Small variations were still observed and were primarily attributable to differences in reaction rates and minor shifts in activation overpotentials.

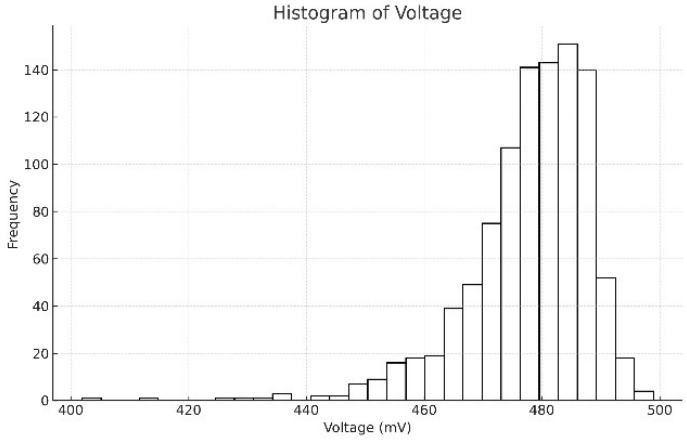


Figure 26. Histogram of Simulated Cell Voltage Values from Monte Carlo Simulations

Power density, being a function of both voltage and current, displayed the broadest distribution shown in Figure 27. The histogram revealed a bell-shaped curve with an extended tail

toward lower values. This variability is a direct consequence of the multiplicative nature of power calculation, where small changes in either current or voltage compound to yield significant differences in energy output. Simulations involving high resistance or thick biofilms consistently appeared in the lower end of the distribution, confirming the compounded performance penalty associated with these conditions.

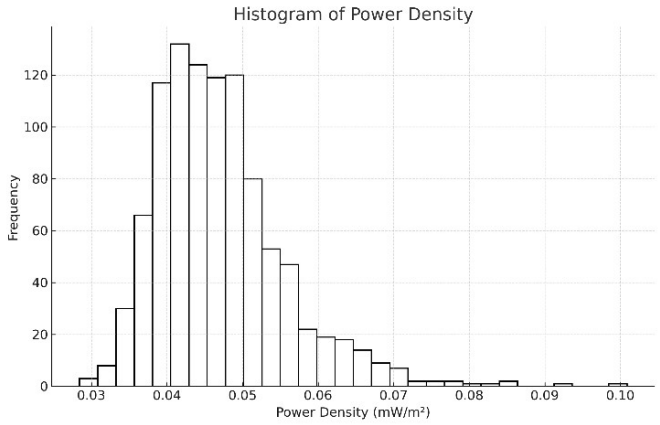


Figure 27. Histogram of Power Density Output from Monte Carlo Simulations

To better understand how each input parameter individually influenced system outputs, scatter plots were constructed comparing each parameter to each output metric.

The relationship between k_{bio} and current, shown in Figure 27, revealed a positive trend, though not strictly linear. Higher reaction rates were associated with increased electron transfer, thereby improving current output. This trend reflects the embedded kinetic relationships within the anode reaction model, where faster microbial metabolism reduces activation losses and promotes greater substrate consumption. The corresponding voltage values showed a weaker but still positive trend with k_{bio} , indicating that improved kinetics modestly enhance anode potential. Power density exhibited a clearer positive relationship with k_{bio}, aligning with the increased energy production from more efficient electrochemical conversion.

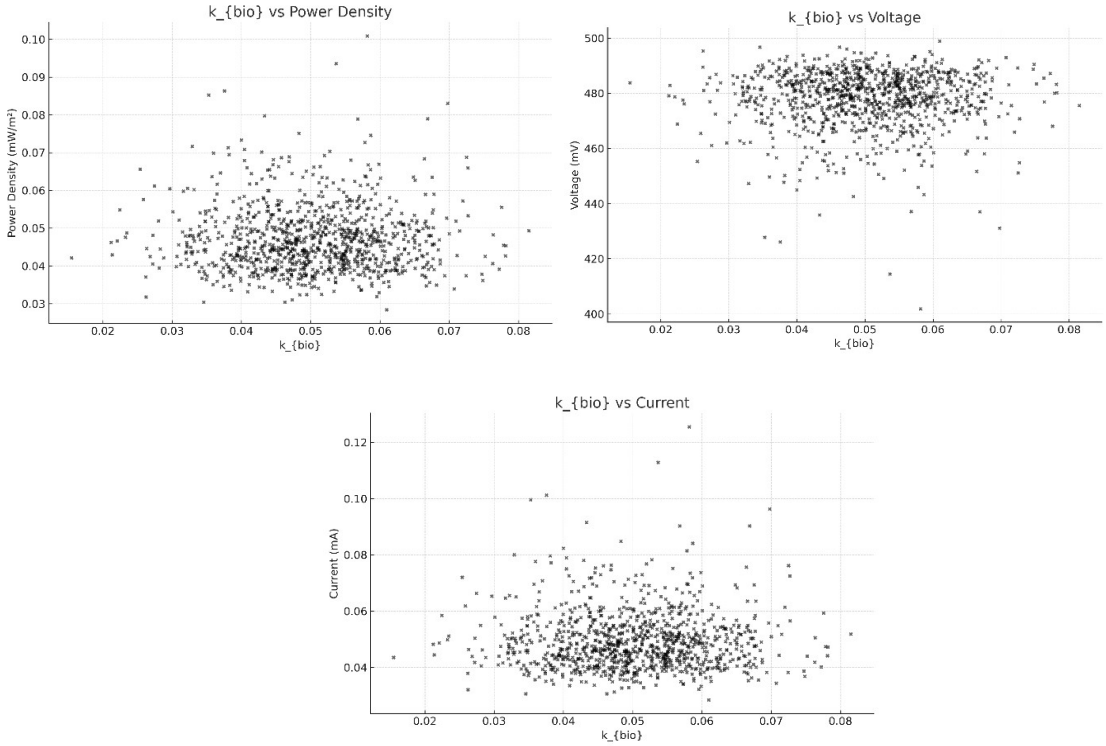


Figure 28. Scatter Plot Showing the Relationship between k_{bio} and Power Density, Voltage and Current

The effect of external resistance on MFC performance was pronounced across all three-output metrics shown in Figure 29. A strong inverse relationship was observed between resistance and current, affirming that increased circuit impedance substantially restricts electron flow. This linear trend is governed directly by Ohm's law and confirms the dominant role of external resistance in shaping electrical output. Voltage also declined with increasing resistance, although the rate of decrease was somewhat dampened due to the stabilizing effect of the fixed cathodic and internal resistances. Power density was highly sensitive to resistance, with higher values of R consistently producing lower energy output. The combined reduction in current and voltage across high-resistance scenarios underscores the detrimental impact of excessive load on system performance.

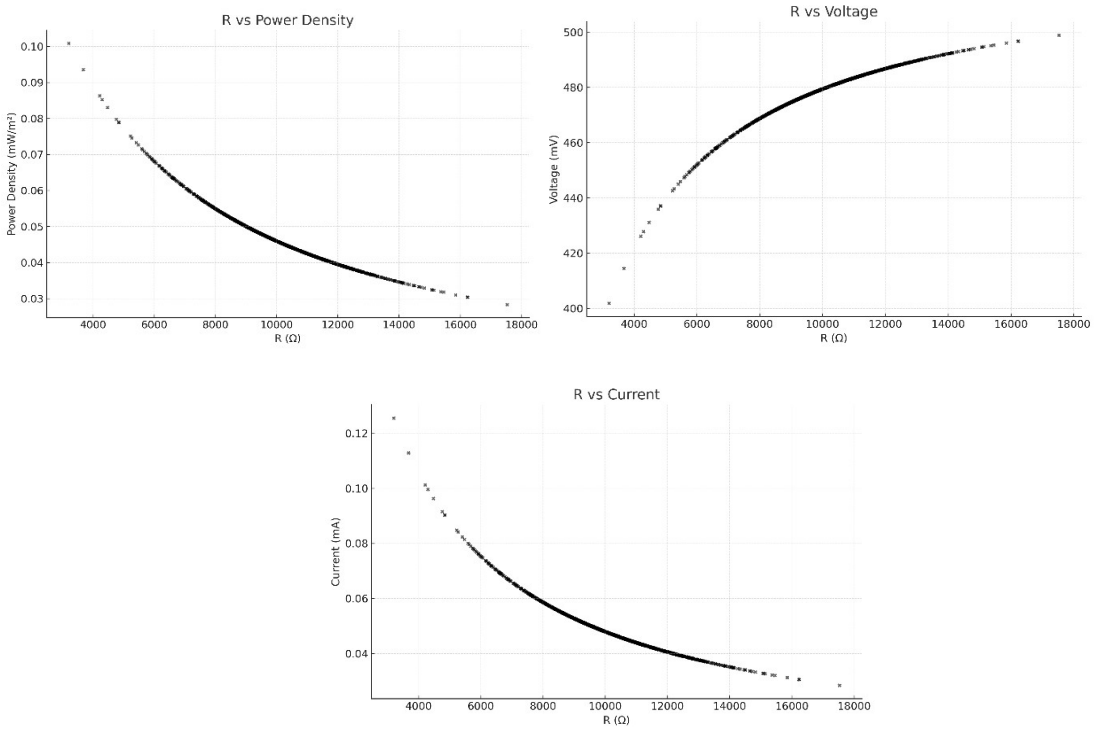


Figure 29. Scatter Plot Showing the Relationship between R and Power Density, Voltage and Current

Biofilm thickness exhibited a more nuanced influence on MFC behavior shown in Figure 30. Current output displayed a mild negative correlation with increasing L_f, indicating that thicker biofilms impose diffusion barriers and elevate internal transport resistance. These conditions reduce the rate of substrate oxidation and impede effective electron transfer to the anode. Voltage was less responsive to changes in biofilm thickness, with only minor deviations observed across the simulation space. Power density followed a similar trend to current, decreasing gradually with thicker biofilms. This behavior is consistent with the theoretical expectation that excessive biofilm accumulation limits the electroactive zone and diminishes both microbial efficiency and electron availability.

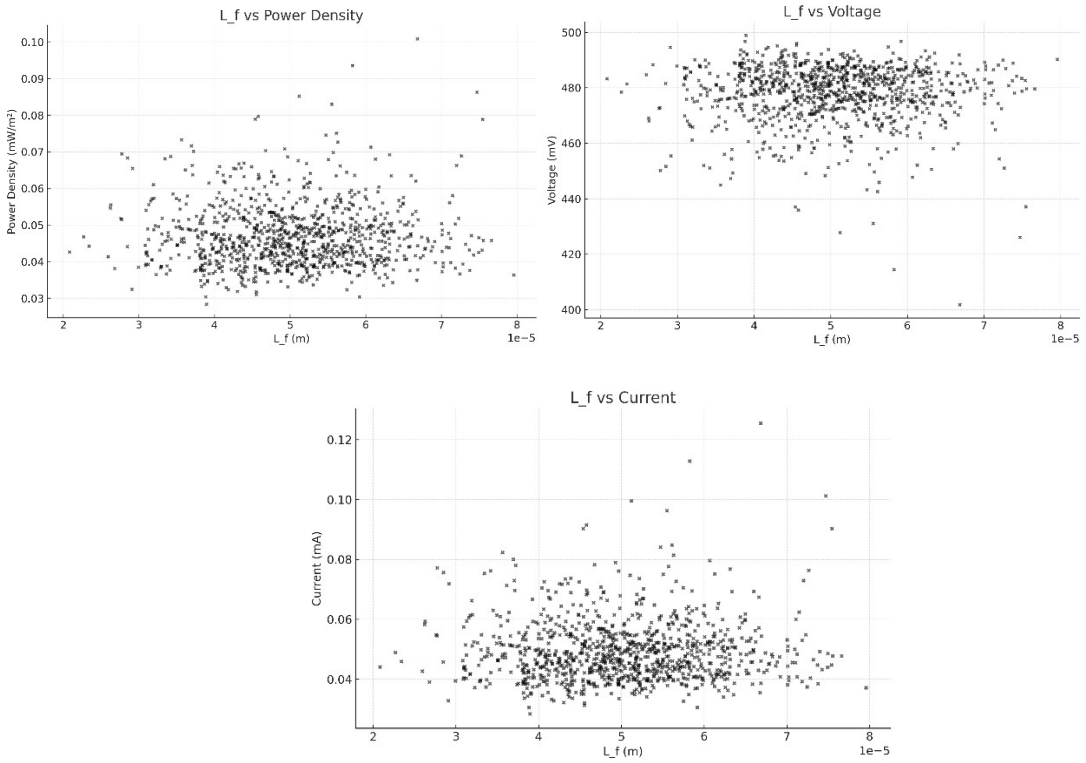


Figure 30. Scatter Plot Showing the Relationship between L_f and Power Density, Voltage and Current

In summary, the visualization of simulation results highlights distinct patterns in how uncertainty affects model predictions. Resistance emerged as the most influential parameter, with a clear and substantial impact on all outputs. The bioelectrochemical reaction rate played a secondary but important role, particularly in enhancing current and power density under favourable kinetic conditions. Biofilm thickness had a moderate effect, primarily limiting performance through increased mass transfer resistance. These graphical results not only validate the sensitivity trends observed in deterministic simulations but also underscore the robustness of the model in capturing realistic system dynamics across a probabilistic parameter space.

4.4.9 Conclusion

This chapter investigated the simulation results of a dual-chamber microbial fuel cell model, focusing on various influencing factors. These factors include the initial glucose concentration, internal resistance of the cell, wastewater flow rate, and temperature, all of which affect the performance of the cell, as well as the concentration, voltage, and COD removal efficiency of wastewater during the cell's operation cycle. The underlying principles were analyzed using model equations. The main conclusions are as follows:

1. The established dual-chamber MFC model can calculate and determine the concentration of substances in the anode and cathode chambers, the COD of the wastewater, and the trends in the cell's current and output voltage over time.
2. For the dual-chamber MFC, increasing the initial glucose concentration is beneficial for enhancing the operating voltage and extending the stable discharge duration of the cell. However, it has a limited impact on the cell's overall performance.
3. When the external resistance is set at an optimal value, reducing the cell's internal resistance increases the operating voltage of the dual-chamber MFC and significantly enhances the maximum power density. Lowering the internal resistance is an effective way to improve the performance of the dual-chamber MFC. Therefore, finding new electrode materials to reduce internal resistance is a crucial approach to enhancing the performance of dual-chamber MFCs.
4. In the dual-chamber configuration, increasing the wastewater flow rate is beneficial for improving the maximum power density of the cell. Further increases in the flow rate led to additional improvements in the maximum power density.
5. The MFC system demonstrated a COD removal rate of 0.0633 kg COD/m^3/day—approximately 4.7 times higher than the 0.01346 kg COD/m^3/day observed in the WWTP—indicating its superior efficiency in organic pollutant degradation and potential as an advanced wastewater treatment alternative.

These findings highlight the importance of optimizing operational parameters and material properties to enhance the performance of dual-chamber MFCs for wastewater treatment and energy recovery.

Chapter 5 Conclusion

This research presents a comprehensive numerical modeling approach to optimize the performance of microbial fuel cells for wastewater treatment. While MFCs offer a promising bioelectrochemical alternative to conventional treatment methods, their widespread application is hindered by challenges such as low power output, charge imbalances, and high operational costs. This study developed and applied mathematical models to address these issues to analyze key operational parameters, predict MFC behavior under varying conditions, and propose optimization strategies for improved efficiency and scalability.

A steady-state model was constructed to simulate the interactions between microbial communities, electrochemical reactions, and mass transport phenomena within an MFC. The model solved mass balance equations for critical species, including acetate, protons, oxygen, and carbon dioxide using finite difference methods. The simulations provided insights into the influence of parameters such as substrate concentration, internal resistance, wastewater flow rate, and temperature on system performance. By comparing the model predictions to experimental data, the study demonstrated a high degree of accuracy in replicating real-world MFC behavior, validating the model's applicability for performance optimization.

The modeling framework was further extended to assess the feasibility of integrating MFC technology into a full-scale wastewater treatment plant, specifically the Guelph Water Resource Recovery Centre. The simulations indicated that MFCs could achieve a significantly higher chemical oxygen demand removal rate (0.0633 kg COD/m^3/day), approximately 4.7 times greater than the existing WRRC treatment processes. This underscores the potential of MFCs to enhance pollutant degradation while simultaneously recovering energy from wastewater.

In addition to the deterministic simulations, a Monte Carlo uncertainty analysis was conducted to evaluate the sensitivity of key MFC performance outputs—current, voltage, and power density—to variations in bioelectrochemical reaction rate, external resistance, and biofilm thickness. This probabilistic approach revealed that external resistance exerts the greatest influence on output variability, followed by microbial kinetics and biofilm morphology. The consistency of these trends with electrochemical theory and deterministic predictions reinforces the robustness and predictive strength of the developed numerical model. By incorporating stochastic variability, the simulation

framework more closely reflects real-world conditions, offering a more reliable basis for designing and optimizing MFC systems in wastewater treatment applications.

Despite these promising results, the models also revealed several challenges associated with large-scale MFC deployment. Oxygen transport limitations, internal resistance effects, and pH imbalances were identified as significant factors restricting overall performance. The study explored potential solutions, including optimized electrode materials, improved reactor configurations, and dynamic operational strategies, to mitigate these issues and enhance MFC efficiency. By demonstrating the power of numerical modeling in understanding and improving MFC performance, this research contributes to the ongoing efforts to develop sustainable wastewater treatment solutions.

While this research demonstrates the effectiveness of numerical modeling in optimizing microbial fuel cell performance, several limitations must be acknowledged. The models developed in this study were based on idealized assumptions, including uniform biofilm growth, constant operational temperature, and simplified mass transfer dynamics. In practical systems, variations in microbial community behavior, fluctuating environmental conditions, and complex substrate compositions could lead to deviations from model predictions. Moreover, the electrochemical parameters and microbial kinetics were primarily derived from literature values, which may not fully capture site-specific variations or long-term operational dynamics. Although the model successfully captured key trends in MFC performance, scaling the framework from laboratory to full-scale applications may introduce additional challenges related to oxygen transport limitations, internal resistance, and pH control. These limitations highlight the need for further experimental validation and model refinement to improve predictive accuracy under real-world conditions.

Future research should focus on enhancing the robustness and applicability of the developed modeling framework. Integrating real-time monitoring data into the simulation environment could enable dynamic calibration, allowing the model to adapt to operational fluctuations and improve predictive reliability. The application of machine learning techniques, such as predictive analytics and adaptive control algorithms, offers a promising approach to optimizing MFC performance in complex wastewater treatment scenarios. Additionally, further investigation into alternative electrode and membrane materials—with improved conductivity, chemical stability, and biofouling resistance—is essential to mitigate internal resistance and oxygen transport limitations. Pilot-scale experiments across diverse wastewater compositions and environmental conditions will be critical to validate

model predictions and evaluate system scalability and long-term stability. By addressing these research directions, future work can accelerate the practical deployment of MFCs as a sustainable and energy-efficient solution for wastewater treatment.

.

References

Adelaja, O., Keshavarz, T., & Kyazze, G. (2015). The effect of salinity, redox mediators and temperature on anaerobic biodegradation of petroleum hydrocarbons in microbial fuel cells. *Journal of Hazardous Materials, 283*, 211-217. doi:https://doi.org/10.1016/j.jhazmat.2014.08.066

Aelterman, P., Rabaey, K., Pham, H., Boon, N., & Verstraete, W. (2006). Continuous Electricity Generation at High Voltages and Currents Using Stacked Microbial Fuel Cells. *Environmental Science & Technology, 40*(10), 3388-3394. doi: 10.1021/es0525511

Aelterman, P., Versichele, M., Marzorati, M., Boon, N., & Verstraete, W. (2008). Loading rate and external resistance control the electricity generation of microbial fuel cells with different three-dimensional anodes. *Bioresource Technology, 99*(18), 8895-8902. Retrieved from https://doi.org/10.1016/j.biortech.2008.04.061

Ahmadian-Alam, L., & Mahdavi, H. (2018). A novel polysulfone-based ternary nanocomposite membrane consisting of metal-organic framework and silica nanoparticles: As proton exchange membrane for polymer electrolyte fuel cells. *Renewable Energy, 126*, 630-639. doi:10.1016/j.renene.2018.03.075

Ahn, Y., & Logan, B. (2010). Effectiveness of domestic wastewater treatment using microbial fuel cells at ambient and mesophilic temperatures. *Bioresource Technology, 101*, 469-475. doi:10.1016/j.biortech.2009.07.039

Ahn, Y., & Logan, B. E. (2012). A multi-electrode continuous flow microbial fuel cell with separator electrode assembly design. *Applied Microbiology and Biotechnology, 93*, 2241–2248. Retrieved from https://doi.org/10.1007/s00253-012-3916-4

Atanassov, P., Banta, S., Barton, S. C., Cooney, M., & Liaw, B. (2007). Enzymatic Biofuel Cells. *The Electrochemical Society Interface*. doi:10.1149/2.F04072IF

Baker, B., Aldridge, C., & Omer, A. (2016). Water: availability and use. *Mississippi State University Extension*.

Banu, R. J., Ushani, U., & Yukesh Kannah, R. (2017). Activated Sludge Process and Energy. In *Optimization and Applicability of Bioprocesses* (pp. 187-210).

Behera, M., & Ghangrekar, M. (2009). Performance of microbial fuel cell in response to change in sludge loading rate at different anodic feed pH. *Bioresour Technol, 100*(21), 5114-5121. doi:10.1016/j.biortech.2009.05.020

Behera, M., & Ghangrekar, M. (2009). Performance of microbial fuel cell in response to change in sludge loading rate at different anodic feed pH. *Bioresource Technology, 100*(21), 5114-5121. doi:https://doi.org/10.1016/j.biortech.2009.05.020

Behera, M., Jana, P., More, T., & Ghangrekar, M. (2010). Rice mill wastewater treatment in microbial fuel cells fabricated using proton exchange membrane and earthen pot at different pH. *Bioelectrochemistry, 79*(2), 228-233. doi:https://doi.org/10.1016/j.bioelechem.2010.06.002

Behera, S., Kumari, U., Shankar, R., & Mondal, P. (2018). Performance analysis of a double-chambered microbial fuel cell employing a low-cost sulfonated polystyrene proton exchange membrane. *Ionics, 24*(11), 3573-3590. doi:10.1007/s11581-018-2480-z

Bimastyaji, S. R. (2017). Challenges and opportunities of microbial fuel cells (MFCs) technology development in Indonesia. *Sriwijaya International Conference on Engineering, Science and Technology . 101.* MATEC Web of Conferences. doi:https://doi.org/10.1051/matecconf/201710102018

Bobade, V., & Lomte, A. (2015). Challenges in UASB reactor system design: A Review. *APCChE 2015 Congress incorporating Chemeca 2015.* Melbourne, Victoria.

Bohn, I., Björnsson, L., & Mattiasson, B. (2007). EFFECT OF TEMPERATURE DECREASE ON THE MICROBIAL POPULATION AND PROCESS PERFORMANCE OF A MESOPHILIC ANAEROBIC BIOREACTOR. *Environmental Technology, 28*(8). doi:https://doi.org/10.1080/09593332808618843

Brown, J. L. (2012). Fuel Cells Treat Wastewater, Generate Electricity. *Civil Engineering Magazine Archive, 82*(7). doi:https://doi.org/10.1061/ciegag.0000643

Capodaglio, A. G., Cecconet, D., & Molognoni, D. (2017). An integrated mathematical model of microbial fuel cell processes: Bioelectrochemical and microbiologic aspects. *Processes, 5*(4). doi:10.3390/pr5040073

Carrette, L., Friedrich, K., & Stimming, U. (2001). *Fuel Cells.*

Chao, D., Zhou, W., Xie, F., Ye, C., Li, H., Jaroniec, M., & Qiao, S.-Z. (2020). Roadmap for advanced aqueous batteries: From design of materials to applications. *Science Advances, 5*(10). doi:10.1126/sciadv.aax4279

Chauhan, S., Sharma, V., Varjani, S., Sindhu, R., & Bhargava, P. (2022). Mitigation of tannery effluent with simultaneous generation of bioenergy using dual chambered microbial fuel cell. *Bioresource Technology, 351*, 127084. Retrieved from https://doi.org/10.1016/j.biortech.2022.127084

Cheng, S., Liu, H., & Logan, B. E. (2006). Increased performance of single-chamber microbial fuel cells using an improved cathode structure. *Electrochemistry Communications, 8*, 489-494.

Choi, C., & Cui, Y. (2012). Recovery of silver from wastewater coupled with power generation using a microbial fuel cell. *Bioresource Technology, 107*, 522-525. doi:https://doi.org/10.1016/j.biortech.2011.12.058

Chokshi, K., Pancha, I., Ghosh, A., & Mishra, S. (2016). Microalgal biomass generation by phycoremediation of dairy industry wastewater: An integrated approach towards sustainable biofuel production. *Bioresource Technology, 221*, 455-460. Retrieved from https://doi.org/10.1016/j.biortech.2016.09.070

Clauwaert, P., Aelterman, P., Pham, T. H., De Schamphelaire, L., Carballa, M., Rabaey, K., & Verstraete, W. (2008). Minimizing losses in bio-electrochemical systems: the road to applications. *Appl Microbiol Biotechnol, 79*, 901-913. Retrieved from https://doi.org/10.1007/s00253-008-1522-2

Clauwaert, P., van der Ha, D., Boon, N., Verbeken, K., Verhaege, M., Rabaey, K., & Verstraete, W. (2007). Open Air Biocathode Enables Effective Electricity Generation with Microbial Fuel Cells. *Environmental Science & Technology, 41*(21), 7564-7569.

Corbella, C., & Puigagut, J. (2018). Improving domestic wastewater treatment efficiency with constructed wetland microbial fuel cells: Influence of anode material and external resistance.

Science of The Total Environment, 631-632, 1406-1414. Retrieved from https://doi.org/10.1016/j.scitotenv.2018.03.084

CPCB. (2021). *National Inventory of Sewage Treatment Plants.* Retrieved May 2024, from https://cpcb.nic.in/openpdffile.php?id=UmVwb3J0RmlsZXMvMTIyOF8xNjE1MTk2MzIyX21lZGlhcGhvdG85NTY0LnBkZg

Daud, M. K., Rizvi, H., Akram, M. F., Ali, S., Rizwan, M., Nafees, M., & Jin, Z. (2018). Review of Upflow Anaerobic Sludge Blanket ReactorTechnology: Effect of Different Parameters and Developmentsfor Domestic Wastewater Treatment. *Journal of Chemistry*. Retrieved from https://doi.org/10.1155/2018/1596319

del Campo, A., Lobato, J., Cañizares, P., Rodrigo, M., & Fernandez Morales, F. (2013). Short-term effects of temperature and COD in a microbial fuel cell. *Applied Energy, 101*, 213-217. doi:10.1016/j.apenergy.2012.02.064

Dhote, J., Ingoleb, S., & Chavhana, A. (2012). REVIEW ON WASTEWATER TREATMENT TECHNOLOGIES. *International Journal of Engineering Research & Technology, 1*(5).

Divya Priya, A., & Pydi Setty, Y. (2019). Cashew apple juice as substrate for microbial fuel cell. *Fuel, 246*, 75-78. doi:10.1016/j.fuel.2019.02.100

Do, M., Ngo, H., Guo, W., Liu, Y., Chang, S., Nguyen, D., . . . Ni, B. (2018). Challenges in the application of microbial fuel cells to wastewater treatment and energy production: A mini review. *Science of The Total Environment, 639*, 910-920. doi:https://doi.org/10.1016/j.scitotenv.2018.05.136

Dun, J., Hu, Y., Bi, Z., & Cao, Y. (2009). Improved performance of air-cathode single-chamber microbial fuel cell for wastewater treatment using microfiltration membranes and multiple sludge inoculation. *Journal of Power Sources, 187* , 471-479. doi:10.1016/j.jpowsour.2008.11.022

Falk, M., Narvμez Villarrubia, C., Babanova, S., Atanassov, P., & Shleev, S. (2013). Biofuel Cells for Biomedical Applications: Colonizing theAnimal Kingdom. *ChemPhysChem, 14*(10), 2005-2347. doi:10.1002/cphc.201300044

Fan, Y., Hu, H., & Liu, H. (2007). Enhanced Coulombic efficiency and power density of air-cathode. *Journal of Power Sources, 171*, 348-354.

Fan, Y., Hu, H., & Liu, H. (2007). Enhanced Coulombic efficiency and power density of air-cathode microbial fuel cells with an improved cell configuration. *Journal of Power Sources, 171*, 348-354.

Farissi, S., Ramesh, S., Muthuchamy, M., & Muthukumar, A. (2022). Chapter 4 - Biodegradation and photocatalysis of pharmaceuticals in wastewater. In M. Shah, S. Rodriguez-Couto, & R. Kapoor, *Development in Wastewater Treatment Research and Processes* (pp. 69-97). Elsevier. Retrieved from https://doi.org/10.1016/B978-0-323-85657-7.00007-9

Fernandes, H., Jungles, M., Hoffmann, H., Antonio, R., & Costa, R. (2013). Full-scale sequencing batch reactor (SBR) for domestic wastewater: Performance and diversity of microbial communities. *Bioresource Technology, 132*, 262-268. Retrieved from https://doi.org/10.1016/j.biortech.2013.01.027

Fraiwan, A., & Choi, S. (2016). A stackable, two-chambered, paper-based microbial fuel cell. *Biosensors and Bioelectronics*, 27-32. doi:10.1016/j.bios.2016.04.025

Galvani, L., & Aldini, J. (1792). *De viribus electricitatis.* W. Junk.

Ge, Z., Zhang, F., Grimaud, J., Hurst, J., & He, Z. (2013). Long-term investigation of microbial fuel cells treating primary sludge or digested sludge. *Bioresource Technology, 136*, 506-514. doi:10.1016/j.biortech.2013.03.016

Geng, Y., Yuan, L., Liu, T., Li, Z., Zheng, X., & Sheng, G. (2020). Thermal/alkaline pretreatment of waste activated sludge combined with a microbial fuel cell operated at alkaline pH for efficient energy recovery. *Applied Energy*, 115291. doi:10.1016/j.apenergy.2020.115291

Ghasemi, M., Sedighi, M., & Usefi, M. M. (2022). A comprehensive review on membranes in microbial desalination cells; processes, utilization, and challenges. *International Journal of Energy Research, 46*, 14716-14739. doi:10.1002/er.8265

Gorbunov, A., Jost, O., Pompe, W., & Graff, A. (2002). Solid–liquid–solid growth mechanism of single-wall carbon nanotubes. *Carbon, 40*, 113-118.

Gude, V. G. (2016). Wastewatertreatment inmicrobial fuelcellseanoverview. *JournalofCleanerProduction, 122*, 287-307. Retrieved from https://doi.org/10.1016/j.jclepro.2016.02.022

Guelph, C. o. (2022). *Annual Performance Report* . guelph.

Gulamhussein, M., & Randall, D. G. (2020). Design and operation of plant microbial fuel cells using municipal sludge. *Journal of Water Process Engineering, 38*. doi:10.1016/j.jwpe.2020.101653

Haavisto, J., Kokko, M., Lay, C.-H., & Puhakka, J. (2017). Effect of hydraulic retention time on continuous electricity production from xylose in up-flow microbial fuel cell. *International Journal of Hydrogen Energy, 42*(45), 27494-27501. Retrieved from https://doi.org/10.1016/j.ijhydene.2017.05.068

Hamedani, E., Abasalt, A., & Talebi, S. (2024). Application of microbial fuel cells in wastewater treatment and green energy production: A comprehensive review of technology fundamentals and challenges. *Fuel, 370*. doi:https://doi.org/10.1016/j.fuel.2024.131855

Hang, T.-J., Chang, Y.-H., Chao, W.-L., Jane, W.-N., & Chang, Y.-T. (2018). Effect of hydraulic retention time on electricity generation using a solid plain-graphite plate microbial fuel cell anoxic/oxic process for treating pharmaceutical sewage. *Journal of Environmental Science and Health, 53*(13), 1185–1197. doi:10.1080/10934529.2018.1530338

Hassan, M., Kanwal, S., Singh, R., S.A, M., Anwar, M., & Zhao, C. (2024). Current challenges and future perspectives associated with configuration of microbial fuel cell for simultaneous energy generation and wastewater treatment. *International Journal of Hydrogen Energy, 50*, 323-350. Retrieved from https://doi.org/10.1016/j.ijhydene.2023.08.134

He, C.-S., Mu, Z.-X., Yang, H.-Y., Wang, Y.-Z., Mu, Y., & Yu, H.-Q. (2015). Electron acceptors for energy generation in microbial fuel cells fed with wastewaters: A mini-review. *Chemosphere, 140*, 12-17. doi:https://doi.org/10.1016/j.chemosphere.2015.03.059

He, Z., Huang, Y., Manohar, A. K., & Mansfeld, F. (2008). Effect of electrolyte pH on the rate of the anodic and cathodic reactions in an air-cathode microbial fuel cell. *Bioelectrochemistry, 74*(1), 78-82. doi:10.1016/j.bioelechem.2008.07.007

Hena, S., Fatimah, S., & Tabassum, S. (2015). Cultivation of algae consortium in a dairy farm wastewater for biodiesel production. *Water Resources and Industry, 10*, 1-14. Retrieved from https://doi.org/10.1016/j.wri.2015.02.002

Hernandez-Flores, G., Poggi-Varaldo, H., Solorza-Feria, O., Ponce-Noyola, M., Romero-Casta~ non, T., Rinderknecht-Seijas, N., & Galı´ndez-Mayer, J. (2015). Characteristics of a single chamber microbial fuel cell equipped with a low cost membrane. *International Journal of Hydrogen Energy, 40*, 17380-17387.

Hoanga, A., Nizetic, S., Ngc, K., Papadopoulosd, A., Le, A., Kumar, S., . . . Pham, V. (2022). Microbial fuel cells for bioelectricity production from waste as sustainable prospect of future energy sector. *Chemosphere*. doi:10.1016/j.chemosphere.2021.132285

Huang, L., Zeng, R. J., & Angelidaki, I. (2008). Electricity production from xylose using a mediator-less microbial fuel cell. *Bioresource Technology*, 4178–4184. Retrieved from https://doi.org/10.1016/j.biortech.2007.08.067

Ishii, S., Watanabe, K., Yabuki, S., Logan, B. E., & Sekiguchi, Y. (2008). Comparison of electrode reduction activities of Geobacter sulfurreducens and an enriched consortium in an air-cathode microbial fuel cell. *Applied and Environmental Microbiology, 74*(23), 7348-7355. doi:10.1128/AEM.01639-08

IWA. (2005). *Anaerobic Digestion Model No.1 (ADM1).* IWA Publishing. doi:https://doi.org/10.2166/9781780403052

Jadhav, D. A., Ghosh Ray, S., & Ghangrekar, M. M. (2017). Third generation in bio-electrochemical system research – A systematic review on mechanisms for recovery of valuable by-products from wastewater. *Renewable and Sustainable Energy Reviews, 76*, 1022-1031. doi:10.1016/j.rser.2017.03.096

Jiang , J., Zhao, Q., Wei, L., & Wang, K. (2010). Extracellular biological organic matters in microbial fuel cell using sewage sludge as fuel. *Water Research, 44*, 2163-2170. doi:10.1016/j.watres.2009.12.033

Jothinathan, D., Pandey, A., Choure, K., & Rathinavel, L. (2024). Microbial Fuel Cell for the Treatment of Wastewater Pollutants and Resource Recovery. In R. Selvasembian, J. Mal, S. Das, D. Verma, & I. Anastopoulos, *Emerging Trends in Microbial Electrochemical Technologies for Sustainable Mitigation of Water Resources Contamination* (pp. 133–157). Springer, Cham. Retrieved from https://doi.org/10.1007/978-3-031-74636-9_6

Jung, S. P., & Pandir, S. (2019). Important Factors Influencing Microbial Fuel Cell Performance. *Microbial Electrochem Technol*, 377-406. doi: 10.1016/B978-0-444-64052-9.00015-7

Karthikeyan, R., Wang, B., Xuan, J., Wong, J., Lee, P., & Leung, M. (2015). Interfacial electron transfer and bioelectrocatalysis of carbonized plant material as effective anode of microbial fuel cell. *Electrochimica Acta, 157*, 314-323. doi:https://doi.org/10.1016/j.electacta.2015.01.029

Katuri, K. P., Scott, K., Head, I. M., Picioreanu, C., & Curtis, T. P. (2011). Microbial fuel cells meet with external resistance. *Bioresource Technology, 102*(3), 2758-2766. Retrieved from https://doi.org/10.1016/j.biortech.2010.10.147

Khandaker, S., Das, S., Hossain, M., Islam, A., Miah, M., & Awual, M. (2021). Sustainable approach for wastewater treatment using microbial fuel. *Journal of Molecular Liquids*. doi: Khandaker), awual75@yahoo.com (M.R. Awual).

Kiani Raad, N., Farrokhi, F., Alireza Mousavi, S., Darvishi, P., & Mahmoudi, A. (2020). Simultaneous power generation and sewage sludge stabilization using an air cathode-MFCs. *Biomass and Bioenergy, 140*, 105642. doi:10.1016/j.biombioe.2020.105642

Kim , M., Iwuchukwu, I., Wang, Y., Shin, D., Sanseverino, J., & Frymier, P. (2011). An analysis of the performance of an anaerobic dual anode-chambered microbial fuel cell. *Journal of Power Sources, 196*, 1909–1914. doi:10.1016/j.jpowsour.2010.09.064

Kim, H., Park, H., Hyun, M., Chang, I., Kim, M., & Kim, B. (2002). A mediator-less microbial fuel cell using a metal reducing bacterium,Shewanella putrefaciens. *Enzyme and Microbial Technology*, 14-152.

Kim, J., Jung, S., Regan, J., & Logan, B. (2007). Electricity generation and microbial community analysis of alcohol powered microbial fuel cells. *Bioresource Technology, 98*, 2568-2577.

Kim, K.-Y., Yang, W., & Logan, B. E. (2015). Impact of electrode configurations on retention time and domestic wastewater treatment efficiency using microbial fuel cells. *Water Research, 80*, 41-46. Retrieved from https://doi.org/10.1016/j.watres.2015.05.021

Krieg, T., Mayer, F., Sell, D., & Holtmann, D. (2019). Insights into the applicability of microbial fuel cells in wastewater treatment plants for a sustainable generation of electricity. *Environmental Technology, 40*(9), 1101-1109. doi:https://doi.org/10.1080/09593330.2017.1401668

Kumar, A., Siggins, A., Katuri, K., Mahony, T., O'Flaherty, V., Lens, P., & Leech, D. (2013). Catalytic response of microbialbio film sgrown under fixed anode potentials depends on electro chemica lcell configuration. *Chemical Engineering Journal, 230*, 532-536. doi: http://dx.doi.org/10.1016/j.cej.2013.06.044

Kumar, M., Boda, S., Shah, A., Kumar, S., & Sarkar, I. (2024). Scaling-Up Attempts of Microbial Electrochemical Technologies for the Removal of Water Pollutants. In R. Selvasembian, J. Mal, S. Das, D. Verma, & I. Anastopoulos, *Emerging Trends in Microbial Electrochemical Technologies for Sustainable Mitigation of Water Resources Contamination* (pp. 287-312). Springer, Cham. Retrieved from https://doi.org/10.1007/978-3-031-74636-9_12

Kumar, R., Singh, L., Wahid, Z., & Din, M. (2015). Exoelectrogens in microbial fuel cells towardbioelectricity generation: a review. *International Journal of Energy Research, 39*(8), 1011-1152. doi:https://doi.org/10.1002/er.3305

Kumar, R., Singh, L., Zularisam, A. W., & Hai, F. I. (2017). Microbial fuel cell is emerging as a versatile technology: a review on its possible applications, challenges and strategies to improve the performances. *International Journal of Energy Research, 42*(2), 369-394. doi:10.1002/er.3780

Kumar, S., Kumar, V., Malyan, S., Sharma, J., Mathimani, T., Maskarenj, M., . . . Pugazhendhi, A. (2019). Microbial fuel cells (MFCs) for bioelectrochemical treatment of different wastewater streams. *Fuel, 254*. Retrieved from https://doi.org/10.1016/j.fuel.2019.05.109

Kuntke, P., Śmiech, K., Bruning, H., Zeeman, G., Saakes, M., Sleutels, T., . . . Buisman, C. (2012). Ammonium recovery and energy production from urine by a microbial fuel cell. *Water Research, 46*(8), 2627-2636.

Larrosa-Guerrero, A., Scott, K., Head, I., Mateo, F., Ginesta, A., & Godinez, C. (2010). Effect of temperature on the performance of microbial fuel cells. *Fuel, 89*(12), 3985-3994. Retrieved from https://doi.org/10.1016/j.fuel.2010.06.025

Lee, S. H., Ban, J. Y., Oh, C.-H., Park, H.-K., & Choi, S. (2016). A solvent-free microbial-activated air cathode battery paper platform made with pencil-traced graphite electrodes. *Scientific Reports, 6*, 28588. doi: 10.1038/srep28588

Lettinga, G., Rebac, S., & Zeeman, G. (2001). Challenge of psychrophilic anaerobic wastewater treatment. *Trends in Biotechnology, 19*(9), 363-370. Retrieved from https://doi.org/10.1016/S0167-7799(01)01701-2

Li, L. H., S. Y., Yuan, Z. H., Kong, X. Y., & Li, Y. (2013). Effect of temperature change on power generation of microbial fuel cell. *Environmental Technology, 34*(13-14), 1929–1934. doi:https://doi.org/10.1080/09593330.2013.828101

Li, W.-W., Yu, H.-Q., & He, Z. (2014). Towards sustainable wastewater treatment by using microbial fuel cells-centered technologies. *Energy & Environm,ental Science*(3), 911-924. doi:10.1039/c3ee43106a

Li, W.-W., Yu, H.-Q., & He, Z. (2014). Towards sustainable wastewater treatment by using microbial fuel cells-centered technologies. *Energy and Environmental Science, 7*(3), 911-924. doi:10.1039/c3ee43106a

Li, X. (2006). *Principles of fuel cells.* New York: Taylor & Francis.

Li, Z., Yao, L., Kong, L., & Liu, H. (2008). Electricity generation using a baffled microbial fuel cell convenient for stacking. *Bioresource Technology, 99*, 1650-1655. Retrieved from https://doi.org/10.1016/j.biortech.2007.04.003

Liang, P., Duan, R., Yong, J., Zhang, X., Qiu, Y., & Huang, X. (2018). One-year operation of 1000-L modularized microbial fuel cell for municipal wastewater treatment. *Water Research, 141*, 1-8. doi:10.1016/j.watres.2018.04.066

Liu, H., Cheng, S., & Logan, B. (2004). Production of Electricity from Acetate or Butyrate Using a Single-Chamber Microbial Fuel Cell. *Environmental Science & Technology, 39*(2).

Liu, H., Cheng, S., & Logan, B. (2005). Power Generation in Fed-Batch Microbial Fuel Cells as a Function of Ionic Strength, Temperature, and Reactor Configuration. *Environmental Science & Technology, 39*(14).

Liu, H., Cheng, S., Huang, L., & Logan, B. E. (2007). Scale-up of membrane-free single-chamber microbial fuel cells. *Journal of Power Sources, 179*, 274–279. Retrieved from https://doi.org/10.1016/j.jpowsour.2007.12.120

Liu, Y., Climent, V., Berna, A., & Feliu, J. (2011). Effect of Temperature on the Catalytic Ability of Electrochemically Active Biofilm as Anode Catalyst in Microbial Fuel Cells. *Electroanalysis, 23*(2), 387-394. doi:https://doi.org/10.1002/elan.201000499

Liu, Z., Liu, J., Zhang, S., & Su, Z. (2009). Study of operational performance and electrical response on mediator-less microbial fuel cells fed with carbon-and protein-rich substrates. *Biochemical Engineering Journal, 45*(3), 185-191. doi:10.1016/j.bej.2009.03.011

Logan, B. E. (2009). Exoelectrogenic bacteria that power microbial fuel cells. *Nature Reviews Microbiology*, 375-381.

Logan, B., Hamelers, B., Rozendal, R., Schröder, U., Keller, J., Freguia, S., . . . Rabaey, K. (2006). Microbial Fuel Cells: Methodology and Technology. *Environmental Science & Technology, 40*(17), 5181-5192. doi:10.1021/es0605016

Logroño, W., Pérez, M., Urquizo, G., Kadier, A., Echeverría, M., Recalde, C., & Rákhely, G. (2017). Single chamber microbial fuel cell (SCMFC) with a cathodic microalgal biofilm: A preliminary assessment of the generation of bioelectricity and biodegradation of real dye textile wastewater. *Chemosphere, 176*, 378-388. Retrieved from https://doi.org/10.1016/j.chemosphere.2017.02.099

Ma, D., Jiang, Z.-H., Lay, C.-H., & Zhou, D. (2016). Electricity generation from swine wastewater in microbial fuel cell: Hydraulic reaction time effect. *International Journal of Hydrogen Energy, 41*(46), 21820-21826. Retrieved from https://doi.org/10.1016/j.ijhydene.2016.08.019

Mahmoudi, A., Alireza Mousavi, S., & Darvishi, P. (2024). Performance and recent development in sewage sludge-to-bioenergy using microbial fuel cells: A comprehensive review. *International Journal of Hydrogen Energy, 50*, 1432-1455. doi:https://doi.org/10.1016/j.ijhydene.2023.10.338.

Malekmohammadi, S., & Ahmad Mirbagheri, S. (2021). A review of the operating parameters on the microbial fuel cell for wastewater treatment and electricity generation. *Water Science & Technology, 84*(6), 1309-1323. Retrieved from https://doi.org/10.2166/wst.2021.333

Marcus, A. K., Torres, C. I., & Rittmann, B. E. (2007). Conduction-based modeling of the biofilm anode of a microbial fuel cell. *Biotechnology and Bioengineering, 98*(6), 1171 - 1182. doi:10.1002/bit.21533

McCarty, P. L., Bae, J., & Kim, J. (2011). *Domestic wastewater treatment as a net energy producer--can this be achieved?* California: PubMed®.

Min, B., & Logan, B. E. (2004). Continuous Electricity Generation from Domestic Wastewater and Organic Substrates in a Flat Plate Microbial Fuel Cell. *Environmental Science & Technology, 38*(21), 5809-5814. doi:10.1021/es0491026

Min, B., Kim, J., Oh, S., Regan, J. M., & Logan, B. E. (2005). Electricity generation from swine wastewater using microbial fuel cells. *Water Res*, 4961–4968. doi:10.1016/j.watres.2005.09.039

Minteer, S. D., Liaw, B., & Cooney, M. J. (2007). Enzyme-based biofuel cells. *Current Opinion in Biotechnology, 18*(3), 228-234. doi:https://doi.org/10.1016/j.copbio.2007.03.007.

Mitov, M., & Hubenova, Y. (2015). Microbial X cells - Innovative multipurpose bioelectrochemical systems. *Bulgarian Journal of Science Education, 24*, 404-416.

Miyahara, M., Hashimoto, K., & Watanabe, K. (2013). Use of cassette-electrode microbial fuel cell for wastewater treatment. *Journal of Bioscience and Bioengineering, 115*(2), 176-181. doi:10.1016/j.jbiosc.2012.09.003

Moharir, P., & Tembhurkar, A. (2018). Effect of recirculation on bioelectricity generation using microbial fuel cell with food waste leachate as substrate. *International Journal of Hydrogen Energy, 43*, 10061-10069. doi:10.1016/J.IJHYDENE.2018.04.072

Molognoni, D., Puig, S., Balaguer, M. D., Liberale, A., Capodaglio, A. G., Callegari, A., & Colprim, J. (2014). Reducing start-up time and minimizing energy losses of Microbial Fuel Cells using Maximum Power Point Tracking strategy. *Journal of Power Sources, 269*, 403 - 411. doi:10.1016/j.jpowsour.2014.07.033

Morozan, A., Jousselme, B., & Palacin, S. (2011). Low-platinum and platinum-free catalysts for the oxygenreduction reaction at fuelcell cathodes. *Energy & Environmental Science*(4), 1238-1254. doi:https://doi.org/10.1039/C0EE00601G

Munoz-Cupa, C., Hu, Y., Xu, C., & Bassi, A. (2021). An overview of microbial fuel cell usage in wastewater treatment, resource recovery and energy production. *Science of The Total Environment, 754*.

Munoz-Cupa, C., Hu, Y., Xu, C., & Bassi, A. (2021). An overview of microbial fuel cell usage in wastewater treatment, resource recovery and energy production. *Science of the Total Environment, 754*. doi:10.1016/j.scitotenv.2020.142429

N M, S., Meda, U. S., Patil, J. H., Moses, V., & P L, M. (2022). Wastewater Treatment Using Anaerobic Fluidized Bed Membrane Bioreactor Coupled with Microbial Fuel Cells for Circular Economy. *ECS Transactions. 107*, pp. 4435-4448. The Electrochemical Society. doi:10.1149/10701.4435ecst

Nor, M., Mubarak, M., Elmi, H., Ibrahim, N., Wahab, M., & Ibrahim, Z. (2015). Bioelectricity generation in microbial fuel cell using natural microflora and isolated pure culture bacteria from anaerobic palm oil mill effluent sludge. *Bioresource Technology, 190*, 458-465. Retrieved from https://doi.org/10.1016/j.biortech.2015.02.103

Nurmayani, S., Sugiarti, Y., & Putra, R. (2016). Utilization of industrial dairy waste as microalgae cultivation medium: a potential study for sustainable energy resources. *IOP Conference Series: Materials Science and Engineering*. Retrieved from https://doi.org/10.1088/1757-899X/128/1/012033

O'Toole, G., Kaplan, H., & Kolter, R. (2000). BIOFILM FORMATION AS MICROBIAL. *Annu. Rev. Microbiol*, 49-79. Retrieved from https://www.annualreviews.org/docserver/fulltext/micro/54/1/annurev.micro.54.1.49.pdf?expires=1736355476&id=id&accname=ar-190818&checksum=F98FB85C02982B9542152AE691D5C082

Pandey, A., Srivastava, S., & Kumar, S. (2020). Development and cost-benefit analysis of a novel process for biofuel production from microalgae using pre-treated high-strength fresh cheese whey wastewater. *Environ Sci Pollut Res, 27*, 23963–23980. Retrieved from https://doi.org/10.1007/s11356-020-08535-4

Pandit, S., Savla, N., Sonawane, J. M., Sani, A. M., Gupta, P. K., Mathuriya, A. S., . . . Prasad, R. (2021). Agricultural Waste and Wastewater as Feedstock for Bioelectricity Generation Using Microbial Fuel Cells: Recent Advances. *Fermentation, 7*(3), 169. Retrieved from https://doi.org/10.3390/fermentation7030169

Pandit, S., Sengupta, A., Kale, S., & Das, D. (2011). Performance of electron acceptors in catholyte of a two-chambered microbial. *Bioresource Technology, 102*, 2736-2744.

Pant, D., Van Bogaert, G., Diels, L., & Vanbroekhoven, K. (2010). A review of the substrates used in microbial fuel cells (MFCs) for sustainable energy production. *Bioresource Technology*, 1533-1543. doi:10.1016/j.biortech.2009.10.017

Park, H., Tinh, V., & Kim, D. (2022). Surface hydrophilization toward the proton conductive porous PTFE substrate impregnating SPEEK for polymer electrolyte membranes. *Progress in Organic Coatings, 163*. Retrieved from https://doi.org/10.1016/j.porgcoat.2021.106643

Park, I., Christy, M., Kim, P., & Nahm, K. (2014). Enhanced electrical contact of microbes using Fe3O4/CNT nanocomposite anode in mediator-less microbial fuel cell. *Biosensors and Bioelectronics, 58*, 75-80. doi:https://doi.org/10.1016/j.bios.2014.02.044.

Parker, W. J. (2005). Application of the ADM1 model to advanced anaerobic digestion. *Bioresource Technology, 96*(16), 1832-1842. Retrieved from https://doi.org/10.1016/j.biortech.2005.01.022

Patel, D., Bapodra, S. L., Madamwar, D., & Desai, C. (2021). Electroactive bacterial community augmentation enhances the performance of a pilot scale constructed wetland microbial fuel cell for treatment of textile dye wastewater. *Bioresource Technology, 332*. Retrieved from https://doi.org/10.1016/j.biortech.2021.125088

Pearce, G. (2008, March 1). UF/MF pre-treatment to RO in seawater and wastewater reuse applications: a comparison of energy costs. *Desalination, 222*(1-3), 66-73.

Peng, J., Wang, X., Yin, F., & Xu, G. (2019). Characterizing the removal routes of seven pharmaceuticals in the activated sludge process. *Science of The Total Environment, 650*, 2437-2445. Retrieved from https://doi.org/10.1016/j.scitotenv.2018.10.004

Pinto, R., Srinivasan, B., Guiot, S., & Tartakovsky, B. (2011). The effect of real-time external resistance optimization on microbial fuel cell performance. *Water Research, 45*(4), 1571-1578. Retrieved from https://doi.org/10.1016/j.watres.2010.11.033

Pinto, R., Srinivasan, B., Manuel, M.-F., & Tartakovsky, B. (2010). A two-population bio-electrochemical model of a microbial fuel cell. *Bioresource Technology, 101*(14), 5256 - 5265. doi:10.1016/j.biortech.2010.01.122

Raad, N. K., Farrokhi, F., Mousavi, S. A., Darvishi, P., & Mahmoudi, A. (2020). Simultaneous power generation and sewage sludge stabilization using an air cathode-MFCs. *Biomass and Bioenergy, 140*. doi:10.1016/j.biombioe.2020.105642

Rabaey, K., & Verstraete, W. (2005). Microbial fuel cells: Novel biotechnology for energy generation. *Trends in Biotechnology, 23*(6), 291 - 298. doi:10.1016/j.tibtech.2005.04.008

Rabaey, K., Boon, N., Siciliano, S. D., Verhaege, M., & Verstraete, W. (2004). Biofuel cells select for microbial consortia that self-mediate electron transfer. *Applied and Environmental Microbiology, 70*(9), 5373-5382. doi:10.1128/AEM.70.9.5373-5382.2004

Rabaey, K., Clauwaert, P., Aelterman, P., & Verstraete, W. (2005). Tubular microbial fuel cells for efficient electricity generation. *Environmental Science and Technology, 39*(20), 8077 - 8082. doi:10.1021/es050986i

Rahimnejad, M., Adhami, A., Darvari, S., Zirepour, A., & Oh, S.-E. (2015). Microbial fuel cell as new technology for bioelectricity generation: A review. *Alexandria Engineering Journal, 54*(3), 745-756. doi:https://doi.org/10.1016/j.aej.2015.03.031.

Rahimnejad, M., Ghoreyshi, A., Najafpour, G., Younesi, H., & Shakeri, M. (2012). A novel microbial fuel cell stack for continuous production of clean energy. *International Journal of Hydrogen Energy, 37*(7), 5992-6000. doi:10.1016/j.ijhydene.2011.12.154

Rasmussen, M., Abdellaoui, S., & Minteer, S. (2016). Enzymatic biofuel cells: 30 years of critical advancements. *Biosensors and Bioelectronics, 76*, 91-102.

Ren, Z., Ward, T. E., & Regan, J. M. (2007). Electricity production from cellulose in a microbial fuel cell using a defined binary culture. *Environmental Science and Technology, 41*(13), 4781 - 4786. doi:10.1021/es070577h

Roy, H., Rahman, T. U., Tasnim, N., Arju, J., Rafid, M. M., Islam, M. R., . . . Islam, M. S. (2023). Microbial Fuel Cell Construction Features and Application for Sustainable Wastewater Treatment. *Membranes, 13*(5), 490. Retrieved from https://doi.org/10.3390/membranes13050490

Rozendal, R., Hamelers, H. V., & Buisman, C. J. (2006). Effects of Membrane Cation Transport on pH and Microbial Fuel Cell Performance. *Environmental Science & Technology, 40*(17). doi:10.1021/es060387r

Sajana, T., Ghangrekar, M., & Mitra, A. (2013). Effect of pH and distance between electrodes on the performance of a sediment microbial fuel cell. *Water Science and Technology, 68*(3), 537-543. doi:10.2166/wst.2013.271

Saket, P., Mittal, Y., Bala, K., Joshi, A., & Yadav, A. K. (2022). Innovative constructed wetland coupled with microbial fuel cell for enhancing diazo dye degradation with simultaneous electricity generation. *Bioresource Technology, 345*. Retrieved from https://doi.org/10.1016/j.biortech.2021.126490

Samsudeen, N., Radhakrishnan, T., & Matheswaran, M. (2015). Performance Comparison of Triple and DualChamber Microbial Fuel Cell Using DistilleryWastewater as a Substrate. *Environmental Progress & Sustainable Energy*, 315-633. doi:https://doi.org/10.1002/ep.12005

Sangamnere, R., Misra, T., Bherwani, H., Kapley, A., & Kumar, R. (2023). A critical review of conventional and emerging wastewater treatment technologies. *Sustain. Water Resour. Manag, 9*(58). Retrieved from https://doi.org/10.1007/s40899-023-00829-y

Santoro, C., Arbizzani, C., Erable, B., & Ieropoulos, I. (2017). Microbial fuel cells: From fundamentals to applications. A review. *Journal of Power Sources, 356*, 225-244. Retrieved from https://doi.org/10.1016/j.jpowsour.2017.03.109.

Santoro, C., Arbizzani, C., Erable, B., & Ieropoulos, I. (2017). Microbial fuel cells: From fundamentals to applications. A review. *Journal of Power Sources, 356*, 225-244. doi:https://doi.org/10.1016/j.jpowsour.2017.03.109.

Saratale, G., Saratale, R., Shahid, M., Zhen, G., Kumar, G., Shin, H.-S., . . . Kim, S.-H. (2017). A comprehensive overview on electro-active biofilms, role of exo-electrogens and their microbial niches in microbial fuel cells (MFCs). *Chemosphere, 178*, 534-547. doi:https://doi.org/10.1016/j.chemosphere.2017.03.066

Saravanana, A., Senthil, P. K., Srinivasand, S., Jeevananthame, S., & Kamaleshe, R. (2022). Sustainable strategy on microbial fuel cell to treat the wastewater for the production of green energy. *Chemosphere, 290*, 133295. doi:https://doi.org/10.1016/j.chemosphere.2021.133295

Sciarria, T., Tenca, A., D'Epifanio, A., Mecheri, B., Merlino, G., Barbato, M., . . . Adani, F. (2013). Using olive mill wastewater to improve performance in producing electricity from domestic

wastewater by using single-chamber microbial fuel cell. *Bioresource Technology*, 246-253. Retrieved from https://doi.org/10.1016/j.biortech.2013.08.033

Seow, T. W., Lim, C., Hanif Md Nor, M., Mubarak, M., Lam, C., Yahya, A., & Ibrahim, Z. (2016). Review on Wastewater Treatment Technologies. *International Journal of Applied Environmental Sciences, 11*, 111-126.

Sharma, Y., & Li, B. (2010). Optimizing energy harvest in wastewater treatment by combining anaerobic hydrogen producing biofermentor (HPB) and microbial fuel cell (MFC). *International Journal of Hydrogen Energy, 35*(8), 3789-3797. doi:10.1016/j.ijhydene.2010.01.042

Shukla, A. K., Suresh, P., Berchmans, S., & Rajendran, A. (2004). Biological fuel cells and their applications. *Current Science, 87*(4), 455-468.

Silveira , G., de Aquino Neto, S., & Schneedorf, J. (2020). Development, characterization and application of a low-cost single. *Energy, 208*. doi:https://doi.org/10.1016/j.energy.2020.118395

Singh Mathuriya, A., & Yakhmi, J. (2016). Microbial fuel cells – Applications for generation of electrical powerand beyond. *Critical Reviews in Microbiology, 42*(1), 127-143. doi:10.3109/1040841X.2014.905513

Slate, A. J., Whitehead, K. A., Brownson, D. A., & Banks, C. E. (2019). Microbial fuel cells: an overview of current technology. *Renewable and Sustainable Energy Reviews, 101*, 60-81. doi:10.1016/j.rser.2018.09.044

Sobieszuk, P., Zamojska-Jaroszewicz, A., & Makowski, Ł. (2017). Influence of the operational parameters on bioelectricity generation in continuous microbial fuel cell, experimental and computational fluid dynamics modelling. *Journal of Power Sources, 371*, 178-187. Retrieved from https://doi.org/10.1016/j.jpowsour.2017.10.032

Stirling, J. L., Bennetto, H. P., Delaney, G. M., Mason, J. R., Roller, S. D., Tanaka, K., & Thurston, C. F. (1983). Microbial fuel cells. *Biochem Soc Trans, 11*(4), 451-453. doi:https://doi.org/10.1042/bst0110451

Suor, D., Ma, J., Wang, Z., Li, Y., Tang, J., & Wu, Z. (2014). Enhanced power production from waste activated sludge in rotating-cathode microbial fuel cells: the effects of aquatic worm predation. *Chemical Engineering Journal, 248*, 415-421. doi:10.1016/j.cej.2014.02.095

Suzuki, K., Kato, Y., Yui, A., Yamamoto, S., Ando, S., Rubaba, O., . . . Futamata, H. (2018). Bacterial communities adapted to higher external resistance can reduce the onset potential of anode in microbial fuel cells. *Journal of Bioscience and Bioengineering, 125*(5), 565-571. Retrieved from https://doi.org/10.1016/j.jbiosc.2017.12.018

Toronto water. (2020). *NORTH TORONTO TREATMENT PLANT.* Toronto. Retrieved Decmber 2023, from https://www.toronto.ca/wp-content/uploads/2021/05/9732-2020-TNT-Annual-Report-FINAL.pdf

Tran, H., Lesage, G., Lin, C., Nguyen, T., Bui, X.-T., Nguyen, M., . . . Nguyen, D. (2022). Chapter 3 - Activated sludge processes and recent advances. In D. D.-D. Xuan-Thanh Bui, *Current Developments in Biotechnology and Bioengineering* (pp. 49-79). Elsevier.

Tremouli, A., Martinos, M., & Lyberatos, G. (2017). The Effects of Salinity, pH and Temperature on the Performance of a Microbial Fuel Cell. *Waste and Biomass Valorization, 8*(6), 2037 - 2043. doi:10.1016/j.bioelechem.2008.07.007

Ullah, Z., & Zeshan, S. (2020). Effect of substrate type and concentration on the performance of a double chamber microbial fuel cell. *Water Science and Technology, 81*(7), 1336-1344. doi:10.2166/wst.2019.387

Venkata Mohan, S., Mohanakrishna, G., & Sarma, P. (2010). Composite vegetable waste as renewable resource for bioelectricity generation through non-catalyzed open-air cathode microbial fuel cell. *Bioresource Technology, 101*(3), 970-976. doi:10.1016/j.biortech.2009.09.005

Venkata Mohan, S., Velvizhi, G., Modestra, J., & Srikanth, S. (2014). Microbial fuel cell :Critical factors regulating bio-catalyzed electro chemical process and recent advancements. *Renewable and Sustainable Energy Reviews, 40*, 779-797. doi: http://dx.doi.org/10.1016/j.rser.2014.07.109

Verma, M., Singh, V., & Mishra, V. (2023). Bioelectricity generation by using cellulosic waste and spent engine oil in a concentric photobioreactor-microbial fuel cell. *Journal of Environmental Chemical Engineering, 11*(5), 110566.

Virdis, B., Rabaey, K., Yuan, Z., & Keller, J. (2008). Microbial fuel cells for simultaneous carbon and nitrogen removal. *Water Research, 42*(12), 3013-3024. doi:https://doi.org/10.1016/j.watres.2008.03.017.

Vologni, V., Kakarla, R., Angelidaki, I., & Min, B. (2013). Increased power generation from primary sludge by a submersible microbial fuel cell and optimum operational conditions. *Bioprocess and Biosystems Engineering, 36*(5), 631-642. doi:10.1007/s00449-013-0918-2

Wang, Z., Su, G., Zhang, Z., Dong, H., Wang, Y., Zhao, H., . . . H9c2, 2.-H.-p. p.-i. (2018). 25-Hydroxyl-protopanaxatriol protects against H2O2-induced H9c2. *Biomedicine & Pharmacotherapy, 99*, 33-42. doi:https://doi.org/10.1016/j.biopha.2018.01.039

Watanabe, K. (2008). Recent Developments in Microbial Fuel Cell Technologies for Sustainable Bioenergy. *Journal of Bioscience and Bioengineering, 106*(6), 528-536. Retrieved from https://doi.org/10.1263/jbb.106.528

Winfield, J., Gajda, I., Greenman, J., & Ieropoulos, I. (2016). A review into the use of ceramics in microbial fuel cells. *Bioresour Technol, 215*, 296-303. doi:10.1016/j.biortech.2016.03.135

Woodward, L., Perrier, M., Srinivasan, B., Pinto, R. P., & Tartakovsky, B. (2010). Comparison of real-time methods for maximizing power output in microbial fuel cells. *AIChE Journal, 56*(10), 2742-2750. Retrieved from https://doi.org/10.1002/aic.12157

Wu, S., Li, H., Zhou, X., Liang, P., Zhang, X., Jiang, Y., & Huang, X. (2016). A novel pilot-scale stacked microbial fuel cell for efficient electricity generation and wastewater treatment. *Water Research*, 396-403. doi:10.1016/j.watres.2016.04.043

Xiao, B., Han, Y., Liu, X., & Liu, J. (2014). Relationship of methane and electricity production in two-chamber microbial fuel cell using sewage sludge as substrate. *International journal of hydrogen energy, 39*(29), 16419-16425. doi:10.1016/j.ijhydene.2014.08.024

Xiao, B., Yang, F., & Liu, J. (2011). Enhancing simultaneous electricity production and reduction of sewage sludge in two-chamber MFC by aerobic sludge digestion and sludge pretreatments. *Journal of Hazardous Materials, 189*, 444-449. doi:10.1016/j.jhazmat.2011.02.058

Xu, M., Li, P., Tang, T., & Hu, Z. (2015). Roles of SRT and HRT of an algal membrane bioreactor system with a tanks-in-series configuration for secondary wastewater effluent polishing. *Ecological Engineering, 85*, 257-264. Retrieved from https://doi.org/10.1016/j.ecoleng.2015.09.064

Yang, W., Li, J., Ye, D., Zhang, L., Zhu, X., & Liao, Q. (2016). A hybrid microbial fuel cell stack based on single and double chamber microbial fuel cells for self-sustaining pH control. *Journal of Power Sources, 306*, 685-691. doi:10.1016/j.jpowsour.2015.12.073

Yaqoob, A. A., Khatoon, A., Mohd Setapar, S. H., Umar, K., Parveen, T., Mohamad Ibrahim, M. N., . . . Rafatullah, M. (2020). Outlook on the Role of Microbial Fuel Cells in Remediation of Environmental Pollutants with Electricity Generation. *Catalysts, 10*(8), 819. doi:10.3390/catal10080819

Ye, Y., Ngo, H. H., Guo, W., Liu, Y., Chang, S. W., Nguyen, D. D., . . . Zhang, X. (2019). Feasibility study on a double chamber microbial fuel cell for nutrient recovery from municipal wastewater. *Chemical Engineering Journal, 358*, 236-242. Retrieved from https://doi.org/10.1016/j.cej.2018.09.215

Yetilmezsoy, K., & Sakar, S. (2008). Development of empirical models for performance evaluation of UASB reactors treating poultry manure wastewater under different operational conditions. *Journal of Hazardous Materials, 153*(1–2), 532-543. Retrieved from https://doi.org/10.1016/j.jhazmat.2007.08.087

You, J., Greenman, J., & Leropoulos, I. (2018). Novel Analytical Microbial Fuel Cell Design for Rapid in Situ Optimisation of Dilution Rate and Substrate Supply Rate, by Flow, Volume Control and Anode Placement. *Energies, 11*(9), 2377. Retrieved from https://doi.org/10.3390/en11092377

Zeng, Y., Choo, Y. F., Kim, B.-H., & Wu, P. (2010). Modelling and simulation of two-chamber microbial fuel cell. *Journal of Power Sources, 195*, 79-89. doi:10.1016/j.jpowsour.2009.06.101

Zeng, Y., Choo, Y. F., Kim, B.-H., & Wu, P. (2010). Modelling and simulation of two-chamber microbial fuel cell. *Journal of Power Sources, 195*(1), 79-89. doi:10.1016/j.jpowsour.2009.06.101.

Zhang, L., Chen, Q., Zhou, S., Yuan, Y., & Yuan, H. (2012). Methanogenesis control using 2-bromoethanesulfonate for enhanced power recovery from sewage sludge in air-cathode microbial fuel cells. *Int. J. Electrochem. Sci.*, 6512-6523.

Zhang, L., Li, J., Zhu, X., Ye, D., Fu, Q., & Liao, Q. (2017). tartup Performance and Anodic Biofilm Distribution in Continuous-Flow Microbial Fuel Cells with Serpentine Flow Fields: Effects of External Resistance. *Industrial & Engineering Chemistry Research, 56*(14), 3767–3774. Retrieved from https://doi.org/10.1021/acs.iecr.6b04619

Zhang, L., Wang, J., Fu, G., & Zhang, Z. (2020). Simultaneous electricity generation and nitrogen and carbon removal. *Journal of Cleaner Production, 276*. doi: https://doi.org/10.1016/j.jclepro.2020.123203

Zhang, Y., Liu, M., Zhou, M., Yang, H., Liang, L., & Gu, T. (2019). Microbial fuel cell hybrid systems for wastewater treatment and bioenergy production: Synergistic effects, mechanisms and challenges. *Renewable and Sustainable Energy Reviews, 103*, 13-29. doi:10.1016/j.rser.2018.12.027.

Zhang, Y., Min, B., Huang, L., & Angelidaki, I. (2011). Electricity generation and microbial community response to substrate changes in microbial fuel cell. *Bioresource Technology*, 1166-1173.

Zhang, Y., Olias, L., Kongjan, P., & Angelidaki, I. (2011). Submersible microbial fuel cell for electricity production from sewage sludge. *Water Science & Technology, 64*(1), 50-55. doi:10.2166/wst.2011.678

Appendix A

Raw Influent Data and Final Effluent Data from Guelph WWTP

	pH	CBOD5 (mg/L)	BOD5 (mg/L)	TSS (mg/L)	TP (mg/L)	TKN (mg/L)	TAN (mg/L)
January	7.50	250	253	259	5.48	35.0	27.9
February	7.40	193	217	277	4.74	35.0	26.6
March	7.40	185	192	232	4.18	28.0	21.0
April	7.40	150	168	194	4.11	30.0	22.6
May	7.40	163	185	234	4.50	28.0	21.3
June	7.50	190	204	258	4.74	27.0	21.2
July	7.60	202	246	300	5.10	28.0	19.5
August	7.60	196	216	269	5.48	36.0	21.9
September	7.60	226	248	328	6.22	44.0	23.9
October	7.60	192	220	320	6.16	44.0	24.4
November	7.60	262	264	340	5.44	50.0	28.3
December	7.70	242	283	324	4.97	46.0	27.8
Annual Average	7.53	204	225	278	5.09	35.9	23.9
Winter Average	7.52	226	242	286	4.96	38.8	26.3
Summer Average	7.53	188	212	272	5.19	33.9	22.1

Figure 31. Raw Influent Data from Guelph WWTP (Guelph, 2022)

		Jan	Feb	Mar	Apr	May	June	July	Aug	Sept	Oct	Nov	Dec	Annual Avg.	Winter Avg.	Summer Avg.
Min pH		7.1	6.9	7.0	6.9	6.9	6.9	7.1	7.0	6.7	6.6	6.6	7.2	6.9	7.0	6.9
Max pH		7.2	7.2	7.2	7.1	7.1	7.2	7.2	7.3	7.1	7.6	7.5	7.5	7.3	7.3	7.2
Average pH		7.2	7.1	7.0	7.0	7.0	7.1	7.2	7.2	6.8	6.9	7.4	7.4	7.1	7.2	7.0
Temp	^{0}C	13.4	12.6	12.2	13.5	15.9	18.5	20.5	21.4	21.3	19.5	18.0	15.4	16.9	14.3	18.7
CBOD5	Concentration (mg/L)	2.0	2.4	2.0	2.7	2.0	2.0	2.0	2.0	2.0	2.1*	2.0	2.0	2.1	2.1	2.1
CBOD5	Loading (kg/d)	104.8	149.2	132.0	165.9	112.1	102.1	94.7	93.2	94.5	99.3	91.3	88.8	110.7	113.2	108.8
BOD5	Concentration (mg/L)	2.1	3.7	2.3	5.1	2.3	2.0	2.0	2.0	2.1	2.0*	2.3	2.0	2.5	2.5	2.5
BOD5	Loading (kg/d)	110.8	247.0	154.5	313.5	126.8	102.1	94.7	93.2	100.5	93.8	102.5	88.8	135.7	140.7	132.1
TSS	Concentration (mg/L)	2.0	2.0	2.0	3.0	2.0	2.0	2.0	2.0	4.0	2.0	2.0	2.0	2.3	2.0	2.4
TSS	Loading (kg/d)	105	125	123	164	136	109	107	109	160	94	101	93	118.8	109.4	125.6
TP	Concentration (mg/L)	0.09	0.09	0.10	0.12	0.10	0.13	0.18	0.13	0.15	0.12	0.14	0.11	0.12	0.11	0.13
TP	Loading (kg/d)	4.6	5.0	6.4	7.1	5.6	6.2	8.1	6.1	6.6	5.3	6.3	4.7	6.0	5.4	6.4
TKN	Concentration (mg/L)	2.10	2.06	3.08	2.09	1.43	1.96	2.08	1.26	1.41	1.25	1.75	1.03	1.79	2.00	1.64
TAN	Concentration (mg/L)	0.45	1.61	2.71	1.21	0.48	0.27	0.15	0.14	0.27	0.32	0.60	0.18	0.70	1.11	0.41
TAN	Loading (kg/d)	22.8	98.5	185.4	73.6	27.2	13.8	6.9	6.5	12.6	14.6	27.1	8.2	41.4	68.4	22.2
NO3-N	Concentration (mg/L)	31.8	28.0	23.1	26.7	27.9	27.9	30.9	27.7	26.6	28.3	31.5	35.7	28.8	30.0	28.0
NO2-N	Concentration (mg/L)	0.12	0.22	0.36	0.27	0.09	0.18	0.09	0.03	0.06	0.09	0.20	0.06	0.15	0.19	0.12
E. Coli	(CFU/100 mL)	17	10	10	10	11	16	37	30	24	11	14	23	17.8	14.8	19.9
TCR	(mg/L)	0.00	0.00	0.00	0.00	0.00	0.00	0.00	0.00	0.00	0.00	0.00	0.00	0.0	0.0	0.0
SBR	(mg/L)	1.09	1.25	1.25	1.30	1.27	1.41	1.10	1.33	1.42	1.33	1.17	1.17	1.26	1.19	1.31

Figure 32. Final Effluent Quality (Guelph, 2022)